NONLINEAR ANALYSIS OF COMPOSITE LAMINATED PLATES SUBJECTED TO IMPACT

by

Hiroto Matsuhashi

B.S. Aerospace Engineering, State University of New York at Buffalo (1990)

Submitted to the Department of Aeronautics and Astronautics
in partial fulfillment of the requirement for the degree of

MASTER OF SCIENCE
IN AERONAUTICS AND ASTRONAUTICS

at the

MASSACHUSETTS INSTITUTE OF TECHNOLOGY

September 1992

Copyright © Massachusetts Institute of Technology, 1992.
All rights reserved.

Signature of Author _____
Department of Aeronautics and Astronautics
August 4, 1992

Certified by _____
Professor Michael J. Graves
Thesis Supervisor

Accepted by _____
Professor Harold Y. Wachman
Chairman, Departmental Graduate Committee

Aero
MASSACHUSETTS INSTITUTE OF TECHNOLOGY
SEP 22 1992
LIBRARIES

NONLINEAR ANALYSIS OF COMPOSITE LAMINATED PLATES SUBJECTED TO IMPACT

by

Hiroto Matsuhashi

Submitted to the Department of Aeronautics and Astronautics
on August 4, 1992 in partial fulfillment of the requirement for the degree of
MASTER OF SCIENCE IN AERONAUTICS AND ASTRONAUTICS

ABSTRACT

Nonlinear transient global response of shear deformable composite laminated plates subjected to impact loading was investigated analytically and compared with linear transient global response, which was also reviewed in this study, and with existing experimental data. Based on energy equations derived by applying geometrical nonlinearity in strain-displacement relations, the impacted plate response model was developed employing the Lagrangian equations of motion and the Rayleigh-Ritz method in conjunction with assumed mode shapes. The resulting system of second-order nonlinear differential equations with respect to time was solved using the fourth-order Runge-Kutta numerical time integration scheme to produce a transient response in terms of force- and displacement-time histories at the point of impact where a nonlinear local contact law was assumed. Comparison between linear and nonlinear analysis clearly showed the importance of considering the geometrical nonlinear effect of membrane stiffening. Comparison of the analytical results with existing experimental data indicated that the nonlinear plate impact response model with partial geometrical nonlinearity accounting for the flexible boundary was able to predict the impact response well especially for the primary frequency response. However, the secondary frequency response predicted by the model showed relatively poor correlations with the existing experimental data. Further refinement needs to be done to bring this nonlinear impact response analysis into better agreement with the experimental data.

Thesis Supervisor: Michael J. Graves

Title: Assistant Professor, Department of Aeronautics and Astronautics, Massachusetts Institute of Technology

Acknowledgements

There are many people who I would like to acknowledge for their technical and/or personal support and encouragement throughout these last two years of my graduate study at MIT or probably the last seven years of my life in the United States.

A special thanks to my advisor, Prof. Michael Graves for providing me with precious advice and fruitful discussions, and letting me realize the importance of *thinking*. His always positive and optimistic attitude helped me a lot when I needed some encouragement. I would like to thank Prof. John Dugundji for his excellent technical suggestions and comments. The approach suggested by Prof. Dugundji in Chapter 4 of this thesis helped to determine the vector of this investigation into a nonlinear world. I would also like to thank Prof. Paul Lagace for participating in many of my meetings with Michael, giving a number of suggestions, allowing me to use CRAY almost unlimitedly, and most importantly, providing me with the opportunity to work in TELAC. Also, I would like to show my appreciation to Prof. Herbert Reismann in State University of New York at Buffalo for introducing me to the joy of working in the field of aerospace structures and making it possible for me to be here.

My life at MIT became a very enjoyable and meaningful one because of the following individuals. Thanks to all of the fellow graduate students in TELAC for their help and companionships. Thanks to Aaron, Narendra, Hary, Jeff, Laura, Stacy, Steve, Wilson, Kim, Mary,

Peter, Ed, Randy, James, Wai-Tuck, Claudia, and Mak. Special thanks to Wilson Tsang for providing extensive help in impact analysis, Narendra Bhat for answering and discussing many of my questions and problems, both technical and personal, and Ed Wolf for providing information on experiments he performed and his consistent experimental data. (Also, thanks for the lecture notes of 18.086 to Steve, Stacy, Aaron, and Jeff.) I would like to thank many of my friends in both the United States and Japan for their support, encouragement, and friendship over the years. Special thanks to Dai Tanno for his invaluable advice, friendship, and being my role model in some aspects for last seven years.

Finally, I would like to thank Mr. Shin-ichiro Komazawa and Recruit Scholarship Foundation in Japan for their funding support which made it possible for me to attend my first semester at MIT.

Foreword

This investigation was conducted in the Technology Laboratory for Advanced Composites (TELAC) of the Department of Aeronautics and Astronautics at the Massachusetts Institute of Technology. Some of the computations in this investigation were performed using MIT's CRAY X-MP EA/464 supercomputer. This work was sponsored by joint Navy/FAA Contract No. N00019-89-C-0058.

Dedication

I would like to dedicate this thesis to my loving parents, Toshiaki and Akiko Matsuhashi, who allowed their only son to study abroad for seven long years. I will not forget their unselfish and supportive attitude for rest of my life.

Normal science does and must continually strive to bring theory and fact into closer agreement, and that activity can easily be seen as testing or as a search for confirmation or falsification. Instead, its object is to solve a puzzle for whose very evidence the validity of the paradigm must be assumed. Failure to achieve a solution discredits only the scientist and not the theory.

"The Structure of Scientific Revolutions"

— Thomas S. Kuhn, 1962

Table of Contents

List of Figures

List of Tables

Nomenclature

u, v, w	displacement components along the x, y, z coordinates
ψ_x, ψ_y	rotations of a plane section about the y, x axes
ε_{ij}	strain tensor components $(i, j = 1, 2, 3)$
ε°_{ij}	strain tensor components at midplane $(i, j = 1, 2)$
κ_{ij}	curvature tensor components $(i, j = 1, 2)$
A_{ij}	in-plane stiffness component of the plate $(i, j = 1, 2, 6)$
B_{ij}	bending-stretching stiffness component of the plate $(i, j = 1, 2, 6)$
D_{ij}	bending stiffness component of the plate $(i, j = 1, 2, 6)$
G_{ij}	transverse shear stiffness component of the plate $(i, j = 4, 5)$
N_x, N_y, N_{xy}	in-plane stress resultants
M_x, M_y, M_{xy}	bending moment resultants
Q_x, Q_y	shear force resultants
U	internal strain energy
W	work done by the external forces
T	kinetic energy
t	time
$(\cdot)$	derivative sign with respect to time
a, b	plate dimensions in x, y directions
F, F_z	impact force
m_I	mass of impactor

u_I	displacement of impactor
k	local contact stiffness constant
n	local contact nonlinearity exponent
α	indentation at the contact point
E	Young's modulus of elasticity
l	length of beam
β	geometrical nonlinearity factor
$A_i(t)$, $B_i(t)$, $C_i(t)$, $D_i(t)$, $E_i(t)$	modal amplitudes
$f_i(x)$, $g_i(y)$, $h_i(x)$, $l_i(y)$, $m_i(x)$, $n_i(y)$, $o_i(x)$, $p_i(y)$, $q_i(x)$, $r_i(y)$	assumed mode shape functions
L	Lagrangian function
$\underline{q}$, $\underline{\lambda}$	generalized coordinates for linear terms
$\underline{\lambda}^{[3]}$	system of generalized coordinates for nonlinear cubic terms
$\underline{M}$	inertia matrix for reduced system of equations
$\underline{K}^*$	stiffness matrix for linear term of reduced system of equations
$\underline{K}_{III}{}^*$	stiffness matrix for nonlinear cubic term of reduced system of equations
$\underline{R}$	generalized force vector of reduced system of equations

Chapter 1

Introduction

1.1 Motivation

Advanced composite laminated materials such as graphite/epoxy have been successfully employed as structural components in aircrafts, missiles, and space vehicles. The performance of these composites has shown their superiority over metals in applications requiring high strength-to-weight and stiffness-to-weight ratios [1]. The composite laminates are, however, particularly susceptible to impact damage with foreign objects such as tool drops, runway kickup, bird strikes, and hail; these impacts can produce significant damage in terms of fiber breakage, matrix cracking, and delamination which may be embedded inside the composites [2,3]. Such damage is sometimes hardly detectable by the naked eye, but can cause significant reductions in the strength and stiffness of the structure [4]. Therefore, to utilize composites to their full advantage their response to impact must be understood, and the damage caused by impact must be predictable.

The response of the structure to an impact can be assumed to occur at two levels; a *global* response of the structure and a *local* response under the point of impact [2]. As a first step to understanding the impact damage issue in composite laminates, an accurate prediction of the transient global response during an impact event is necessary. Then, the output of the global response analysis can be used to produce useful information to compute stresses and strains at the local level. Those results coupled with other appropriate analyses such as failure criteria may be used to predict damage in the structure and, ultimately, the residual strength. Again, an accurate prediction of the transient global response is a first key to reach the goal – prediction of the damage and residual strength.

1.2 Objective

This report focuses on the problem of analyzing the transient global response of composite laminated plates subjected to impact. In particular, it deals with impact modeling using both linear and nonlinear laminated plate theory with first-order shear deformation. The results of those analyses are compared to a particular impact condition observed experimentally [19].

The linear plate theory is based on the assumption that a membrane force effect, which may be a function of out-of-plane displacement, is negligible. Consequently, linear strain-displacement relations are employed. On the other hand, nonlinear plate theory can account for the membrane force effect by adding second-order nonlinear

terms to the linear strain-displacement relations. The membrane force effect may be crucial in predicting the transient global response depending on impact conditions such as impactor mass, impactor velocity, plate geometry, and boundary conditions. No material nonlinearity is considered in this investigation.

1.3 Review of Previous Work

The impact of a foreign object with a composite laminated plate is a complex event occurring over a very short period of time (on the order of milliseconds typically). There are several features which preclude a simple modeling and solution for the analytical prediction of this impact event. Some of those features might include a shearing deformation effect, an influence of bending-twisting coupling in the constitutive behavior, a nonlinear constitutive relation between plate and projectile, and a geometric nonlinearity of the plate depending on a boundary condition.

Many researchers have developed models to predict the global response of laminated plates with shear deformation effect due to an impact event, but relatively few researchers have considered the geometrical nonlinearity in plate analysis. Abrate [47] presented an extensive review in the field of impact on laminated composite materials and Chia [48] described a review for the geometrically nonlinear behavior of composite plates. Some of the prominent work, as well as recent developments, are reviewed in this section.

1.3.1 Linear Plate Analysis

Yang, Norris, and Stavsky [5] deduced a two-dimensional linear theory of the motion of heterogeneous plates from the three-dimensional theory of elasticity. They included transverse shear deformations [11] and rotary inertia in their formulation of the plate theory. Although they were investigating the propagation of elastic waves in a heterogeneous plate, the governing equations of the free vibration of the plate are the same as for the problem of impact transverse to the plate.

The impact of a sphere on a half-space was treated by Timoshenko and Goodier [6]. In their approach, wave effects in the half-space and ball were neglected. Greszczuk [7] studied the impact of both isotropic and transversely isotropic half-spaces by a sphere. Internal stresses in the body were determined using the finite element method. The results showed that the largest contact stresses were under the point of impact within the composite, and that the critical stress was usually shear. This analysis neglected global bending of the laminate and inertial forces. These effects need to be considered to accurately model the dynamics of composite plates.

For plates, the basic approach presented by Timoshenko [8] for the analysis of transverse impact of a beam by a sphere was extended by Karas [9] to the analysis of the central impact of a rectangular simply supported plate. Sun and Chattopadhyay [10] extended this approach to analyze laminated composite plates under initial stress including transverse shear deformation [11]. They obtained the contact force and the dynamic response of the plate by solving an integral equation numerically.

Whitney and Pagano [11] showed that the influence of shearing deformation in composite laminates can be significant because of high through-the-thickness shearing compliances. Their results showed that Reissner-Mindlin plate theory, in which planar rotations are introduced as independent variables, can accurately represent the displacement of composite plates compared to exact elasticity solutions. Laterally loaded models that do not account for shearing deformation (i.e., Kirchhoff-Love) can be unrealistically stiff. In impact analyses where contact load introduction is essentially a point load, these errors may be severe.

Tan and Sun [12] used a two-dimensional finite element approach to study the impact of a laminated plate by a rod. The plate was modeled using shear flexible plate elements, while the rod was represented using higher order rod elements. Very good agreement with experimental results was reported for both contact force and strains at several locations on the surface of the plate. However, these results were limited to relatively low impact force (i.e., maximum force was approximately 200 Newtons) and four-sides free boundary condition or hung plate condition. Sun and Chen [13] used essentially the same model to conduct a study of the influence of the local indentation law studied by Yang and Sun [14], impactor mass, laminate pre-stress, and impactor velocity on the impact event. Experimental impact tests were not conducted to verify their analysis.

A three-dimensional finite element method modeling each ply of the laminate was developed by Wu and Springer [15]. This model was extended to predict the damage state on a local level. The three

dimensional model incorporated through the thickness effects, but the accuracy of the model was governed by the degree of refinement of the mesh used. If the damage state occurred on a very local level, a high degree of refinement in the mesh was required, and the solution cost increased correspondingly.

Graves and Koontz [16] developed approximate closed-form solutions for orthotropic plates subjected to impact loadings. Experimental impact tests using four-sides simply supported boundary conditions were also conducted to determine threshold values of damage initiation. The analysis was then correlated with the experimental results so that predictions of damage initiation in other laminates could be made. The magnitude of the resultant transverse shear was considered the critical parameter controlling impact damage.

Cairns and Lagace [17] developed the equations of motion of an impacted composite plate using the Rayleigh-Ritz method. Assumed mode shapes were used in the in-plane x and y directions to satisfy both the geometric and force boundary conditions. Some of the experimental data were compared with this type of analysis by Ryan [18] and Wolf [19]; however, comparisons using a relatively heavy impactor mass (i.e., 1.53 kg) did not give good correlations. Typically, analysis predicted longer impact durations, lower peak forces, and smaller deflections.

Similar types of analyses were also performed by Qian and Swanson [20]. They also obtained strain data experimentally and compared with analysis. Although the comparison gave good agreement, the strain data could not be measured at the point of impact and may have resulted in poor correlation with local damage

assessment. Also, the impactor mass used for comparison was relatively small (approximately 0.023 kg).

In general, the predictions for impact using linear plate theory show good agreement with experimental data for limited impact conditions such as using a relatively small impactor mass or using four-sides free boundary conditions. However, there are some difficulties in prediction for cases using relatively large impactor masses (i.e., 1.53 kg) and using some other boundary conditions. These limitations need to be further studied and clarified.

1.3.2 Nonlinear Plate Analysis

The nonlinear transient response of composite plates was considered by Reddy [21] and Chen and Sun [22]. Including transverse shear in a finite element analysis of the large deflection response, Reddy [21] found for undamped laminated plates that the bending-stretching coupling increased the amplitude of the center deflection in a simply supported antisymmetric two-layer cross ply plate under suddenly applied patch loading. Using a method of solution similar to that stated above, Chen and Sun [22] studied the effect of initial stress on the nonlinear transient response of a composite plate. Also, wave propagation in composite plates was discussed by Sun and Shafey [23] using a nonlinear shear-deformable theory. It was found that large deflections have a substantial stiffening effect on the phase velocity.

Recently, several researchers studied nonlinear plate theory with a first or higher-order shear deformation included [24–28]. Among

them, Kant and Mallikarjuna [26] developed a finite element model for nonlinear dynamics of laminated plates to analyze impact response. Although they did not compare the analytical results with experimental data, the numerical results clearly showed that the nonlinear theory predicted smaller deflection compared to linear theory.

1.4 Contributions of this Thesis

In this thesis, the energy equations for both linear and nonlinear plate theories are derived. Lagrangian equations of motion and the Rayleigh-Ritz method are used in conjunction with assumed mode shapes to yield the impacted plate response models. This modeling procedure based on Cairns' work [2] uses assumed mode shapes instead of the finite element method employing shape functions in order to attempt to reduce computational intensity. The results of these models, in particular impact force-time histories during impact, are compared with the existing experimental data obtained by Wolf [19]. The importance of considering the geometrical nonlinear effect of membrane stiffening depending on boundary conditions is discussed for particular impacting events.

1.5 Thesis Outline

Chapter 2 deals with an impact modeling technique using linear laminated plate theory including first-order shear deformation. This is a review chapter from Cairns [2]. In Chapter 3, some of the parametric

studies using the impact model developed in Chapter 2 are presented in order to clarify the source of problem. The parameters to be varied are the number of modes, the time increment for numerical integration, and the local stiffness parameters. Chapter 4 presents a one-dimensional beam version of the impact analysis using geometrical nonlinearity. Chapter 5 which is a highlight of this report deals with impact modeling using nonlinear laminated plate theory with first-order shear deformation. In Chapter 6, results obtained using the nonlinear impact model developed in Chapter 5 are discussed and also compared with existing experimental results. In Chapter 7, the conclusions and recommendations are given.

Chapter 2

Review of Impact Modeling Using Linear Laminated Plate Theory with First-Order Shear Deformation

2.1 Overview

This chapter reviews the impact modeling for the *global* response of composite laminated plates using shear deformable *linear* plate theory as discussed by Cairns [2]. Also, a similar analytical review was done by Tsang [29]. It starts with a linear strain-displacement relations assumption. Energy equations are developed using constitutive equations based on linear strain-displacement relations and laminated plate theory. Using Lagrangian equations of motion and the Rayleigh-Ritz method in conjunction with assumed mode shapes for both x and y directions yields a system of second-order linear ordinary differential equations with respect to time for the plate equations of motion. Also, a

impactor equation of motion can be developed using Newton's second law of motion. These plate and impactor equations of motion are coupled in terms of a Hertzian local contact relation. The coupled differential equations are solved using a numerical integration scheme over time.

2.2 Development of the Equations of Motion

2.2.1 Assumptions

The following assumptions are made to develop a system of equations of motion for both a plate and an impactor.

a) Linear strain-displacement relations and stress-strain relations are assumed.

b) Through-the-thickness strain, ε_{33}, is negligible and, out-of-plane displacement, w, is a function of in-plane coordinates, x and y, only.

c) The plate deforms both in bending and in shear.

d) First-order shear deformation terms are included.

e) The contact force between the impactor and the plate is a point load.

f) Constant material properties are assumed throughout the impact event.

g) No structural damping is considered.

h) Impactor is assumed to be rigid.

i) Local indentation of the plate is accounted for by a nonlinear Hertzian stiffness relation.

A schematic of the laminated plate impact model is shown in Figure 2.1. There will be additional assumptions later to reduce the system of equations.

2.2.2 Linear Laminated Plate Theory with First-Order Shear Deformation

Strain-Displacement Relations

Analogous to the Timoshenko beam theory, the shear deformable plate theory assumes that plane sections originally perpendicular to the midplane of the plate remain plane, but not necessarily perpendicular to the midplane (Figure 2.2).

The displacement field is assumed to be described as,

$$\begin{aligned} u_1(x,y,z) &= u(x,y) + z\psi_x(x,y) \\ u_2(x,y,z) &= v(x,y) + z\psi_y(x,y) \\ u_3(x,y,z) &= w(x,y) \end{aligned} \tag{2.2.1}$$

where (u, v, w) denote displacement components of a point along the (x,y,z) coordinates, and ψ_x and ψ_y denote the rotations of a plane section, originally perpendicular to the midplane, about the y and x axes, respectively.† The linear strain tensor components associated with the displacement fields (2.2.1) are given by,

†Classical plate theory (Kirchhoff plate theory) can be recovered by setting, $\psi_x = -\frac{\partial w}{\partial x}$, $\psi_y = -\frac{\partial w}{\partial y}$.

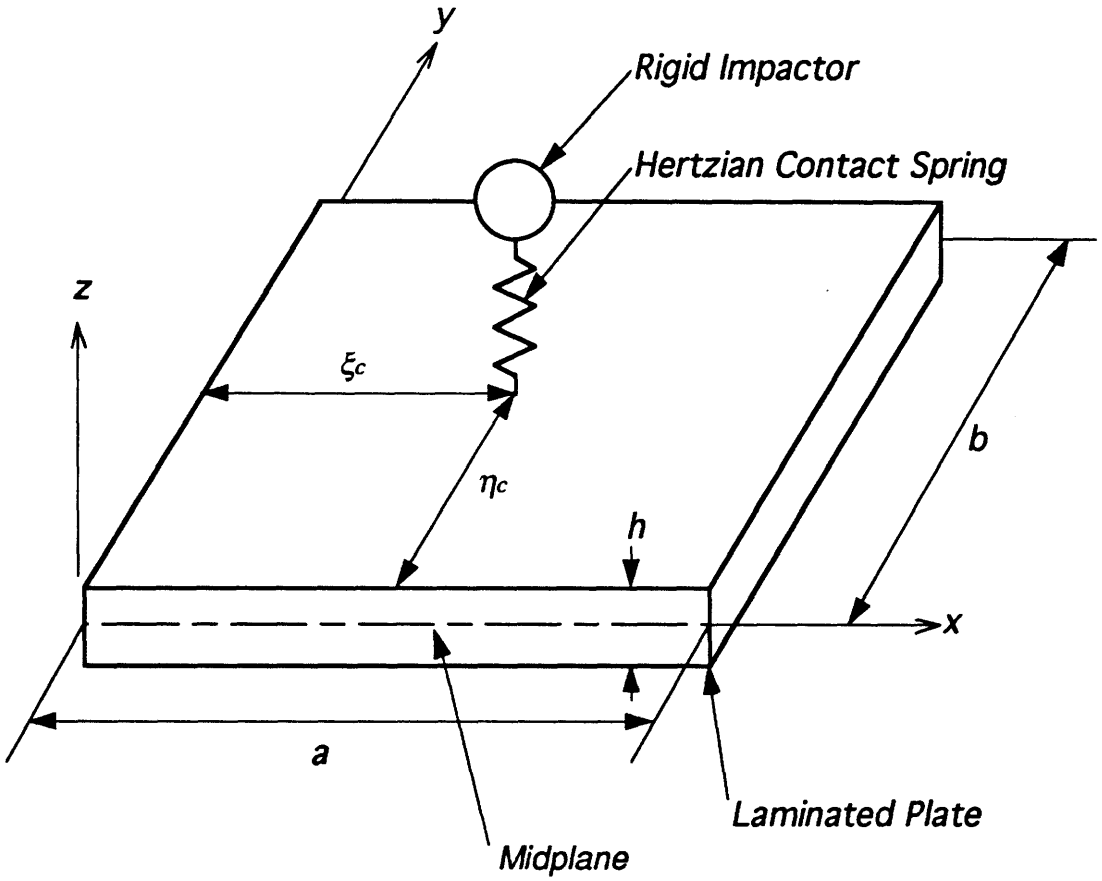

Figure 2.1 : Schematic of Laminated Plate Impact Model

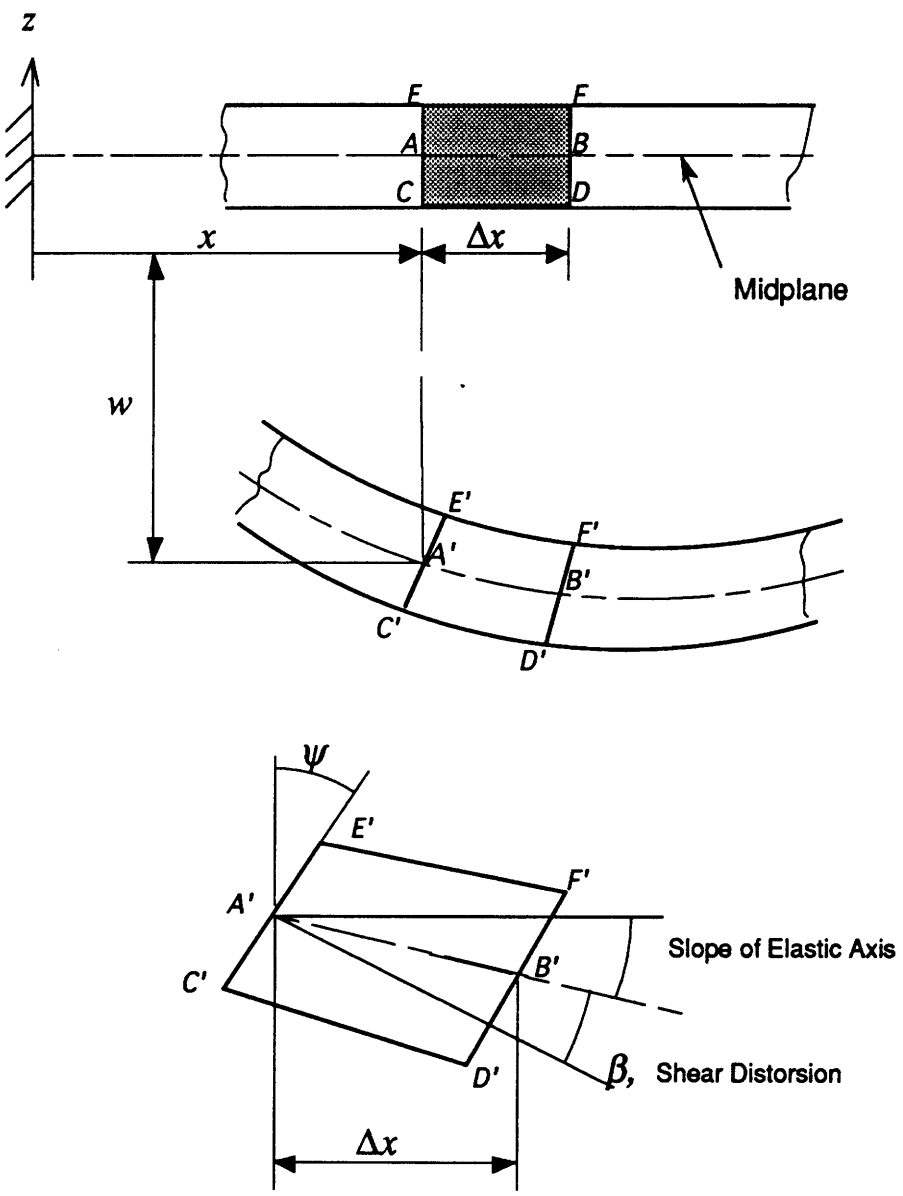

Figure 2.2 : Shear Deformation in a Beam

$$
\begin{aligned}
\varepsilon_{11} &= \frac{\partial u}{\partial x} + z\frac{\partial \psi_x}{\partial x} \\
\varepsilon_{22} &= \frac{\partial v}{\partial y} + z\frac{\partial \psi_y}{\partial y} \\
2\varepsilon_{12} &= \frac{\partial u}{\partial y} + \frac{\partial v}{\partial x} + z\left(\frac{\partial \psi_x}{\partial y} + \frac{\partial \psi_y}{\partial x}\right) \\
2\varepsilon_{13} &= \psi_x + \frac{\partial w}{\partial x} \\
2\varepsilon_{23} &= \psi_y + \frac{\partial w}{\partial y} \\
\varepsilon_{33} &= 0
\end{aligned}
\tag{2.2.2}
$$

Note that the transverse shear strains are non-zero.

Eq. (2.2.2) can be expressed using vector notations.

$$
\underline{\varepsilon} = \begin{Bmatrix} \varepsilon_{11} \\ \varepsilon_{22} \\ 2\varepsilon_{12} \end{Bmatrix}, \qquad \underline{\gamma} = \begin{Bmatrix} 2\varepsilon_{23} \\ 2\varepsilon_{13} \end{Bmatrix} \tag{2.2.3}
$$

By including time, t, as another variable, the strains can be written as,

$$
\begin{aligned}
\underline{\varepsilon}(x,y,z,t) &= \underline{\varepsilon}^{\circ}(x,y,t) + z\,\underline{\kappa}(x,y,t) \\
\underline{\gamma}(x,y,z,t) &= \underline{\gamma}(x,y,t)
\end{aligned}
\tag{2.2.4}
$$

where,

$$
\underline{\varepsilon}^{\circ} = \begin{Bmatrix} \varepsilon^{\circ}_{11} \\ \varepsilon^{\circ}_{22} \\ \varepsilon^{\circ}_{12} \end{Bmatrix} = \begin{Bmatrix} \dfrac{\partial u}{\partial x} \\ \dfrac{\partial v}{\partial y} \\ \dfrac{\partial u}{\partial y} + \dfrac{\partial v}{\partial x} \end{Bmatrix}, \qquad \underline{\kappa} = \begin{Bmatrix} \kappa_{11} \\ \kappa_{22} \\ \kappa_{12} \end{Bmatrix} = \begin{Bmatrix} \dfrac{\partial \psi_x}{\partial x} \\ \dfrac{\partial \psi_y}{\partial y} \\ \dfrac{\partial \psi_x}{\partial y} + \dfrac{\partial \psi_y}{\partial x} \end{Bmatrix} \tag{2.2.5}
$$

Eqs. (2.2.3), (2.2.4), and (2.2.5) represent linear strain-displacement relations including shear deformation.

Constitutive Behavior of the Plate

The basic laminate constitutive equations can be defined as,

$$\begin{Bmatrix}\{N\}\\ \{M\}\end{Bmatrix}=\begin{bmatrix}[A] & [B]\\ [B]^{T} & [D]\end{bmatrix}\begin{Bmatrix}\underline{\varepsilon}^{\circ}\\ \underline{\kappa}\end{Bmatrix}$$
$$\begin{Bmatrix}Q_x\\ Q_y\end{Bmatrix}=\begin{bmatrix}G_{55} & G_{45}\\ G_{45} & G_{44}\end{bmatrix}\begin{Bmatrix}\varepsilon_5\\ \varepsilon_4\end{Bmatrix} \qquad (2.2.6)$$

where $[A]$, $[B]$, and $[D]$ are the in-plane, bending-stretching, and bending stiffnesses of the plate, respectively. Each of the matrix components are given as,

$$\left(A_{ij},\ B_{ij},\ D_{ij}\right)=\sum_{n=1}^{N}\int_{z_n}^{z_{n+1}} C_{ij}^{(n)}\left(1,\ z,\ z^2\right)dz \qquad (i,j=1,2,6) \qquad (2.2.7)$$

where n denotes nth ply and there are total of Nplies. Also, where C_{ij} are assumed to be the plane stress material constants† for this investigation and i, j = 1,2,4,5,6 by letting,

$$\underline{\varepsilon}=\begin{Bmatrix}\varepsilon_{11}\\ \varepsilon_{22}\\ 2\varepsilon_{12}\end{Bmatrix}=\begin{Bmatrix}\varepsilon_1\\ \varepsilon_2\\ \varepsilon_6\end{Bmatrix}, \qquad \underline{\gamma}=\begin{Bmatrix}2\varepsilon_{23}\\ 2\varepsilon_{13}\end{Bmatrix}=\begin{Bmatrix}\varepsilon_4\\ \varepsilon_5\end{Bmatrix} \qquad (2.2.8)$$

† It is assumed that the normal stress in the through-the-thickness direction does not contribute to the strain energy.

The transverse shear stiffness matrix [G] and each of the matrix components are defined as,

$$G_{ij} = \sum_{n=1}^{N} K_i K_j \int_{z_n}^{z_{n+1}} C_{ij}^{(n)}\, dz \qquad (i, j = 4, 5) \qquad (2.2.9)$$

The value of the shearing correction term, $K_i K_j$, used here is the isotropic correction factor of 5/6, shown to be adequate for laminates made from thin plies [11].

By assuming symmetric laminates ($B_{ij} = 0$), in-plane stretching behavior will be decoupled from bending behavior. Since we are interested in out-of-plane behavior only, we can extract only the constitutive bending behavior of the plate from Eq. (2.2.6).

$$\begin{Bmatrix} M_x \\ M_y \\ M_{xy} \end{Bmatrix} = \begin{bmatrix} D_{11} & D_{12} & D_{16} \\ D_{12} & D_{22} & D_{26} \\ D_{16} & D_{26} & D_{66} \end{bmatrix} \begin{Bmatrix} \kappa_{11} \\ \kappa_{22} \\ \kappa_{12} \end{Bmatrix}$$
$$\begin{Bmatrix} Q_x \\ Q_y \end{Bmatrix} = \begin{bmatrix} G_{55} & G_{45} \\ G_{45} & G_{44} \end{bmatrix} \begin{Bmatrix} \varepsilon_5 \\ \varepsilon_4 \end{Bmatrix} \qquad (2.2.10)$$

Potential Energy

The potential energy stored in a body under load can be separated into two different parts:

a) the internal strain energy, defined as the product of strain and stress assuming a linear stress-strain behavior as:

$$U = \frac{1}{2}\iiint_V C_{ij}\varepsilon_i\varepsilon_j \, dV \tag{2.2.11}$$

b) the work done by the external forces:

$$W = \iint_S p_i w_i \, dS \qquad i = 1,2,3 \tag{2.2.12}$$

where p_i denotes external force per unit area and w_i denotes displacement from original position.

The total potential energy is simply the difference of these two terms and a function of the displacements only.

Introducing Eqs. (2.2.3), (2.2.4), (2.2.5), and (2.2.10) into the strain energy equation (2.2.11) and integrating over the thickness, the following expression which is now a function of three displacements variables†, w, ψ_x, ψ_y, is obtained:

$$U = \frac{1}{2}\iint \left(\underline{\kappa}^{\mathrm{T}}[D]\,\underline{\kappa} + \underline{\gamma}^{\mathrm{T}}[G]\,\underline{\gamma} \right) dx\,dy \tag{2.2.13}$$

or this strain energy expression can be separated into two kinds of energy expressions, bending strain energy, U_b, and shearing strain energy, U_s.

† In-plane stretching behavior can be decoupled in this case as mentioned previously.

$$U_b = \frac{1}{2}\int_0^b\int_0^a \underline{\kappa}^{\mathrm{T}}[D]\,\underline{\kappa}\; dx\,dy$$

$$= \frac{1}{2}\int_0^b\int_0^a \begin{Bmatrix} \dfrac{\partial \psi_x}{\partial x} \\ \dfrac{\partial \psi_y}{\partial y} \\ \dfrac{\partial \psi_x}{\partial y} + \dfrac{\partial \psi_y}{\partial x} \end{Bmatrix}^{\mathrm{T}} \begin{bmatrix} D_{11} & D_{12} & D_{16} \\ D_{12} & D_{22} & D_{26} \\ D_{16} & D_{26} & D_{66} \end{bmatrix} \begin{Bmatrix} \dfrac{\partial \psi_x}{\partial x} \\ \dfrac{\partial \psi_y}{\partial y} \\ \dfrac{\partial \psi_x}{\partial y} + \dfrac{\partial \psi_y}{\partial x} \end{Bmatrix} dx\,dy$$

$$= \frac{1}{2}\int_0^b\int_0^a \begin{bmatrix} D_{11}\left(\dfrac{\partial \psi_x}{\partial x}\right)^2 + 2D_{12}\left(\dfrac{\partial \psi_x}{\partial x}\right)\left(\dfrac{\partial \psi_y}{\partial y}\right) + 2D_{16}\left(\left(\dfrac{\partial \psi_x}{\partial x}\right)\left(\dfrac{\partial \psi_x}{\partial y}\right) + \left(\dfrac{\partial \psi_x}{\partial x}\right)\left(\dfrac{\partial \psi_y}{\partial x}\right)\right) \\ +D_{22}\left(\dfrac{\partial \psi_y}{\partial y}\right)^2 + 2D_{26}\left(\left(\dfrac{\partial \psi_x}{\partial y}\right)\left(\dfrac{\partial \psi_y}{\partial y}\right) + \left(\dfrac{\partial \psi_y}{\partial x}\right)\left(\dfrac{\partial \psi_y}{\partial y}\right)\right) \\ +D_{66}\left(\left(\dfrac{\partial \psi_x}{\partial y}\right)^2 + 2\left(\dfrac{\partial \psi_x}{\partial y}\right)\left(\dfrac{\partial \psi_y}{\partial x}\right) + \left(\dfrac{\partial \psi_y}{\partial x}\right)^2\right) \end{bmatrix} dx\,dy$$

(2.2.14)

$$U_s = \frac{1}{2}\int_0^b\int_0^a \underline{\gamma}^{\mathrm{T}}[G]\,\underline{\gamma}\; dx\,dy$$

$$= \frac{1}{2}\int_0^b\int_0^a \begin{Bmatrix} 2\varepsilon_{23} \\ 2\varepsilon_{13} \end{Bmatrix}^{\mathrm{T}} \begin{bmatrix} G_{55} & G_{45} \\ G_{45} & G_{44} \end{bmatrix} \begin{Bmatrix} 2\varepsilon_{23} \\ 2\varepsilon_{13} \end{Bmatrix} dx\,dy$$

$$= \frac{1}{2}\int_0^b\int_0^a \begin{bmatrix} G_{55}\left((\psi_x)^2 + 2\psi_x\dfrac{\partial w}{\partial x} + \left(\dfrac{\partial w}{\partial x}\right)^2\right) \\ +2G_{45}\left(\psi_x\psi_y + \psi_x\dfrac{\partial w}{\partial y} + \psi_y\dfrac{\partial w}{\partial x} + \dfrac{\partial w}{\partial x}\dfrac{\partial w}{\partial y}\right) \\ +G_{44}\left((\psi_y)^2 + 2\psi_y\dfrac{\partial w}{\partial y} + \left(\dfrac{\partial w}{\partial y}\right)^2\right) \end{bmatrix} dx\,dy \qquad (2.2.15)$$

Kinetic Energy

The kinetic energy, T, of the plate is given by,

$$T(u,v,w,\psi_x\psi_y)=\frac{1}{2}\iiint_V \rho\left[\dot{u}_1^2+\dot{u}_2^2+\dot{u}_3^2\right]dV \tag{2.2.16}$$

where u_1, u_2, u_3 denote displacements in x, y, z directions respectively and $(\dot{\cdot})$ denotes differentiation with respect to time. Substituting Eq. (2.2.1) into Eq. (2.2.16) and integrating over the thickness yields,

$$\begin{aligned} &T(u,v,w,\psi_x,\psi_y) \\ &=\frac{1}{2}\int_0^b\int_0^a \begin{Bmatrix}\dot{\psi}_x\\ \dot{\psi}_y\\ \dot{u}\\ \dot{v}\\ \dot{w}\end{Bmatrix}^{\mathrm{T}} \begin{bmatrix} I_2 & 0 & 0 & 0 & 0\\ 0 & I_2 & 0 & 0 & 0\\ 0 & 0 & I_1 & 0 & 0\\ 0 & 0 & 0 & I_1 & 0\\ 0 & 0 & 0 & 0 & I_1\end{bmatrix} \begin{Bmatrix}\dot{\psi}_x\\ \dot{\psi}_y\\ \dot{u}\\ \dot{v}\\ \dot{w}\end{Bmatrix} dx\,dy \end{aligned} \tag{2.2.17}$$

where

$$(I_1,\ I_2)=\int_{-h/2}^{h/2}(1,\ z^2)\rho\,dz \tag{2.2.18}$$

Since in-plane displacements u and v can be decoupled here again, Eq. (2.2.17) is reduced to a function of three variables.

$$\begin{aligned} &T(w,\psi_x,\psi_y) \\ &=\frac{1}{2}\int_0^b\int_0^a \begin{Bmatrix}\dot{\psi}_x\\ \dot{\psi}_y\\ \dot{w}\end{Bmatrix}^{\mathrm{T}} \begin{bmatrix} I_2 & 0 & 0\\ 0 & I_2 & 0\\ 0 & 0 & I_1\end{bmatrix} \begin{Bmatrix}\dot{\psi}_x\\ \dot{\psi}_y\\ \dot{w}\end{Bmatrix} dx\,dy \end{aligned} \tag{2.2.19}$$

Using these energy expressions, the differential equations of equilibrium of composite laminated plates can be derived for either the

static or the dynamic case. For static analysis, there is no need to consider the kinetic energy term and time variable; hence, the principle of minimum total potential energy can be used to obtain differential equations of equilibrium.† For the dynamic case, Hamilton's principle can be employed to obtain the differential equations or so-called equations of motion. In this investigation, Lagrangian equations of motion which can be obtained using the Hamilton's principle to extract the equations of motion at a *given point* †† are used.

2.2.3 Plate Equations of Motion

Plate equations of motion are obtained by applying Lagrangian equations of motion and the Rayleigh-Ritz method in conjunction with assumed mode shapes to the energy equations obtained in the previous section.

Assumed Mode Shapes

For spatial discretization of the displacements as functions of x and y , let,

$$\psi_x(x,y,t) = \sum_r \sum_s A_{rs}(t)\, f_r(x)\, g_s(y)$$

$$\psi_y(x,y,t) = \sum_r \sum_s B_{rs}(t)\, h_r(x)\, l_s(y) \qquad (2.2.20)$$

$$w(x,y,t) = \sum_r \sum_s C_{rs}(t)\, m_r(x)\, n_s(y)$$

---

† The principle of minimum total potential energy is defined as $\delta\Pi \equiv \delta U + \delta K = 0$.
†† In this investigation, the impacted point is assumed at the center of the plate .

Cairns [2] rewrote Eq. (2.2.20) using single summation instead of double summation as follows.

$$\begin{aligned} \psi_x(x,y,t) &= \sum_i A_i(t)\, f_r(x)\, g_s(y) \\ \psi_y(x,y,t) &= \sum_i B_i(t)\, h_r(x)\, l_s(y) \\ w(x,y,t) &= \sum_i C_i(t)\, m_r(x)\, n_s(y) \end{aligned} \tag{2.2.21}$$

where,

$$\begin{aligned} f_r(\xi) &= \frac{d}{d\xi}[m_r(\xi)] \\ h_r(\xi) &= m_r(\xi) \\ g_s(\eta) &= n_s(\eta) \\ l_r(\eta) &= \frac{d}{d\eta}[n_r(\eta)] \end{aligned} \tag{2.2.22}$$

where, $\xi = \frac{x}{a}, \qquad \eta = \frac{y}{b}$

and $A_i(t)$, $B_i(t)$, and $C_i(t)$ are modal amplitudes to be determined from the analysis. The functions shown in Eq. (2.2.22) for the planar rotations are derivatives in the lateral displacement. The choice of these functions is appropriate since, in the limit as the plate thickness approaches zero, the slope of the lateral displacement can approach the planar rotations which result in the recovery of classical plate theory or Kirchhoff plate theory. This precludes some of the well known shear locking problems associated with other types of discretization methods [40]. Note that index numbers, i, r, and s, are related by some organized scheme as shown in Table 2.1.

Beam shape functions $m_r(x)$ and $n_s(y)$ represent mode shapes in the x and y directions respectively, and in this analysis, Generalized Beam Functions (GBFs) studied by Dugundji [30] are employed.†

Lagrangian Equations of Motion

Lagrangian function, L, is defined to be,

$$L = T - U \tag{2.2.23}$$

Then, the Lagrangian equations of motion [31] can be expressed as,

$$\frac{d}{dt}\left(\frac{\partial L}{\partial \dot{q}_j}\right) - \frac{\partial L}{\partial q_j} = Q_j \qquad j = 1, 2, \ldots, M \tag{2.2.24}$$

where M denotes the number of degrees of freedom, and q_j denote the generalized coordinates. In this analysis, q_j are A_i, B_i, C_i, and the number of degrees of freedom would be $j = 3\times i = 3\times r\times s$. Since the kinetic energy is a function of only $\dot{q}_j$ and the potential energy is a function of only q_j, Eq. (2.2.24) can be expanded to the following forms.

$$\begin{aligned}
\frac{d}{dt}\left(\frac{\partial T}{\partial \dot{A}_i}\right) + \frac{\partial U}{\partial A_i} &= P_{ai} \\
\frac{d}{dt}\left(\frac{\partial T}{\partial \dot{B}_i}\right) + \frac{\partial U}{\partial B_i} &= P_{bi} \\
\frac{d}{dt}\left(\frac{\partial T}{\partial \dot{C}_i}\right) + \frac{\partial U}{\partial C_i} &= P_{ci}
\end{aligned} \tag{2.2.25}$$

where P_{ai}, P_{bi}, P_{ci} indicate the work done by the external forces.

† See Appendix A for more detail in Generalized Beam Functions.

Table 2.1: Index Numbering System for Beam Functions

Example Case (taken from Tsang [29]):

There are three modes for each x and y direction.

r (x - direction)	s (y - direction)	i
1	1	1
1	2	2
1	3	3
2	1	4
2	2	5
2	3	6
3	1	7
3	2	8
3	3	9

Substituting Eq. (2.2.21) into Eqs. (2.2.14), (2.2.15), (2.2.19), and (2.2.12), then, into Eq. (2.2.25) yields the following system of equations,

$$\begin{bmatrix} \underline{I}_x & \underline{0} & \underline{0} \\ \underline{0} & \underline{I}_y & \underline{0} \\ \underline{0} & \underline{0} & \underline{m} \end{bmatrix} \begin{Bmatrix} \ddot{\underline{A}}_i \\ \ddot{\underline{B}}_i \\ \ddot{\underline{C}}_i \end{Bmatrix} + \begin{bmatrix} \underline{K}_{aa} & \underline{K}_{ab} & \underline{K}_{ac} \\ \underline{K}_{ab}{}^{\mathrm{T}} & \underline{K}_{bb} & \underline{K}_{bc} \\ \underline{K}_{ac}{}^{\mathrm{T}} & \underline{K}_{bc}{}^{\mathrm{T}} & \underline{K}_{cc} \end{bmatrix} \begin{Bmatrix} \underline{A}_i \\ \underline{B}_i \\ \underline{C}_i \end{Bmatrix} = -F \begin{Bmatrix} \underline{R}_{ai} \\ \underline{R}_{bi} \\ \underline{R}_{ci} \end{Bmatrix} \tag{2.2.26}$$

Each element of the inertia matrix, the stiffness matrix, and the generalized force vector is given as follows.

Inertia Matrix:

$$\begin{aligned} \underline{I}_x(i,j) &= I_2 \int_0^b \int_0^a (f_i g_i)(f_j g_j)\, dx\, dy \\ \underline{I}_y(i,j) &= I_2 \int_0^b \int_0^a (h_i l_i)(h_j l_j)\, dx\, dy \\ \underline{m}(i,j) &= I_1 \int_0^b \int_0^a (m_i n_i)(m_j n_j)\, dx\, dy \end{aligned} \tag{2.2.27}$$

where I_1, I_2 are defined in Eq. (2.2.18) and $f_i, g_i, h_i, l_i, m_i, n_i$ are the modal functions (or eigenfunctions) of the beam due to the boundary conditions as defined in Appendix A and also Eq. (2.2.22).

Stiffness Matrix:

$$\underline{K}_{aa}(i,j) = \int_0^b \int_0^a \begin{bmatrix} D_{11}(f_i'' g_i)(f_j'' g_j) + D_{16}(f_i'' g_i)(f_j g_j') \\ + D_{16}(f_i g_i')(f_j'' g_j) + D_{66}(f_i g_i')(f_j g_j') \\ + G_{55}(f_i g_i)(f_j g_j) \end{bmatrix} dx\, dy \tag{2.2.28a}$$

$$\underline{K}_{ab}(i,j)=\int_0^b\int_0^a\begin{bmatrix}D_{12}(f_i'g_i)(h_jl_j')+D_{16}(f_i'g_i)(h_j'l_j)\\+D_{26}(f_ig_i')(h_jl_j')+D_{66}(f_ig_i')(h_j'l_j)\\+G_{45}(f_ig_i)(h_jl_j)\end{bmatrix}dx\,dy \tag{2.2.28b}$$

$$\underline{K}_{ac}(i,j)=\int_0^b\int_0^a\left[G_{45}(f_ig_i)(m_jn_j')+G_{55}(f_ig_i)(m_j'n_j)\right]dx\,dy \tag{2.2.28c}$$

$$\underline{K}_{bb}(i,j)=\int_0^b\int_0^a\begin{bmatrix}D_{22}(h_il_i')(h_jl_j')+D_{26}(h_il_i')(h_j'l_j)\\+D_{26}(h_i'l_i)(h_jl_j')+D_{66}(h_i'l_i)(h_j'l_j)\\+G_{44}(h_il_i)(h_jl_j)\end{bmatrix}dx\,dy \tag{2.2.28d}$$

$$\underline{K}_{bc}(i,j)=\int_0^b\int_0^a\left[G_{45}(h_il_i)(m_j'n_j)+G_{44}(h_il_i)(m_jn_j')\right]dx\,dy \tag{2.2.28e}$$

$$\underline{K}_{cc}(i,j)=\int_0^b\int_0^a\begin{bmatrix}G_{44}(m_in_i')(m_jn_j')+G_{45}(m_in_i')(m_j'n_j)\\+G_{45}(m_i'n_i)(m_jn_j')+G_{55}(m_i'n_i)(m_j'n_j)\end{bmatrix}dx\,dy \tag{2.2.28f}$$

Generalized Force Vector:†

$$\begin{Bmatrix}\underline{R}_{ai}\\\underline{R}_{bi}\\\underline{R}_{ci}\end{Bmatrix}=\begin{Bmatrix}\underline{0}\\\underline{0}\\m_i(\xi_c)n_i(\eta_c)\end{Bmatrix} \tag{2.2.29}$$

where (ξ_c, η_c) are the normalized coordinates of the point of impact as shown in Figure 2.1.

† In this impact modeling, a *transverse* impact is assumed.

The plate equations of motion (2.2.26) are simplified by statically condensing out the rotary inertia terms. The rotary inertia is the inertia associated with the planar rotations and contributes to the formation of shearing waves in the laminates, whereas the lateral inertia governs the formation of bending waves in the laminate. Tan and Sun [12] have argued that for the geometries of interest, the rotary inertia terms are small and may be neglected. As discussed by Cairns and Lagace [17], an examination of the relative amplitudes of the inertia matrix as defined in Eq. (2.2.18) shows that the relative amplitude of the inertia matrices (rotary/lateral) is $h^2/12$. For a practical laminate thickness on the order of 1 to 10 mm, this ratio is on the order of 10^{-7} to 10^{-5}. Since the terms populating the matrices are greater in the shearing stiffness matrices than the bending stiffness matrices, this huge difference in inertia illustrates that the frequency arising from the rotary inertia is much higher than that of the lateral displacement. Consequently, static condensation of the plate equations of motion (2.2.26), neglecting the rotary inertia terms, while retaining the influence of shearing deformation, results in,

$$\underline{m}\ddot{\underline{C}}_i + \underline{K}\underline{C}_i = -F\underline{R}_{ci} \tag{2.2.30}$$

where,

$$\underline{K} = \underline{K}_{cc} - \begin{bmatrix} \underline{K}_{ac}^{\mathrm{T}} & \underline{K}_{bc}^{\mathrm{T}} \end{bmatrix} \begin{bmatrix} \underline{K}_{aa} & \underline{K}_{ab} \\ \underline{K}_{ab}^{\mathrm{T}} & \underline{K}_{bb} \end{bmatrix}^{-1} \begin{bmatrix} \underline{K}_{ac} \\ \underline{K}_{bc} \end{bmatrix} \tag{2.2.31}$$

is the condensed stiffness matrix neglecting rotary inertia.†

† By using the beam functions for free-free boundary conditions, the inversed term in Eq. (2.2.31) becomes singular. Rearranging the matrix is required before inversion. Some details are discussed in Section 5.3.1.

2.2.4 System of Equations of Motion

The system of equations of motion including the impactor equation of motion is now constructed. The impactor is assumed as a point mass whose equation of motion can be drawn from Newton's second law of motion as,

$$m_I \ddot{u}_I = -F \tag{2.2.32}$$

where m_I is the mass of the impactor, u is the displacement of the impactor, and F is the impact force. Eqs. (2.2.30) and (2.2.32) can be combined to give,

$$\underline{M}\ddot{\underline{q}} + \underline{K}^* \underline{q} = -F\underline{R} \tag{2.2.33}$$

where,

$$\underline{M} = \begin{bmatrix} \underline{m} & \underline{0} \\ \underline{0} & m_I \end{bmatrix}, \qquad \underline{K}^* = \begin{bmatrix} \underline{K} & \underline{0} \\ \underline{0} & \underline{0} \end{bmatrix}, \qquad \underline{R} = \begin{Bmatrix} \underline{R}_{ci} \\ 1 \end{Bmatrix} \tag{2.2.34}$$

and the generalized coordinates are now,

$$\ddot{\underline{q}} = \begin{Bmatrix} \ddot{\underline{C}}_i \\ \ddot{u}_I \end{Bmatrix}, \qquad \underline{q} = \begin{Bmatrix} \underline{C}_i \\ u_I \end{Bmatrix} \tag{2.2.35}$$

The plate displacement and the impactor displacement are assumed to be coupled together by the Hertzian contact law† which assumes a nonlinear local contact spring [14]. Rigid impactor contact is illustrated in Figure 2.3. The constitutive equation for the Hertzian stiffness relation can be written as,

---

† This analytical contact law model [41] is summarized in Appendix B for the case of isotropic material.

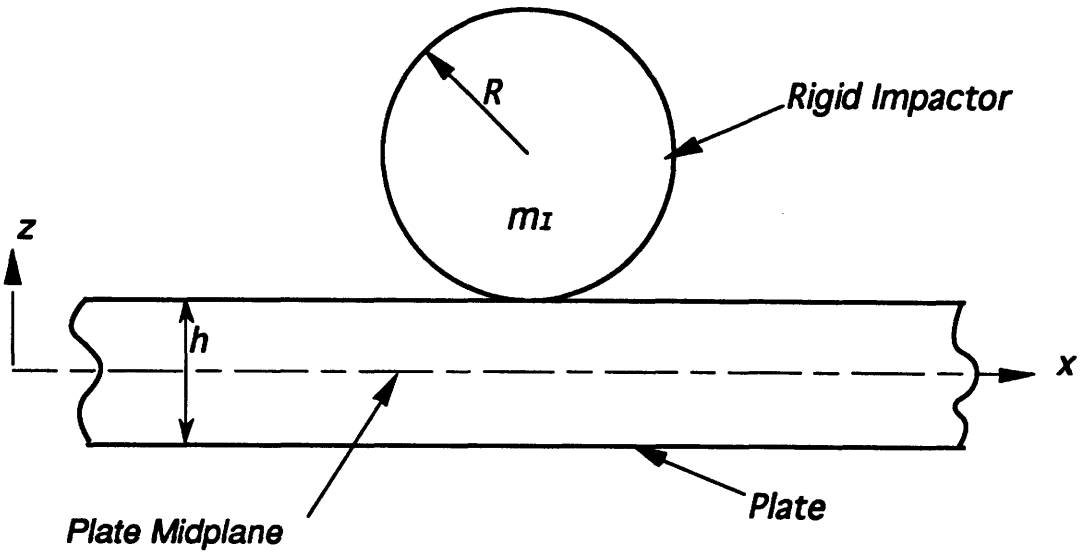

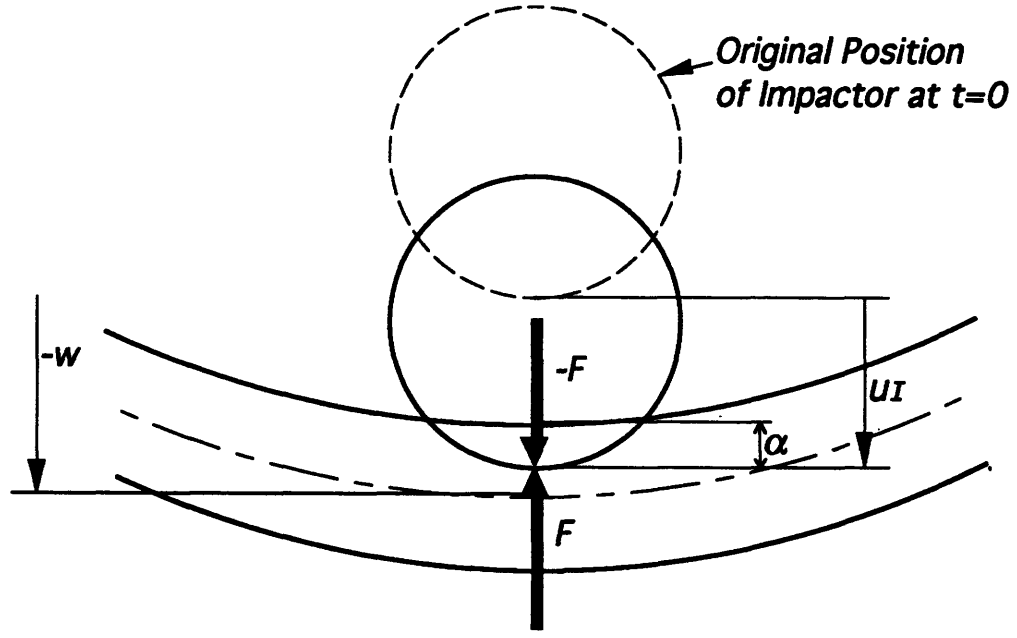

Figure 2.3 : Rigid Impactor in Contact with Flexible Plate

$$F = k\alpha^n \tag{2.2.36}$$

where k is the local contact stiffness of the plate and n is the exponent value controlling the stiffening property of the contact spring. The indentation of the plate is modeled as,†

$$\alpha = u_I + w = \underline{R}^{\mathrm{T}} \underline{q} \tag{2.2.37}$$

The system of equations of motion are expressed in terms of Eqs. (2.2.33), (2.2.36), and (2.2.37). In the next section, the solution method is discussed.

2.3 Solution Method

Eqs. (2.2.33), (2.2.36), and (2.2.37) are solved together to produce $\underline{q}$ and F as functions of time. The initial conditions for this particular analysis are,

$$\underline{q}_{t=0} = \begin{Bmatrix} \underline{0} \\ 0 \end{Bmatrix}, \qquad \dot{\underline{q}}_{t=0} = \begin{Bmatrix} \underline{0} \\ \dot{u}_0 \end{Bmatrix}, \qquad \ddot{\underline{q}}_{t=0} = \begin{Bmatrix} \underline{0} \\ 0 \end{Bmatrix} \tag{2.3.1}$$

where $\dot{u}_0$ indicates the initial impactor velocity.

Following Cairns' formulation [2], the Newmark constant-average-acceleration integration technique or Newmark (beta=1/4) method [32] is employed to solve the coupled second-order ordinary differential equations (2.2.33), and Eqs. (2.2.36) and (2.2.37). Eq. (2.2.33) can be rewritten as,

† The coordinate system for the impactor motion uses the opposite direction of the z-coordinate difined for the plate motion.

$$\underline{M}\ddot{\underline{q}}^{(j+1)} + \underline{K}^{*}\underline{q}^{(j+1)} = -F^{(j+1)}\underline{R} \tag{2.3.2}$$

where the superscript $(j+1)$ represents the $(j+1)$th integration time step. The Newmark integration method assumes the generalized velocity and displacement can be written as,

$$\begin{aligned}
\dot{\underline{q}}^{(j+1)} &= \dot{\underline{q}}^{(j)} + \frac{\Delta t}{2}\left[\ddot{\underline{q}}^{(j+1)} + \ddot{\underline{q}}^{(j)}\right] \\
\underline{q}^{(j+1)} &= \underline{q}^{(j)} + \frac{\Delta t}{2}\left[\dot{\underline{q}}^{(j+1)} + \dot{\underline{q}}^{(j)}\right]
\end{aligned} \tag{2.3.3}$$

where Δt is the integration time increment. Rearranging Eq. (2.3.3) gives,

$$\begin{aligned}
\ddot{\underline{q}}^{(j+1)} &= \frac{4}{\Delta t^2}\left[\underline{q}^{(j+1)} - \underline{q}^{(j)} - \Delta t\,\dot{\underline{q}}^{(j)}\right] - \ddot{\underline{q}}^{(j)} \\
\dot{\underline{q}}^{(j+1)} &= \frac{\Delta t}{2}\left[\underline{q}^{(j+1)} - \underline{q}^{(j)}\right] - \dot{\underline{q}}^{(j)}
\end{aligned} \tag{2.3.4}$$

Substituting Eq. (2.3.4) into Eq. (2.3.2) and rearranging gives,

$$\underline{q}^{(j+1)} = \left(\frac{4}{\Delta t^2}\underline{M} + \underline{K}^{*}\right)^{-1}\left\{-F^{(j+1)}\underline{R} + \underline{M}\left[\frac{4}{\Delta t^2}\underline{q}^{(j)} + \frac{4}{\Delta t}\dot{\underline{q}}^{(j)} + \ddot{\underline{q}}^{(j)}\right]\right\} \tag{2.3.5}$$

There is another relationship given by Eqs. (2.2.36) and (2.2.37). This can be written as,

$$F^{(j+1)} = k\left[\underline{R}^{\mathrm{T}}\underline{q}^{(j+1)}\right]^{n} \tag{2.3.6}$$

Eqs. (2.3.5) and (2.3.6) can give the values of $\underline{q}^{(j+1)}$, $F^{(j+1)}$; however, for $n \neq 1$, those coupled equations require a numerical root finding technique. Tsang [29] used the Newton-Raphson method to evaluate $\underline{q}^{(j+1)}$, $F^{(j+1)}$. Once those values are determined, the next time

integration can be performed using the determined values as previous step values.

2.4 Numerical Example

The developed global plate response model due to impact in Section 2.2 and its solution method in Section 2.3 were implemented in a FORTRAN program by Tsang [29] called "*GLOBAL*". Initially, this code was used to analyze some of the impact cases in this investigation; however, it took more than 10 hours of CPU time to produce the output, such as force-time history during the impact, on a Macintosh IIfx. The required CPU time is strongly dependent on the number of modes used as input as well as the number of time steps. For a 7x7 mode case, it may take less than a half hour of CPU time, but for a 17x17 mode case, it may take more than 15 hours of CPU time on the same machine. In this investigation, *GLOBAL* was installed on MIT's CRAY X-MP EA/464 supercomputer to improve the computational efficiency.

In the following numerical example, an impact problem for a 252 mm by 89 mm AS4/3501-6 graphite/epoxy plate in a $[\pm 45_2/0_2]_S$ configuration was analyzed.

Example Problem

The input data are summarized in Table 2.2. Note that the values of local contact stiffness are approximated values taken from Ryan's experimental work [18]. This case took about 4.5 minutes of CPU time

Table 2.2 : Inputs for *GLOBAL* Analysis – Example Problem

Laminate Material System :	AS4/3501-6 Graphite/Epoxy
Lay-up :	$[\pm 45_2/0_2]_S$
x-direction Boundary Condition :	Clamped-Clamped
y-direction Boundary Condition :	Free-Free
Plate Length (x-direction) :	252 mm
Plate Width (y-direction) :	89 mm
Plate Thickness :	1.608 mm
Plate Density :	1540 kg/m^3
D_{1111} :	17.072 N-m
D_{1122} :	11.272 N-m
D_{1112} :	2.560 N-m
D_{2222} :	15.365 N-m
D_{2212} :	2.560 N-m
D_{1212} :	12.325 N-m
A_{44} :	6.92 MN/m
A_{45} :	0.00 MN/m
A_{55} :	8.06 MN/m
Shear Correction Factor :	0.833
Impactor Mass :	1.53 kg
Impactor Velocity :	3.0 m/s
Local Contact Stiffness :	0.5 GN/m$^{1.5}$
Local Contact Exponent Value :	1.5
Number of Modes in x-direction :	17
Number of Modes in y-direction :	17
Time Step Increment :	5.0 μs
Number of Time Steps :	7,000 time steps

on the Cray X-MP EA/464. As results, force-time history (Figure 2.4) and displacement-time history at the center of the plate (Figure 2.5) are presented. The signatures of both plots are typical as previously reported by Ryan [18] for relatively high impactor mass and low impactor velocity. The force-time history contains many high frequency waves, although the overall trend of the plot is almost a sinusoidal curve. The displacement-time history shows a relatively smooth sinusoidal curve.

These analytical results are compared with experimental results obtained by Wolf [19]. In Figure 2.6, the experimental force-time history during the impact event occurring under the same impacting condition as analysis is over-plotted on the analytical force-time history which is the same as shown in Figure 2.5. Notice that analysis predicts approximately 45% less in peak force than the experiment. Also, the impact duration predicted by analysis is approximately 2.7 times longer than the impact duration observed by experiment.

Experimental displacement-time history was calculated from the experimental force-time history by means of numerical integration. The force-time history devided by the impactor mass gives the approximation of acceleration-time history at the point of impact. Then, integrating the acceleration-time history twice gives the displacement-time history. Although this method gives only an approximated quantity of displacement since we don't include the effective plate mass during the impact, this gives a good correlation as shown by Williamson [33]. In Figure 2.7, this experimental displacement-time history at the center of the plate is compared with the analytical prediction shown in Figure 2.5.

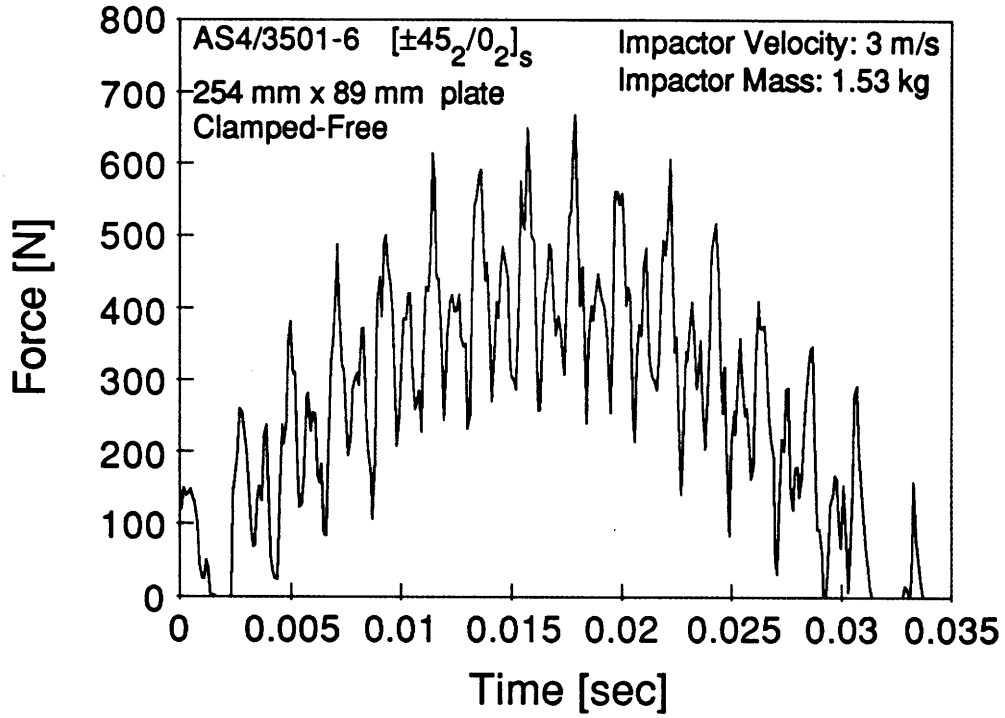

Figure 2.4 : Impact Analysis using Linear Theory : Force-Time History at the Point of Impact for the Example Problem (Input Data are shown in Table 2.2)

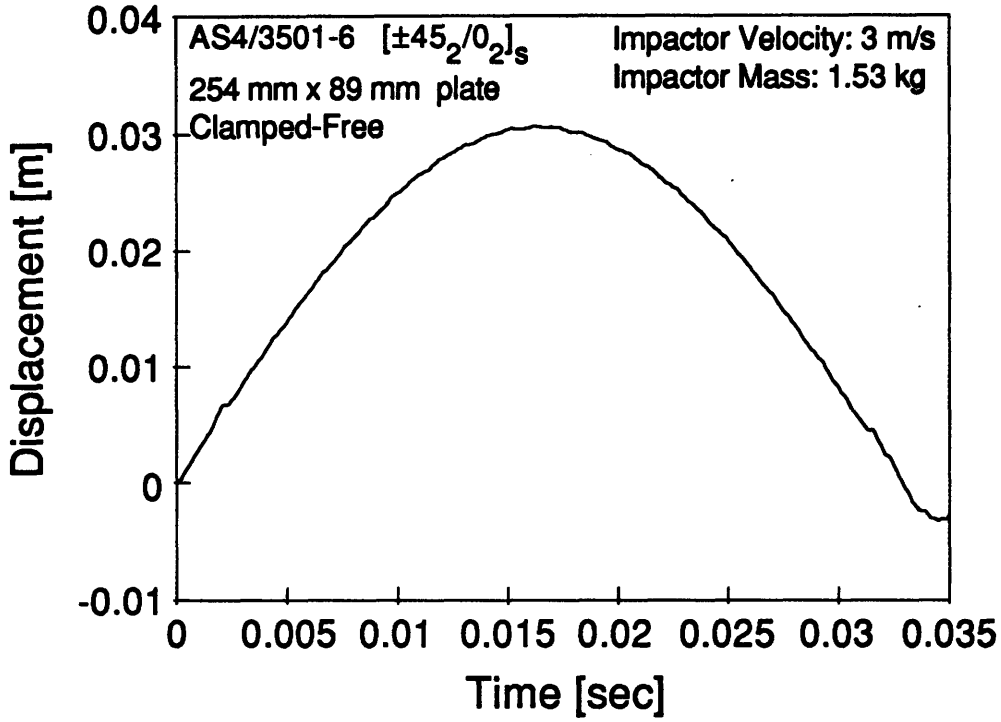

Figure 2.5 : Impact Analysis using Linear Theory : Displacement-Time History at the Point of Impact for the Example Problem (Input Data are shown in Table 2.2)

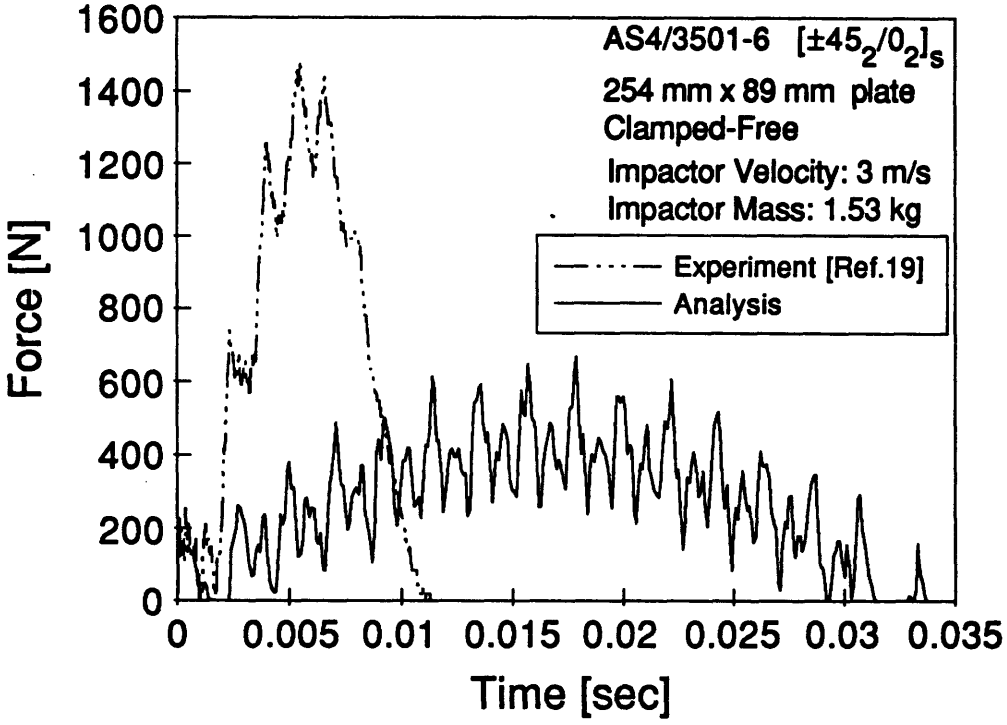

Figure 2.6 : Comparison of Experiment and Analysis : Force-Time History at the Point of Impact for the Example Problem Condition

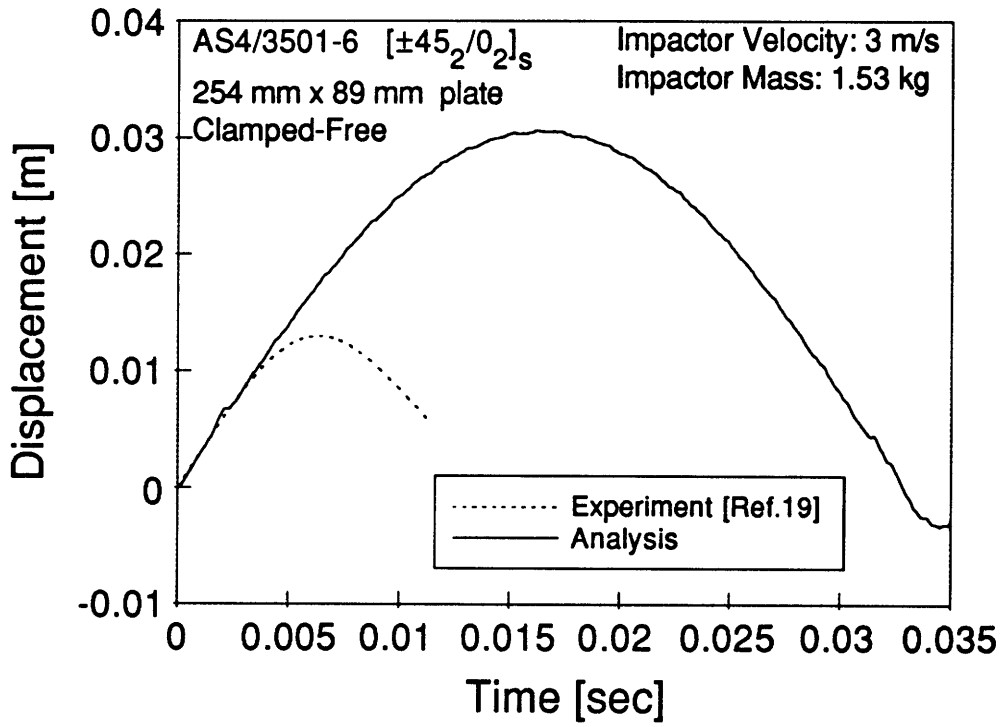

Figure 2.7 : Comparison of Experiment and Analysis : Displacement-Time History at the Point of Impact for the Example Problem Condition

Again, it is observed that there is a large difference between these results. The analysis predicts the maximum displacement approximately 2.4 times larger than the experiment shows. The impact duration predicted by analysis is approximately 2.7 times longer than the impact duration observed by experiment.

For the given example problem case, the analysis does not give predictions which are sufficiently close to the experimental results, and therefore, some refinement or redevelopment in the analysis method is necessary.

2.5 Summary

In this chapter, the impact modeling using linear laminated plate theory with first-order shear deformation was reviewed. The system of equations of motion for both the laminated plate and the impactor was derived and the solution method was also given. As a numerical example, one problem was solved using the impact analysis developed in this chapter and compared with the existing experimental results. However, for the given example problem case, the analysis did not give the predictions which are sufficiently close to the experimental results in terms of force-time and displacement-time histories, and therefore, some refinement or redevelopment in the analysis method is necessary.

In the next two chapters, the source of the problem in the existing linear analysis is described.

Chapter 3

Parametric Studies for Impact Analysis of Linear Laminated Plate Model

3.1 Overview

This chapter describes an initial attempt to address the source of the problem in the analytical method developed in Chapter 2. Some of the input parameters of the analysis are varied to observe their influences on the results of the analysis. The result of interest is the force-time history during the impact event.

The first study is a convergence study. Two parameters, the time increment used for the numerical integration and the number of modes, which control the convergence of the analysis, are varied to check the convergence of the solution. In the example problem of section 2.4 and Ryan's work [18], 17x17 modes were chosen; however, there was no check for convergence done and in fact, Qian and Swanson [34] used a

similar analysis technique and claim that it may require more than 50x50 modes depending on the nature of the impact. The second study is a sensitivity study for the local parameters, Hertzian stiffness constant, k, and local nonlinearity exponent, n. The sensitivity of the force-time history is studied by varying these local parameters. Lastly, there is a discussion of boundary conditions for both the experimental apparatus used by Wolf [19] and the analysis. This issue of the boundary conditions serves as a bridge to Chapter 4.

3.2 Convergence Study

In this section, convergence of the solution for the impact analysis of the linear laminated plate model developed in Chapter 2 is investigated. This provides information on the number of modes and time increment needed for the analysis. The example problem described in Section 2.4 is used for this investigation.

3.2.1 Time Increment

The example problem considered in Section 2.4 is used with the time increment varied with a range of 1–20 μsec. Each maximum force is compared in Figure 3.1. As can be seen, as the time increment becomes smaller, the maximum force increases slightly and becomes relatively stable, which is assumed to be a convergence criteria, in the region of 1–5 μsec. This kind of stability dependent on the time increment is typical and a similar phenomena is presented by Qian and Swanson [34]. Consequently, 5 μsec of time increment appears to

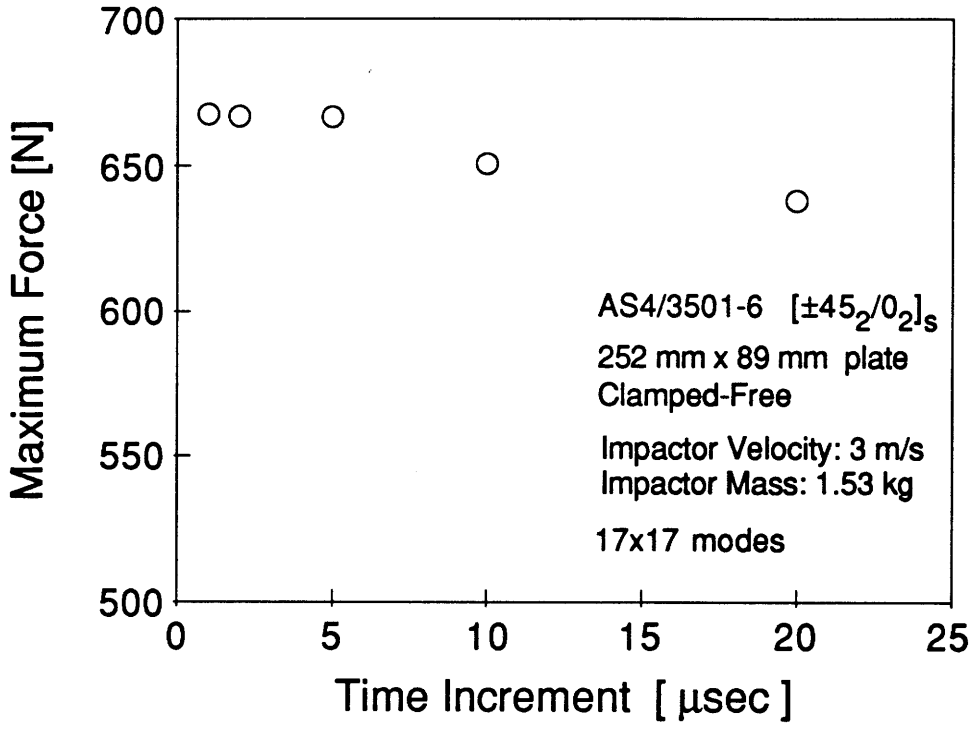

Figure 3.1 : Results of Convergence Study – Time Increment versus Maximum Force

be sufficient for this particular case of impact analysis. However, it is important to remember that the time increment is dependent on the impacting conditions, such as impactor mass, plate geometry, boundary condition, etc. In fact, for smaller impactor mass, 0.008537 kg, a time increment of 0.1–0.2 μsec would be necessary for a converged solution [34].

3.2.2 Number of Modes

A parametric study was performed by varying the number of modes while maintaining a constant time increment of 5 μsec. Again, the maximum force output was used to judge the convergence. The same number of modes in both the x and y directions were assumed in this study with a range of 7x7 to 35x35 modes used as input data of the analysis. As can be seen in Figure 3.2, there is a stable region of maximum force for more than 25x25 to 30x30 modes. As for the time increment, the required number of modes also depends on the impact conditions. For the case investigated by Qian and Swanson [34], more than 50x50 modes may be necessary to provide convergence of the peak contact force.

As a result of this convergence study, the time increment and the number of modes required to obtain the converged force-time history in terms of the maximum force output were captured. However, this convergence study for this example case is essentially a "fine tuning" of the force-time history output. Obviously, varying the time increment and number of modes does not give a force-time history close to the one

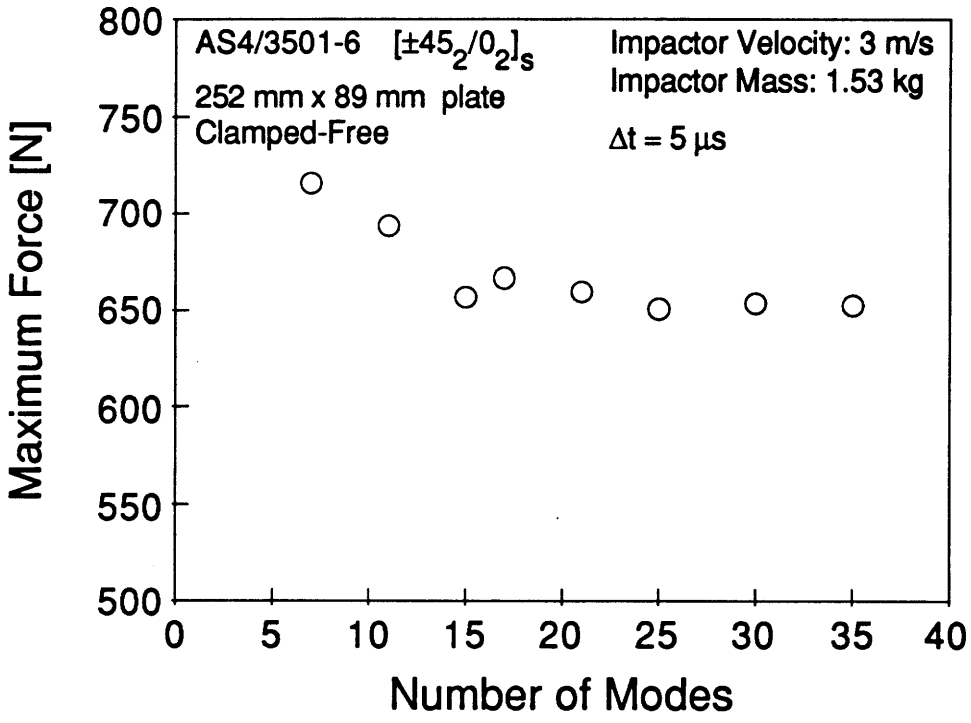

Figure 3.2 : Results of Convergence Study –
Number of Modes versus Maximum Force

observed experimentally as shown in Figure 2.6. After the "fine tuning" of the analysis using 5 μsec of time increment and 25x25 modes, the maximum force output is approximately 656 N which is still half of the peak force observed by experiment.

3.3 Sensitivity Study for Local Parameters

In this section, the sensitivity of the force-time history in terms of the maximum contact force and impact duration due to the change in local parameters, Hertzian stiffness constant and local nonlinearity exponent value are discussed.

As described in Section 2.2 and Eq. 2.2.37, the impact analysis employs a Hertzian contact law which assumes a nonlinear local contact spring.† The constitutive equation for the Hertzian stiffness relation can be written as,

$$F = k\alpha^n \tag{3.3.1}$$

where k is the local contact stiffness of the plate and n is the local nonlinearity exponent value. These local parameters are typically obtained through experiment. By performing static indentation testing [14], force-indentation data can be obtained. The local parameters are then computed by means of a "curve fit" to the experimental force-indentation data. Some researchers [10,12,17,42] assume the local nonlinearity value of $n = 1.5$ for anisotropic material even though this is

† The analytical Hertzian contact law model [41] is summarized in Appendix B for isotropic material case.

strictly true only for local indentation in isotropic material. However, presetting values for k and n is necessary for anisotropic material, so that these local parameters have unique values. In fact, Ryan [18] showed that the method of curve fitting to the experimental force-indentation data usually produced some variations in the local parameters computed. Furthermore, local nonlinearity values other than $n=1.5$ may fit the experimental force-indentation data better. Hence, it might be difficult to compute the exact values of these local parameters. Also, it is not guaranteed that the local parameters obtained from static indentation test can be applied directly to the dynamically occurring indenting event in this particular impacting condition case.

In this study, those local parameters were varied in realistic ranges to determine if there were any significant influences to the impact force output.

3.3.1 Local Stiffness Constant

The input parameter, Hertzian stiffness constant, k, was varied in the range of 0.005 – 8.6 GN/m^n. The local nonlinearity exponent value, n, was assumed to be 1.5 and fixed. In Figure 3.3 and 3.4, the maximum forces and the impact durations for various Hertzian stiffness constants are presented. Using 25x25 modes and 5 μsec of time increment was assumed to give sufficiently converged solutions. The x-axis for Hertzian stiffness constant uses a logarithmic scale. There is little influence observed in terms of the maximum force and the impact

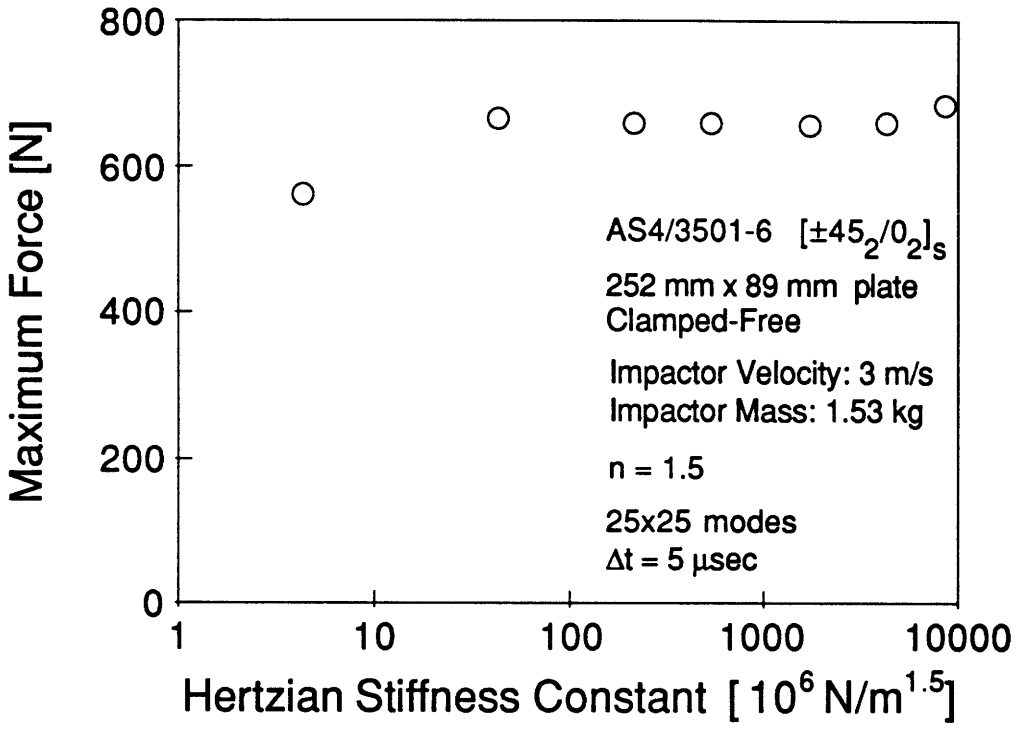

Figure 3.3 : Sensitiveness of the Maximum Impact Forces due to the Change in Hertzian Stiffness Constant, k
(x-axis is in the logarithmic scale)

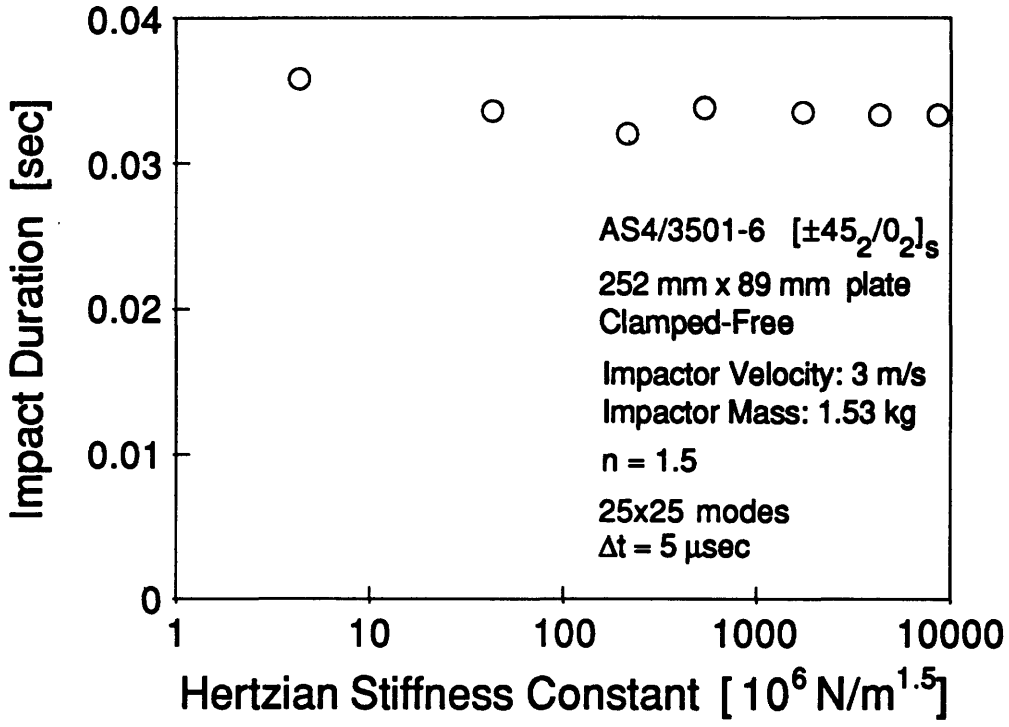

Figure 3.4 : Sensitiveness of the Impact Durations due to the Change in Hertzian Stiffness Constant, k
(x-axis is in the logarithmic scale)

duration due to varying the Hertzian stiffness constant. For example, one of the force-time history comparisons is shown in Figure 3.5 using two different values of the Hertzian stiffness constant, $0.5\,GN/m^{1.5}$, $0.005\,GN/m^{1.5}$. Although there are some changes observed in two curves, the overall trend of the signature of the curves is essentially the same. As can be seen from the Figure 3.5, those deviations of maximum force in Figure 3.3 come from the changes in the peak values of the many "spikes". Typically, a lower Hertzian stiffness value produces a smoother force-time history which contains fewer of the "spikes". This implies that the secondary frequency response refered to as "spikes" may be mostly controlled by the characteristics of the local parameters in this particular example case.

3.3.2 Local Nonlinearity Exponent Value

The input parameter, local nonlinearity exponent value, n, was varied in the range of 1.05 – 2.0. The Hertzian stiffness constant, k, was assumed to be 0.5 $GN/m^{1.5}$ and fixed. In Figures 3.6 and 3.7, the maximum forces and the impact durations for various local nonlinearity exponent values are presented. Using 25x25 modes and 5 μsec of time increment is assumed to give sufficiently converged solutions. Again, there is little influence observed in terms of the maximum force and the impact duration due to varying the local nonlinearity exponent values. For example, one of the force-time history comparisons is shown in Figure 3.8 using two different values of the local nonlinearity exponent; one uses 1.5 and the other uses 1.3.

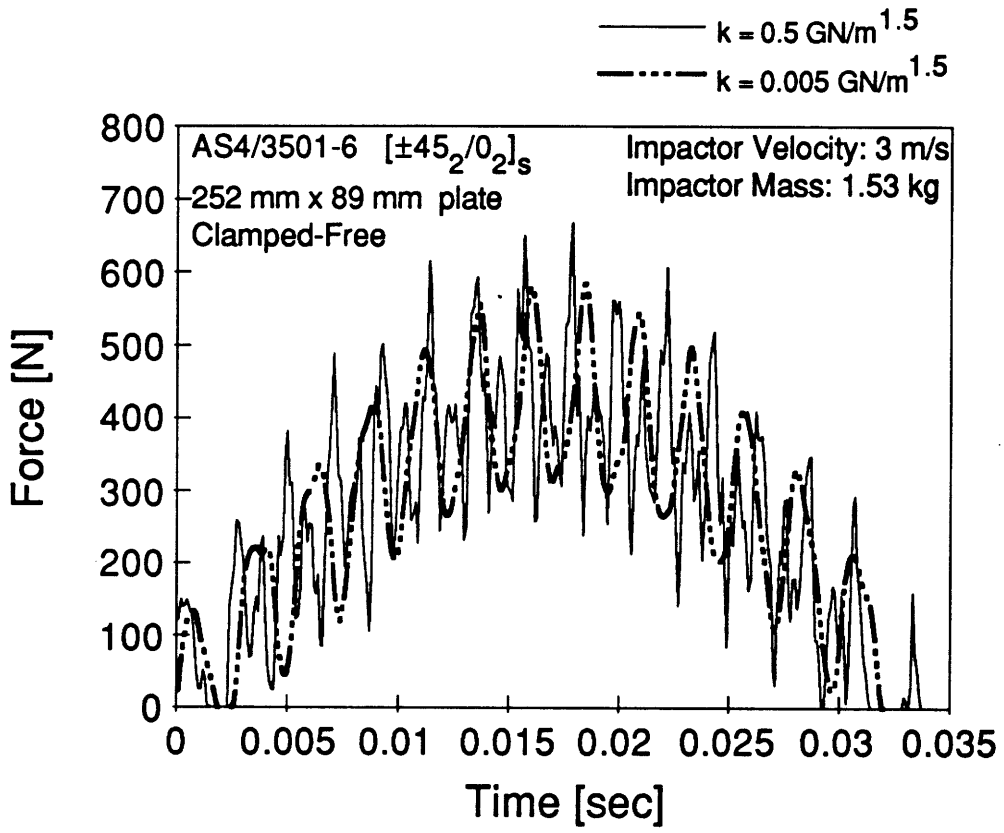

Figure 3.5 : Comparison of the Force-Time Histories using Different Hertzian Stiffness Constants (k = 0.5 GN/m$^{1.5}$ and k = 0.005 GN/m$^{1.5}$)

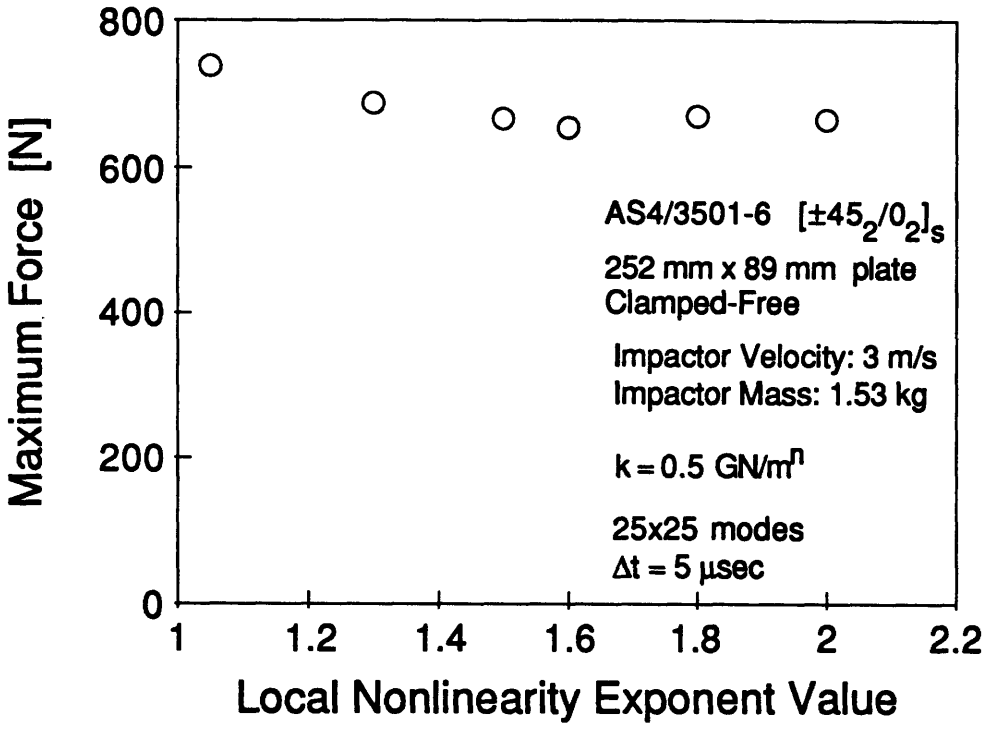

Figure 3.6 : Sensitiveness of the Maximum Impact Forces due to the Change in Local Nonlinearity Exponent Value, *n*

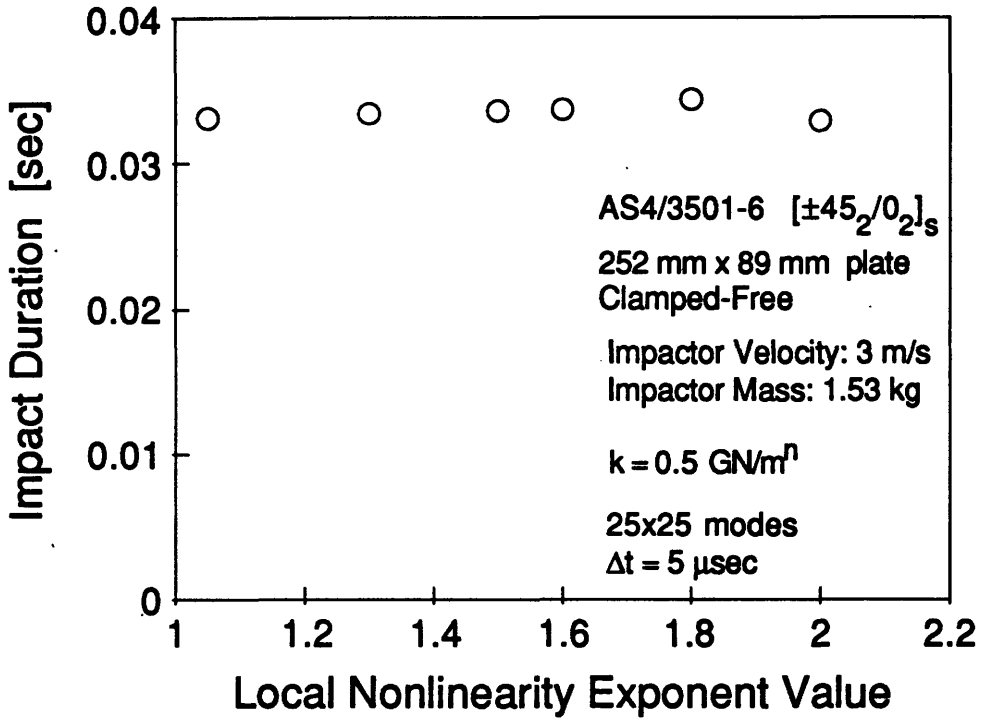

Figure 3.7 : Sensitiveness of the Impact Durations due to the Change in Local Nonlinearity Exponent Value, *n*

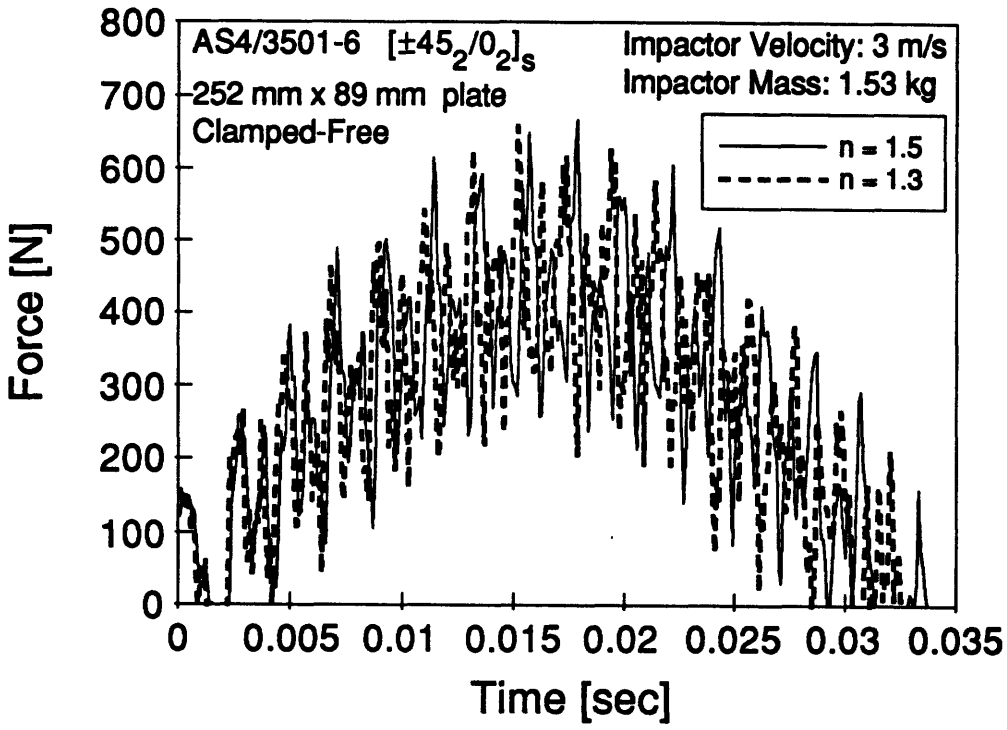

Figure 3.8 : Comparison of the Force-Time Histories using Different Local Nonlinearity Exponent Values ($n = 1.5$ and $n = 1.3$)

Although there are some changes observed in two curves, the overall trend of the signature of the curves is essentially the same.

The sensitivity study provides the following conclusion. For this particular impacting example case, local parameters do not have a significant influence on the force-time history and therefore, the effect of the local-global interaction is negligible in the given realistic range of the local parameters.

This conclusion leads to the following observation. As shown in Figure 3.9, this type of impact model can be analogous to using two springs; one represents local nonlinear stiffness and the other represents the linear plate motion. In the presented sensitivity study, only the characteristics of the local nonlinear stiffness were varied and these local characteristics provided some influence on the secondary frequency response, but did not have much influence on the primary frequency response. The next step is to focus on the characteristics of the other spring, the plate itself, which possibly has a greater effect on the primary frequency response. According to Shivakumar et al [35], the characteristics of the spring representing the plate motion can be governed by the plate geometries and the boundary conditions as well as the material properties of the plate. By assuming that input parameters for the plate geometries and the material properties are correct, the boundary conditions will now be investigated.

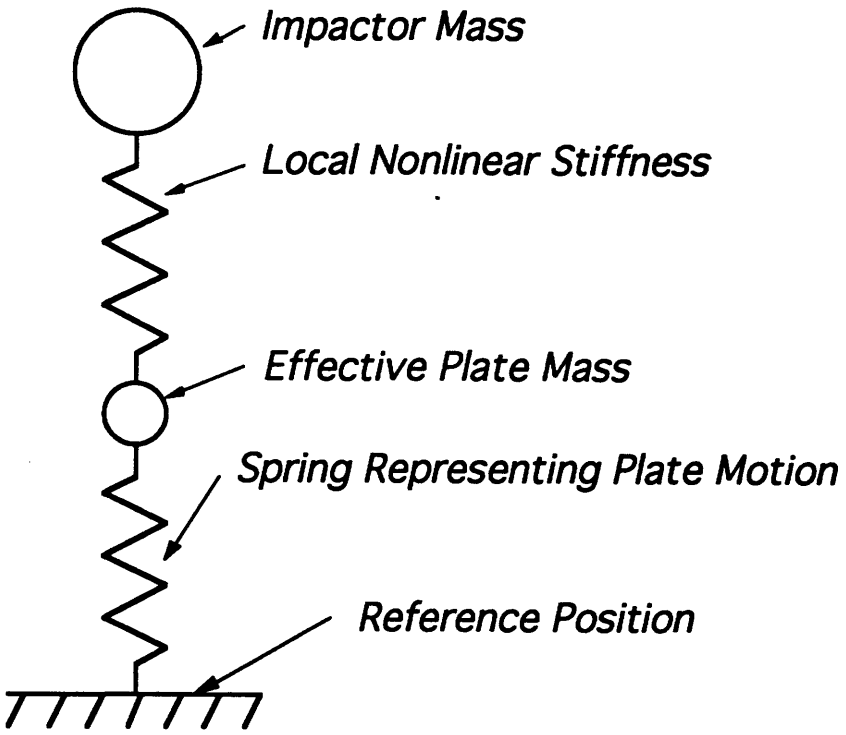

Figure 3.9 : Schematic of Spring-Mass Model

3.4 Issues in Boundary Conditions

According to the experimental set-up by Wolf [19], the plates were *rigidly* clamped in order to pursue the consistency in obtained data by avoiding unexpected slipping at the clamped boundary regions (see Figure 3.10). Because of this rigidly clamped boundary condition, it is possible that there is a significant force in the in-plane direction or so called membrane force which is a function of the out-of-plane displacement of the plate occurring during the impact event. However, linear plate theory cannot account for this membrane force effect which requires the use of geometrical nonlinearity in the analysis.

This geometrical nonlinearity is first considered in the impacted beam problem as a preliminary study for the nonlinear plate impact analysis. Since the plate in the example case is clamped on two opposite sides and free on other sides, its bending can be modeled as a beam and the simplified analysis using a beam model should give some indication of the influence of the membrane force.

3.5 Summary

In this chapter, two studies were performed to address the source of the problem discussed in Section 2.4, that is, the discrepancy in force-time history between the experimental data and the analytical prediction.

The first study was a convergence study where the time increment for numerical integration and the number of modes were

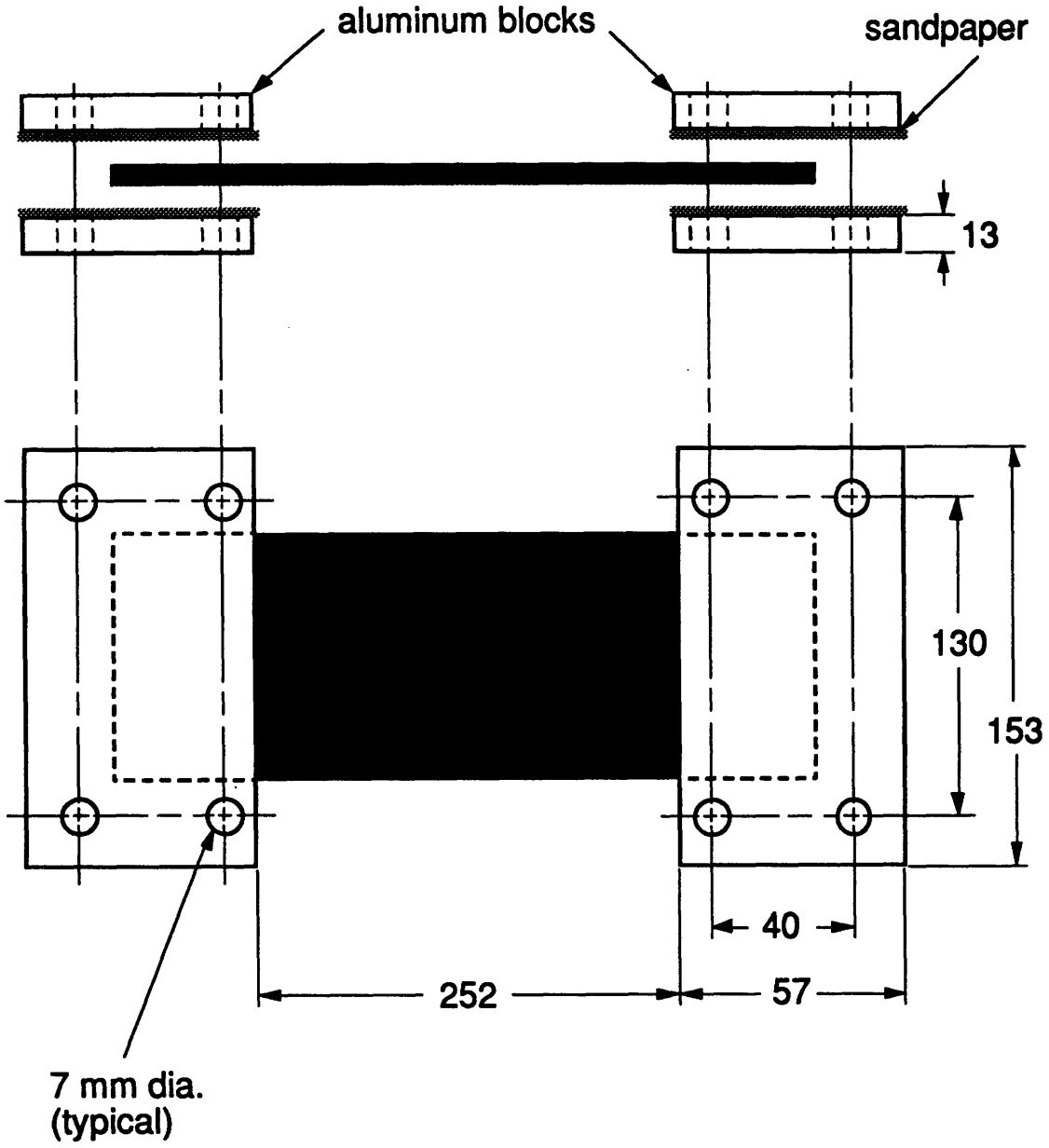

Note: all dimensions in mm.
drawing not to scale.

Figure 3.10 : Impact Specimen Holding Jig Experimental Set-up (taken from Wolf [19])

varied to obtain the converged solution for the example problem in Section 2.4. By making the time increment smaller and also the number of modes greater, the maximum impact force taken from the force-time history was found to be converged. However, the peak force after convergence was still approximately 45% of the experimental peak force.

The second study was a sensitivity study. The sensitivity of the force-time history in terms of the maximum contact force and impact duration due to the change in local parameters, Hertzian stiffness constant and local nonlinearity exponent value were studied. For the example case, local parameters have influence on the secondary frequency response but not on the primary frequency response. Consequently, the effect of the local-global interaction is negligible in the given realistic range of the local parameters.

The effect of the rigidly clamped boundary condition using a simplified beam model including the geometrical nonlinearity is discussed in Chapter 4.

Chapter 4

Impact Analysis of Linear and Nonlinear Beam Model

4.1 Overview

This chapter investigates the effect of membrane force due to the *rigidly* clamped boundary condition in a beam model by including the geometrical nonlinearity. This initial approach is a preliminary study for a plate model assuming that the plate is clamped at two opposite sides and free at the other two sides so that the plate bends like a beam.

A simplified out-of-plane displacement for the beam equation of motion is developed using a support stiffness which is a virtual spring in order to distinguish the boundary condition difference between the *rigidly clamped* and *loosely clamped* cases.† The governing equation of the beam can be solved simultaneously with the equation of motion of the

† Loosely clamped boundary condition means *loose* in the in-plane direction to allow sliding motion as illustrated in Figure 4.2.

rigid impactor and the constitutive relation of the nonlinear contact spring. Also, analogous beam equations of motion are developed using a similar approach taken in Chapter 2. This approach produces an in-plane stretching equation of motion as well as an out-of-plane displacement equation of motion of the beam. The effect of in-plane stretching is also investigated to check the feasibility of a reduction of the system of equations of plate motion used in Chapter 5.

4.2 Development of Beam Equation of Motion Using Support Stiffness

Assume that a Bernoulli-Euler beam with a clamped-clamped boundary condition can be modeled as shown in Figure 4.1 as suggested by Dugundji [36] and Dowell [46]. The basic beam equation of motion for this model is expressed as,

$$EI\frac{d^4w}{dx^4} - F\frac{d^2w}{dx^2} = p_z - m\ddot{w} \tag{4.2.1}$$

where F is a beam force† in the x-direction and can be obtained as follows:

$$F = \frac{EA}{l}u_B \tag{4.2.2}$$

where u_B is the beam elongation and expressed as,

$$u_B = \frac{1}{2}\int_0^l (w')^2\,dx - u_F \tag{4.2.3}$$

† In this formulation, the beam force is assumed to be a function of out-of-plane displacement only. Therefore, in-plane displacement is not considered.

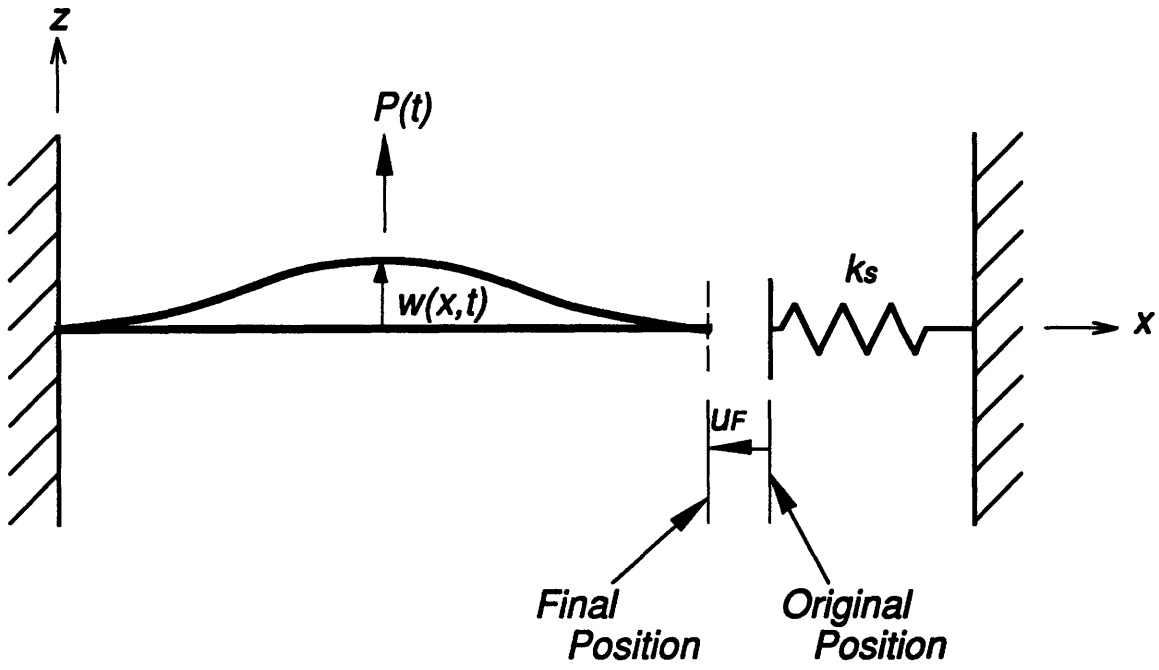

Figure 4.1 : Schematic of Beam Model with Support Stiffness

but also,

$$F = k_s u_F \qquad \text{or} \qquad u_F = \frac{F}{k_s} \tag{4.2.4}$$

Substituting Eqs. (4.2.3) and (4.2.4) into Eq. (4.2.2) yields,

$$F = \beta \frac{EA}{2l} \int_0^l (w')^2 \, dx \tag{4.2.5}$$

where,†

$$\beta = \left(\frac{\frac{k_s l}{EA}}{1 + \frac{k_s l}{EA}} \right) \tag{4.2.6}$$

Note that there are relationships among the support stiffness (k_s), β, and physical meanings of boundary conditions as shown in Figure 4.2.

The fourth-order differential equation of motion of the beam can be obtained by substituting Eq. (4.2.5) into Eq. (4.2.1).

$$EI \frac{\partial^4 w}{\partial x^4} - \left(\beta \frac{EA}{2l} \int_0^l \left(\frac{\partial w}{\partial x} \right)^2 dx \right) \frac{\partial^2 w}{\partial x^2} = p_z - m \frac{\partial^2 w}{\partial t^2} \tag{4.2.7}$$

For the simplified analysis, take the first clamped mode (ϕ_1) only. Let,

$$w(x,t) = \phi_1(x) q_1(t) \tag{4.2.8}$$

Substituting Eq. (4.2.8) into Eq. (4.2.7), and applying the Galerkin's method [43] (multiplying by ϕ_1 and integrating over the length) yields,

---

† β represents a *geometrical nonlinearity factor* which is discussed in Section 6.1.

a) Loosely Clamped Boundary Condition ($k_s = 0$, or $\beta = 0$)

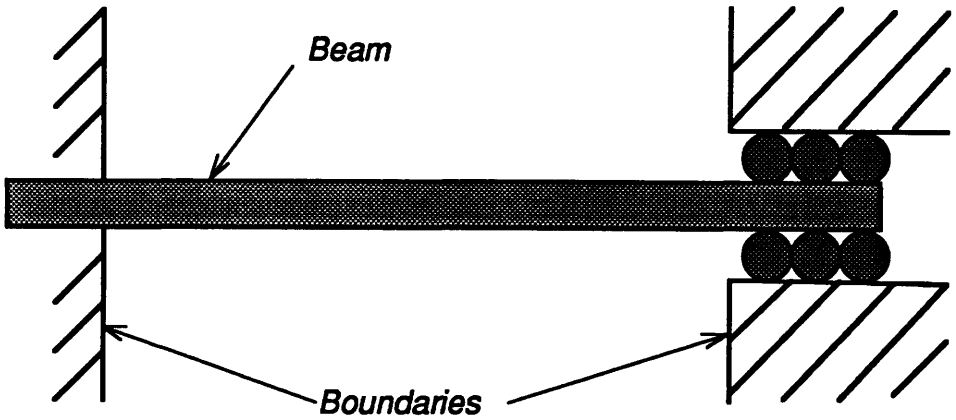

b) Rigidly Clamped Boundary Condition ($k_s = \infty$, or $\beta = 1$)

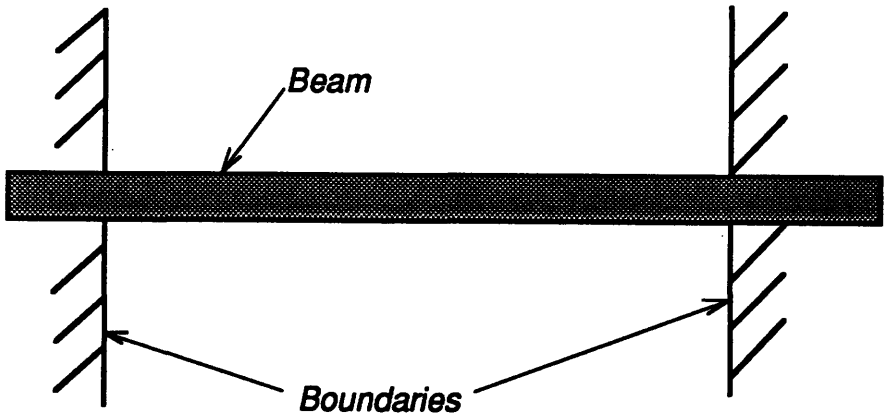

Figure 4.2 : Schematic of Loosely Clamped and Rigidly Clamped Beam Boundary Conditions

$$C_1\ddot{q}_1 + \frac{EI}{ml^4}\left[C_2 q_1 + \beta (C_3)^2 \frac{A}{2I} q_1^3\right] = \phi_1(l/2)\frac{P(t)}{ml} \tag{4.2.9}$$

where C_1, C_2, C_3 are the constants based on the first clamped mode shape as expressed in Eq. (4.2.10).

$$\begin{aligned} C_1 &= \frac{1}{l}\int_0^l \phi_1^2\, dx \\ C_2 &= l^3 \int_0^l (\phi_1'')^2\, dx \\ C_3 &= l \int_0^l (\phi_1')^2\, dx \end{aligned} \tag{4.2.10}$$

where q_1 denotes a modal amplitude and β controls the rigidity of clamped boundary condition. When β is equal to zero, Eq. (4.2.9) describes the linear beam model with loosely clamped boundary conditions. When β is equal to one, Eq. (4.2.9) contains a nonlinear term† and describes the geometrically nonlinear beam model with rigidly clamped boundary conditions.

The governing equation of motion of the beam (4.2.9) can be solved simultaneously with the equation of motion of the rigid impactor (4.2.11) and the constitutive relation of the local nonlinear contact stiffness (4.2.12).

$$m_I \ddot{u} = -P(t) \tag{4.2.11}$$

$$P(t) = k\left[u + q_1 \phi(1/2)\right]^n \tag{4.2.12}$$

Eqs. (4.2.9), (4.2.10), and (4.2.11) are solved using a fourth-order Runge-Kutta numerical integration method. This analysis procedure is

† This nonlinear term is refered to as a *cubic stiffening term*.

implemented in a FORTRAN program called "*NLBEAM*" listed in Appendix C1. In order to investigate the effect of support stiffness or membrane force, this beam model was analyzed for two cases, $\beta = 0$ (linear case) and $\beta = 1$ (nonlinear case).

4.3 Numerical Example

A graphite/epoxy plate made from AS4/3501-6 with the stacking sequence of $[\pm 45_2/0_2]_s$ as shown in Table 2.2 is modeled as a beam and all the input parameters are given in Table 4.1. This example problem is solved using both $\beta = 0$ (linear case) and $\beta = 1$ (nonlinear case).

Results of the force-time history and displacement-time history for each case are shown in Figures 4.3 and 4.4 respectively. In Figure 4.3, it is observed that the nonlinear beam model generates a greater maximum force and shorter impact duration than the linear beam model. This phenomena is similar to what was observed in Figure 2.6 showing a force-time history comparison of experiment and linear plate analysis. In Figure 4.4, the nonlinear beam model produces a smaller displacement than the linear beam model. This also agrees with the Kant and Mallikarjuna [26] claim that the nonlinear theory predicts smaller deflections compared to linear theory. Consequently, the effect of the membrane force in this particular example case can not be neglected and by analogy must be included in the plate analysis.

Table 4.1 : Input Parameters for Beam Analysis

h (thickness) [m] :	0.001608 (= 1.608 mm)
l (length) [m] :	0.252 (= 252 mm)
b (width) [m] :	0.089 (= 89 mm)
E [N/m^2] :	61.8 e+9 (assumed from E_L)
density [kg/m^3] :	1,540
m_I (impactor mass) [kg] :	1.53
V_I (impactor velocity) [m/s] :	3.0
n (local nonlinearity exponent) :	1.5
k (local stiffness) [N/m^n] :	1.0 e+6

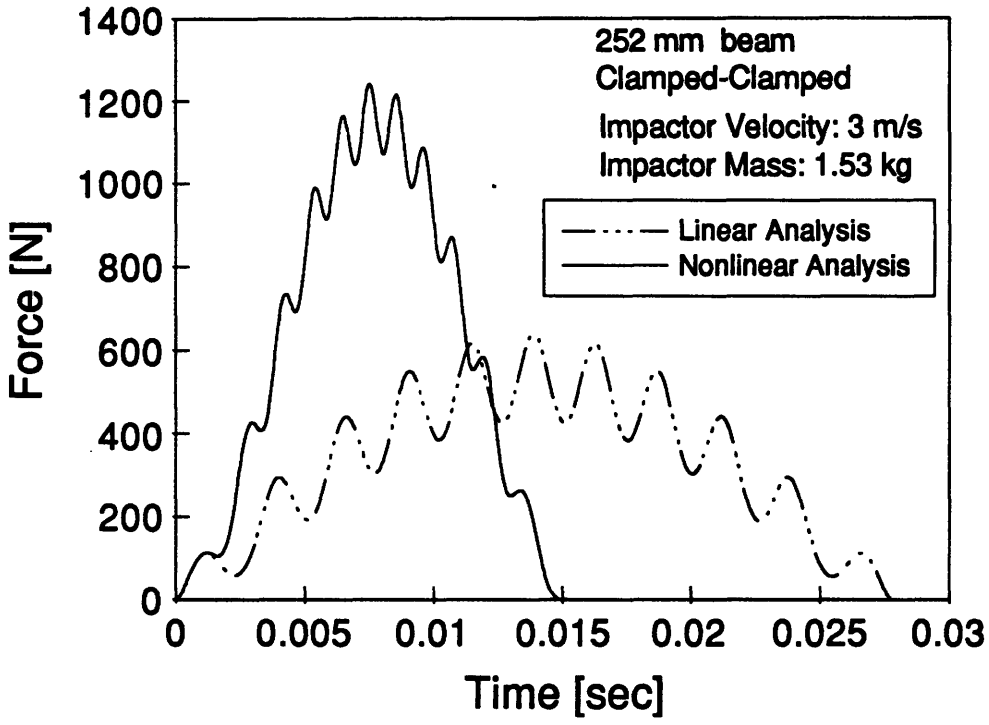

Figure 4.3 : Force Response of Impacted Beam Model – Linear and Nonlinear Analysis

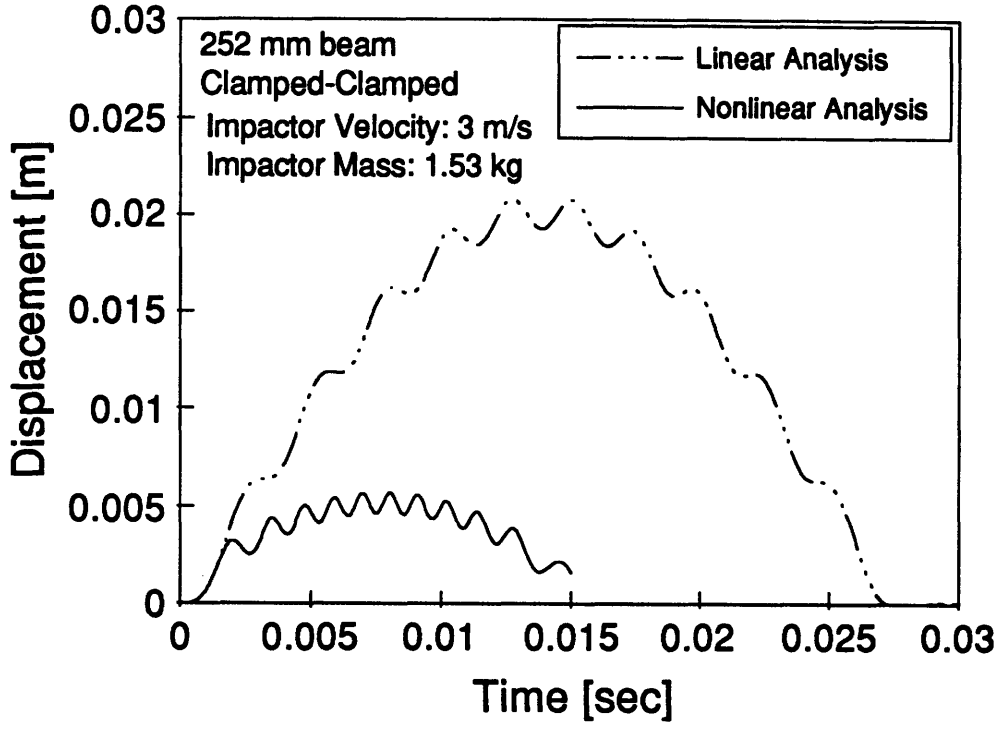

Figure 4.4 : Displacement of Impacted Beam Model – Linear and Nonlinear Analysis

4.4 Importance of In-Plane Displacement

The beam equation of motion developed in Section 4.2 accounts for out-of-plane displacement only. In-plane displacement is not considered.† Using the approach described in Section 2.2 in conjunction with nonlinear strain-displacement relations†† can yield a set of equations including both out-of-plane and in-plane displacements. Assume that the in-plane displacement, u, and the out-of-plane displacement, w, can be expressed by using the first rigidly clamped mode as follows.

$$\begin{aligned} u(x,t) &= p_1(t)\,\varphi_1(x) \\ w(x,t) &= q_1(t)\,\phi_1(x) \end{aligned} \tag{4.2.13}$$

where $p_1(t)$ and $q_1(t)$ denote modal amplitudes in in-plane and out-of-plane directions respectively and $\varphi_1(x)$ and $\phi_1(x)$ denote first mode shapes in in-plane and out-of-plane directions respectively. The resulting coupled system of equations of beam motion is now expressed as follows.

$$\begin{aligned} &J_1\ddot{p}_1 + J_2\left(\frac{EA}{m}\right)p_1 + J_3\left(\frac{EA}{m}\right){q_1}^2 = 0 \\ &J_4\ddot{q}_1 + J_5\left(\frac{EI}{ml^4}\right)q_1 + (J_6)^2\left(\frac{EA}{2ml^4}\right){q_1}^3 + J_7\left(\frac{EA}{m}\right)p_1q_1 = \phi_1(1/2)\frac{P(t)}{ml} \end{aligned} \tag{4.2.14}$$

† The terms, *in-plane* and *out-of-plane*, are used for the beam model. In-plane and out-of-plane refer to longitudinal and transverse directions for the beam model, respectively.

†† The nonlinear strain-displacement relations are discussed in Section 5.2.2.

where,

$$J_1 = \int_0^l \varphi_1^2 dx, \qquad J_2 = \int_0^l (\varphi_1')^2 dx, \qquad J_3 = \int_0^l \varphi_1'(\phi_1')^2 dx,$$

$$J_4 = \frac{1}{l}\int_0^l \phi_1^2 dx, \qquad J_5 = l^3 \int_0^l (\phi_1'')^2 dx, \qquad J_6 = l\int_0^l (\phi_1')^2 dx, \tag{4.2.15}$$

$$J_7 = \frac{1}{l}\int_0^l \varphi_1'(\phi_1')^2 dx$$

The coupled nonlinear differential equations (4.2.14) and also the rigid impactor equation of motion and the constitutive equation of Hertzian local contact relation given in Eqs. (4.2.11) and (4.2.12) can be solved by means of numerical integration and this procedure is implemented in a FORTRAN program "*NLBEAM2*" listed in Appendix C2. The force-time history of the output of this program is compared with the one produced by the nonlinear equation (4.2.9) which contains only out-of-plane displacement (shown in Figure 4.3) in Figure 4.5. The maximum difference in these two curves is less than 1% indicating the effect of in-plane displacement is almost negligible in this example case. Consequently, it will be assumed that nonlinear plate analysis, which is described in Chapter 5, can also be simplified by neglecting the in-plane displacement behavior.

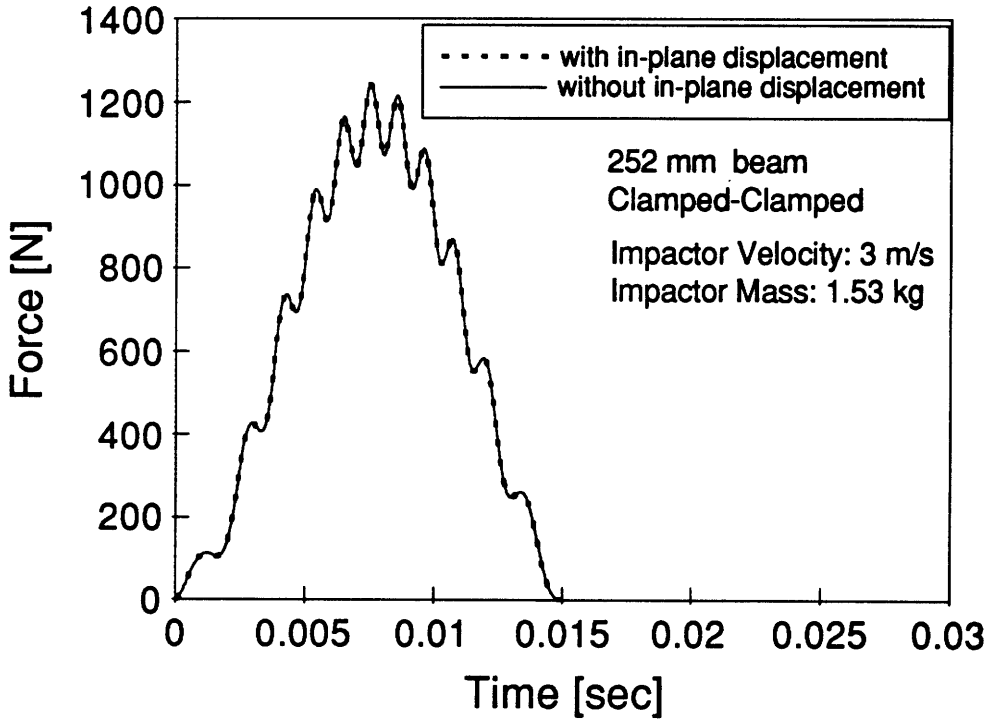

Figure 4.5 : Effect of In-Plane Displacement in Force-Time History – Beam Impact Analyses With and Without In-Plane Displacement

4.5 Summary

In this chapter, the effect of membrane force due to the rigidly clamped boundary condition in a beam model including the geometrical nonlinearity was investigated as a preliminary study for the plate analysis. Two different approaches were taken to obtain the beam equation of motion. One approach used a support stiffness which acts as a virtual spring at the boundary. This approach produced the equation of motion in terms of transverse displacement and included both linear and nonlinear cases by simply changing the support stiffness parameter, β. The nonlinear beam model showed a greater maximum force and shorter impact duration than the linear beam model. Also, the nonlinear beam model produced a smaller displacement than the linear beam model. The other approach was the same as the procedure reviewed in Section 2.2. This approach produced two coupled equations of motion in terms of both in-plane and out-of-plane displacements. From the output of this system of equations, the effect of in-plane displacement was observed. As a result of this preliminary study, it is concluded that the membrane force should be considered in the plate analysis by including geometrical nonlinearity. The effect of in-plane displacement, however, appears to be negligible for the example problem considered.

Chapter 5

Impact Modeling Using Nonlinear Laminated Plate Theory with First-Order Shear Deformation

5.1 Overview

In this chapter, an impact model using a nonlinear laminated plate theory is developed. A geometrical nonlinearity in plate analysis without shear deformation has been considered by several authors, such as Reismann [37], Chia [38], and Whitney [39] and is known as von Kármán nonlinear plate theory. A nonlinear laminated plate theory with shear deformation can be derived from the three-dimensional nonlinear theory of elasticity by combining Timoshenko-type theory and von Kármán nonlinear plate theory as described by Reddy [21]. In this investigation, nonlinear plate equations of motion subjected to impact are obtained from energy equations by means of Lagrangian equations of

motion and a Rayleigh-Ritz method in conjunction with assumed mode shapes.

5.2 Development of the Equations of Motion

5.2.1 Assumptions

The following assumptions were made initially to develop a system of equations of motion for both a plate and an impactor.

a) Nonlinear strain-displacement relations including second-order nonlinear terms in the reference surface strains at $z=0$ are assumed.

b) Linear stress-strain relations are assumed.

c) Through the thickness strain, ε_{33}, is negligible and out-of-plane displacement, w, is a function of in-plane coordinates, x and y, only.

d) The plate deforms both in bending and shear.

e) First-order shear deformation terms are included.

f) The contact force between the impactor and the plate is a point load.

g) Material properties are assumed constant throughout the impact event.

h) No structural damping is considered.

i) Impactor is assumed to be rigid.

j) Local indentation of the plate is accounted for by a nonlinear Hertzian stiffness relation.

A schematic of the laminated plate impact model is shown in Figure 2.1. There are additional assumptions made later to further reduce the system of equations.

5.2.2 Nonlinear Laminated Plate Theory with First-Order Shear Deformation

Strain-Displacement Relations

In the Lagrangian description, the coordinates x_1, x_2, x_3 are regarded as independent variables and the Green strain tensor or the Lagrangian strain components can be defined as,†

$$\varepsilon_{ij} = \frac{1}{2}\left(\frac{\partial u_i}{\partial x_j} + \frac{\partial u_j}{\partial x_i} + \frac{\partial u_k}{\partial x_i}\frac{\partial u_k}{\partial x_j}\right) \tag{5.2.1}$$

By including first-order shear deformation which assumes that cross-sections remain planar but not normal to the plate midplane during deformation, a linear variation of the displacements is assumed through the thickness for the shear deformation. Now, the displacement fields are expressed as follows.

† Reference for general theory of strain may be made to Love, A. E. H., *A Treatise on the Mathematical Theory of Elasticity*, Cambridge University Press, 1927.

$$
\begin{aligned}
u_1(x,y,z,t) &= u(x,y,t) + z\psi_x(x,y,t) \\
u_2(x,y,z,t) &= v(x,y,t) + z\psi_y(x,y,t) \\
u_3(x,y,z,t) &= w(x,y,t)
\end{aligned}
\tag{5.2.2}
$$

u_1, u_2, and u_3 are the displacements in the x, y, and z directions, respectively; u, v, and w are the associated midplane displacements. ψ_x and ψ_y are the rotations in the xz and yz planes owing to bending only. From Eqs. (5.2.1) and (5.2.2), strain-displacement relations can be derived as shown in Eq. (5.2.3).

$$
\begin{aligned}
\varepsilon_{11} &= \frac{\partial u}{\partial x} + \frac{1}{2}\left(\frac{\partial w}{\partial x}\right)^2 + z\frac{\partial \psi_x}{\partial x} \\
\varepsilon_{22} &= \frac{\partial v}{\partial y} + \frac{1}{2}\left(\frac{\partial w}{\partial y}\right)^2 + z\frac{\partial \psi_y}{\partial y} \\
2\varepsilon_{12} &= \frac{\partial u}{\partial y} + \frac{\partial v}{\partial x} + \frac{\partial w}{\partial x}\frac{\partial w}{\partial y} + z\left(\frac{\partial \psi_x}{\partial y} + \frac{\partial \psi_y}{\partial x}\right) \\
2\varepsilon_{13} &= \psi_x + \frac{\partial w}{\partial x} \\
2\varepsilon_{23} &= \psi_y + \frac{\partial w}{\partial y} \\
\varepsilon_{33} &= 0
\end{aligned}
\tag{5.2.3}
$$

Eq. (5.2.3) can also be expressed in terms of vector notation.

$$
\begin{aligned}
\underline{\varepsilon}(x,y,z,t) &= \underline{\varepsilon}^{\circ}(x,y,t) + z\,\underline{\kappa}(x,y,t) \\
\underline{\gamma}(x,y,z,t) &= \underline{\gamma}(x,y,t)
\end{aligned}
\tag{5.2.4a}
$$

where,

$$\underline{\varepsilon}=\begin{Bmatrix}\varepsilon_{11}\\ \varepsilon_{22}\\ 2\varepsilon_{12}\end{Bmatrix}, \qquad \underline{\gamma}=\begin{Bmatrix}2\varepsilon_{23}\\ 2\varepsilon_{13}\end{Bmatrix}$$

$$\underline{\varepsilon}^{\circ}=\begin{Bmatrix}\varepsilon^{\circ}_{11}\\ \varepsilon^{\circ}_{22}\\ \varepsilon^{\circ}_{12}\end{Bmatrix}=\begin{Bmatrix}\dfrac{\partial u}{\partial x}+\dfrac{1}{2}\left(\dfrac{\partial w}{\partial x}\right)^2\\ \dfrac{\partial v}{\partial y}+\dfrac{1}{2}\left(\dfrac{\partial w}{\partial y}\right)^2\\ \dfrac{\partial u}{\partial y}+\dfrac{\partial v}{\partial x}+\dfrac{\partial w}{\partial x}\dfrac{\partial w}{\partial y}\end{Bmatrix}, \qquad \underline{\kappa}=\begin{Bmatrix}\kappa^{\circ}_{11}\\ \kappa^{\circ}_{22}\\ \kappa^{\circ}_{12}\end{Bmatrix}=\begin{Bmatrix}\dfrac{\partial \psi_x}{\partial x}\\ \dfrac{\partial \psi_y}{\partial y}\\ \dfrac{\partial \psi_x}{\partial y}+\dfrac{\partial \psi_y}{\partial x}\end{Bmatrix} \tag{5.2.4b}$$

Eqs. (5.2.4a) and (5.2.4b) represent nonlinear strain-displacement relations including shear deformation. Note that second-order terms in $\underline{\varepsilon}^{\circ}$ are the source of geometrical nonlinearity and are the only differences in the analytical development compared with Eq. (2.2.6) for linear theory.

Constitutive Behavior of the Plate

The basic laminate constitutive equations are the same as those used in the linear analysis and defined by,

$$\begin{Bmatrix}\{N\}\\ \{M\}\end{Bmatrix}=\begin{bmatrix}[A] & [B]\\ [B]^{T} & [\mathrm{D}]\end{bmatrix}\begin{Bmatrix}\underline{\varepsilon}^{\circ}\\ \underline{\kappa}\end{Bmatrix}$$

$$\begin{Bmatrix}Q_1\\ Q_2\end{Bmatrix}=\begin{bmatrix}G_{55} & G_{45}\\ G_{45} & G_{44}\end{bmatrix} \tag{5.2.5}$$

where $[A]$, $[B]$, and $[\mathrm{D}]$ are the in-plane, bending-stretching, and bending stiffnesses of the plate, respectively. Each of the matrix components are given as,

$$\left(A_{ij},\ B_{ij},\ D_{ij}\right)=\sum_{n=1}^{N}\int_{z_n}^{z_{n+1}} C_{ij}^{(n)}\left(1,\ z,\ z^2\right)dz \qquad (i,j=1,2,6) \qquad (5.2.6)$$

where n denotes the nth ply and there are total of Nplies. Also, where C_{ij} are assumed to be the plane stress material constants for this investigation and i, j = 1,2,4,5,6 by letting,

$$\underline{\varepsilon}=\begin{Bmatrix}\varepsilon_{11}\\ \varepsilon_{22}\\ 2\varepsilon_{12}\end{Bmatrix}=\begin{Bmatrix}\varepsilon_1\\ \varepsilon_2\\ \varepsilon_6\end{Bmatrix}, \qquad \underline{\gamma}=\begin{Bmatrix}2\varepsilon_{23}\\ 2\varepsilon_{13}\end{Bmatrix}=\begin{Bmatrix}\varepsilon_4\\ \varepsilon_5\end{Bmatrix} \qquad (5.2.7)$$

The transverse shear stiffness matrix $[G]$ and each of the matrix components are defined as,

$$G_{ij}=\sum_{n=1}^{N} K_iK_j\int_{z_n}^{z_{n+1}} C_{ij}^{(n)}\,dz \qquad (i,j=4,5) \qquad (5.2.8)$$

The value of the shearing correction term, K_iK_j, used here is the isotropic correction factor of 5/6, shown to be adequate for laminates made from thin plies [11].

In Section 4.2, Eq. (2.2.7) could be decoupled by assuming $B_{ij}=0$ for linear plate analysis; however, Eq. (5.2.5) can not be decoupled because the out-of-plane displacement is a function of in-plane displacement for nonlinear plate theory.

Potential Energy

The potential energy stored in a properly constrained body under load can be separated into two parts:

a) the strain energy, defined as the product of strain and stress, or, since we assumed a linear stress-strain behavior as:

$$U = \frac{1}{2}\iiint_V C_{ij}\varepsilon_i\varepsilon_j \, dV \tag{5.2.9}$$

b) the work done by the external forces:

$$W = \iint_S p_i w_i \, dS \qquad i = 1,2,3 \tag{5.2.10}$$

where p_i denotes external force per unit area and w_i denotes displacement from original position.

The total potential energy is simply the difference of these two terms and a function of the displacements only.

Introducing Eqs. (5.2.4a,b) and (5.2.5) into the strain energy equation (5.2.9) and integrating over the thickness yields the following strain energy expression.

$$U = \frac{1}{2}\iint_S \left(\underline{\varepsilon}^{\circ T}[A]\,\underline{\varepsilon}^{\circ} + 2\underline{\varepsilon}^{\circ T}[B]\,\underline{\kappa} + \underline{\kappa}^{T}[D]\,\underline{\kappa} + \underline{\gamma}^{T}[G]\,\underline{\gamma} \right) dS \tag{5.2.11}$$

For convenience, the strain energy is devided into four parts as,

$$U = U_{\mathrm{I}} + U_{\mathrm{II}} + U_{\mathrm{III}} + U_{\mathrm{IV}} \tag{5.2.12}$$

where each of the strain energy parts can be written as follows,

$$U_{\mathrm{I}} = \frac{1}{2}\iint_S \underline{\varepsilon}^{\circ \mathrm{T}}[A]\,\underline{\varepsilon}^{\circ}\,dS$$

$$= \frac{1}{2}\int_0^b\int_0^a \begin{Bmatrix} \dfrac{\partial u}{\partial x} + \dfrac{1}{2}\left(\dfrac{\partial w}{\partial x}\right)^2 \\ \dfrac{\partial v}{\partial y} + \dfrac{1}{2}\left(\dfrac{\partial w}{\partial y}\right)^2 \\ \dfrac{\partial u}{\partial y} + \dfrac{\partial v}{\partial x} + \dfrac{\partial w}{\partial x}\dfrac{\partial w}{\partial y} \end{Bmatrix}^{\mathrm{T}} \begin{bmatrix} A_{11} & A_{12} & A_{16} \\ A_{12} & A_{22} & A_{26} \\ A_{16} & A_{26} & A_{66} \end{bmatrix} \begin{Bmatrix} \dfrac{\partial u}{\partial x} + \dfrac{1}{2}\left(\dfrac{\partial w}{\partial x}\right)^2 \\ \dfrac{\partial v}{\partial y} + \dfrac{1}{2}\left(\dfrac{\partial w}{\partial y}\right)^2 \\ \dfrac{\partial u}{\partial y} + \dfrac{\partial v}{\partial x} + \dfrac{\partial w}{\partial x}\dfrac{\partial w}{\partial y} \end{Bmatrix} dx\,dy$$

(5.2.13)

$$U_{\mathrm{II}} = \frac{1}{2}\iint_S \underline{\varepsilon}^{\circ \mathrm{T}}[B]\,\underline{\kappa}\,dS$$

$$= \frac{1}{2}\int_0^b\int_0^a \begin{Bmatrix} \dfrac{\partial u}{\partial x} + \dfrac{1}{2}\left(\dfrac{\partial w}{\partial x}\right)^2 \\ \dfrac{\partial v}{\partial y} + \dfrac{1}{2}\left(\dfrac{\partial w}{\partial y}\right)^2 \\ \dfrac{\partial u}{\partial y} + \dfrac{\partial v}{\partial x} + \dfrac{\partial w}{\partial x}\dfrac{\partial w}{\partial y} \end{Bmatrix}^{\mathrm{T}} \begin{bmatrix} B_{11} & B_{12} & B_{16} \\ B_{12} & B_{22} & B_{26} \\ B_{16} & B_{26} & B_{66} \end{bmatrix} \begin{Bmatrix} \dfrac{\partial \psi_x}{\partial x} \\ \dfrac{\partial \psi_y}{\partial y} \\ \dfrac{\partial \psi_x}{\partial y} + \dfrac{\partial \psi_y}{\partial x} \end{Bmatrix} dx\,dy$$

(5.2.14)

$$U_{\mathrm{III}} = \frac{1}{2}\iint_S \underline{\kappa}^{\mathrm{T}}[B]\,\underline{\kappa}\,dS$$

$$= \frac{1}{2}\int_0^b\int_0^a \begin{Bmatrix} \dfrac{\partial \psi_x}{\partial x} \\ \dfrac{\partial \psi_y}{\partial y} \\ \dfrac{\partial \psi_x}{\partial y} + \dfrac{\partial \psi_y}{\partial x} \end{Bmatrix}^{\mathrm{T}} \begin{bmatrix} D_{11} & D_{12} & D_{16} \\ D_{12} & D_{22} & D_{26} \\ D_{16} & D_{26} & D_{66} \end{bmatrix} \begin{Bmatrix} \dfrac{\partial \psi_x}{\partial x} \\ \dfrac{\partial \psi_y}{\partial y} \\ \dfrac{\partial \psi_x}{\partial y} + \dfrac{\partial \psi_y}{\partial x} \end{Bmatrix} dx\,dy$$

(5.2.15)

$$U_{IV} = \frac{1}{2}\iint_S \underline{\gamma}^T [G]\,\underline{\gamma}\, dS$$

$$= \frac{1}{2}\int_0^b \int_0^a \begin{Bmatrix} \psi_y + \dfrac{\partial w}{\partial y} \\ \psi_x + \dfrac{\partial w}{\partial x} \end{Bmatrix}^T \begin{bmatrix} G_{55} & G_{45} \\ G_{45} & G_{44} \end{bmatrix} \begin{Bmatrix} \psi_y + \dfrac{\partial w}{\partial y} \\ \psi_x + \dfrac{\partial w}{\partial x} \end{Bmatrix} dx\, dy \qquad (5.2.16)$$

Each of the strain energy components has a specific physical meaning as described by Minguet [40].

U_I : is an energy representing the in-plane stretching, the geometric coupling between in- and out-of-plane deformations, and fourth-order terms representing the stiffness of the large deformation.

U_{II} : is an energy containing linear terms which represent the material coupling between in- and out-of-plane deformations that occurs, for instance, in unsymmetric plates and nonlinear terms representing the in-plane strains.

U_{III} : represents the bending energy of the plate.

U_{IV} : is the energy representing the plate transverse shear deformation. Notice that this is the only term coupling w with ψ_x and ψ_y, and also the only one containing terms which are functions of w alone.

Kinetic Energy

The kinetic energy, T, of the plate is given by,

$$T(u,v,w,\psi_x\psi_y)=\frac{1}{2}\iiint_V \rho\left[\dot{u}_1{}^2+\dot{u}_2{}^2+\dot{u}_3{}^2\right]dV \tag{5.2.17}$$

where u_1, u_2, u_3 denote displacements in x, y, z directions respectively and $(\dot{\cdot})$ denotes differentiation with respect to time. Substituting Eq. (5.2.2) into Eq. (5.2.17) and integrating over the thickness yields,

$$\begin{aligned} &T(u,v,w,\psi_x,\psi_y) \\ &=\frac{1}{2}\int_0^b\int_0^a \begin{Bmatrix}\dot{\psi}_x\\ \dot{\psi}_y\\ \dot{u}\\ \dot{v}\\ \dot{w}\end{Bmatrix}^{\mathrm{T}} \begin{bmatrix} I_3 & 0 & I_2 & 0 & 0\\ 0 & I_3 & 0 & I_2 & 0\\ I_2 & 0 & I_1 & 0 & 0\\ 0 & I_2 & 0 & I_1 & 0\\ 0 & 0 & 0 & 0 & I_1\end{bmatrix} \begin{Bmatrix}\dot{\psi}_x\\ \dot{\psi}_y\\ \dot{u}\\ \dot{v}\\ \dot{w}\end{Bmatrix} dx\,dy \end{aligned} \tag{5.2.18}$$

where,

$$(I_1,\ I_2,\ I_3)=\int_{-h/2}^{h/2}(1,\ z,\ z^2)\rho\,dz \tag{5.2.19}$$

Now, all the energy equations required to produce the plate equations of motion have been presented. General plate equations of motion can be derived using Hamilton's principle [44]:

$$\int_{t_0}^{t_1}\delta L\,dt=0 \tag{5.2.20}$$

where δL is the first variation of the Lagrangian,

$$\delta L = \delta\Pi - \delta T \tag{5.2.21}$$

where Π and T are the total potential and kinetic energies, respectively. The variations of total potential energy and kinetic energy can be obtained by substituting Eqs. (5.2.3), (5.2.5), (5.2.9), (5.2.10), and (5.2.18) into Eq. (5.2.21).

Variation of Total Potential Energy :

$$\begin{aligned}\delta\Pi = \frac{1}{2}\iint_R \Bigg[& N_x \frac{\partial[\delta u]}{\partial x} + N_x \frac{\partial w}{\partial x}\frac{\partial[\delta w]}{\partial x} + M_x \frac{\partial[\delta \psi_x]}{\partial x} \\ & + N_y \frac{\partial[\delta v]}{\partial y} + N_y \frac{\partial w}{\partial y}\frac{\partial[\delta w]}{\partial y} + M_y \frac{\partial[\delta \psi_y]}{\partial y} \\ & + N_{xy} \frac{\partial[\delta u]}{\partial y} + N_{xy} \frac{\partial w}{\partial x}\frac{\partial[\delta v]}{\partial x} + N_{xy}\left(\frac{\partial w}{\partial y}\frac{\partial[\delta w]}{\partial x} + \frac{\partial w}{\partial x}\frac{\partial[\delta w]}{\partial y}\right) \\ & M_{xy} \frac{\partial[\delta \psi_x]}{\partial y} + M_{xy} \frac{\partial[\delta \psi_y]}{\partial x} + Q_x \delta\psi_x + Q_x \frac{\partial[\delta w]}{\partial x} + Q_y \delta\psi_y + Q_y \frac{\partial[\delta w]}{\partial y} \Bigg] dR \\ & - \iint_R q_z \delta w \, dR - \int_{C_1} \hat{N}_n \delta u_n \, dS - \int_{C_2} \hat{N}_s \delta u_s \, dS - \int_{C_3} \hat{M}_n \delta\psi_n \, dS - \int_{C_4} \hat{M}_s \delta\psi_s \, dS - \int_{C_5} \hat{Q}_n \delta w \, dS\end{aligned} \tag{5.2.22}$$

Variation of Total Kinetic Energy :

$$\delta T = \iint_R \left[\begin{array}{l} \left(\dot{u}\dfrac{\partial[\delta u]}{\partial t} + \dot{v}\dfrac{\partial[\delta v]}{\partial t} + \dot{w}\dfrac{\partial[\delta w]}{\partial t} \right) I_1 \\ + \left(\dot{\psi}_x \dfrac{\partial[\delta u]}{\partial t} + \dot{u}\dfrac{\partial[\delta \psi_x]}{\partial t} + \dot{\psi}_y \dfrac{\partial[\delta \psi_y]}{\partial t} + \dot{v}\dfrac{\partial[\delta \psi_y]}{\partial t} \right) I_2 \\ + \left(\dot{\psi}_x \dfrac{\partial[\delta \psi_x]}{\partial t} + \dot{\psi}_y \dfrac{\partial[\delta \psi_y]}{\partial t} \right) I_3 \end{array} \right] dR \qquad (5.2.23)$$

where subscripts n and s denote normal and tangential, respectively, R denotes the midplane of the plate, and the symbol, $\hat{}$, represents a prescribed quantity.

Integrating Eqs. (5.2.22) and (5.2.23) by parts with respect to both time (t) and coordinates (x, y) and setting $\int_{t_0}^{t_1} \delta L \, dt = 0$ yields the following equations of motion.

$$\delta u: \quad \frac{\partial N_x}{\partial x} + \frac{\partial N_{xy}}{\partial y} = I_1 \ddot{u} + I_2 \ddot{\psi}_x \qquad (5.2.24a)$$

$$\delta v: \quad \frac{\partial N_y}{\partial y} + \frac{\partial N_{xy}}{\partial x} = I_1 \ddot{v} + I_2 \ddot{\psi}_y \qquad (5.2.24b)$$

$$\begin{aligned} \delta w: \quad & N_x \frac{\partial^2 w}{\partial x^2} + 2N_{xy}\frac{\partial^2 w}{\partial x \partial y} + N_y \frac{\partial^2 w}{\partial y^2} \\ & + \left(\frac{\partial N_x}{\partial x} + \frac{\partial N_{xy}}{\partial y} \right) \frac{\partial w}{\partial x} + \left(\frac{\partial N_y}{\partial y} + \frac{\partial N_{xy}}{\partial x} \right) \frac{\partial w}{\partial y} \\ & + \frac{\partial Q_x}{\partial x} + \frac{\partial Q_y}{\partial y} = q_z + I_1 \ddot{w} \end{aligned} \qquad (5.2.24c)$$

$$\delta\psi_x: \quad \frac{\partial M_x}{\partial x}+\frac{\partial M_{xy}}{\partial y}-Q_x = I_2\ddot{u}+I_3\ddot{\psi}_x \tag{5.2.24d}$$

$$\delta\psi_y: \quad \frac{\partial M_y}{\partial y}+\frac{\partial M_{xy}}{\partial x}-Q_y = I_2\ddot{v}+I_3\ddot{\psi}_y \tag{5.2.24e}$$

The natural boundary conditions of the plate are given by,

$$\begin{aligned}
&\delta u_{n0}: && N_n-\hat{N}_n=0 \quad \text{on } C_1\\
&\delta u_{s0}: && N_s-\hat{N}_s=0 \quad \text{on } C_2\\
&\delta\psi_n: && M_n-\hat{M}_n=0 \quad \text{on } C_3\\
&\delta\psi_s: && M_s-\hat{M}_s=0 \quad \text{on } C_4\\
&\delta w_0: && Q_n-\hat{Q}_n=0 \quad \text{on } C_5
\end{aligned} \tag{5.2.25}$$

where the subscript, 0, represents a quantity at the midplane. Note that C_1 thru C_5 denote the segments of the total boundary C such that on $C-C_1$, $C-C_2$, $C-C_3$, $C-C_4$, and $C-C_5$, essential boundary conditions are specified:

$$\begin{aligned}
&u_{n0}=\hat{u}_{n0} \quad \text{on } C-C_1\\
&u_{s0}=\hat{u}_{s0} \quad \text{on } C-C_2\\
&\psi_n=\hat{\psi}_n \quad \text{on } C-C_3\\
&\psi_s=\hat{\psi}_s \quad \text{on } C-C_4\\
&w_0=\hat{w}_0 \quad \text{on } C-C_5
\end{aligned} \tag{5.2.26}$$

For a rectangular plate, with coordinate axes parallel to the edges of the plate, the natural and essential boundary conditions take the following simple form:

	Natural		Essential	
Specify	N_x	or	u_0	
	N_y	or	v_0	
	M_x	or	ψ_x	
	M_y	or	ψ_y	
	Q_x (or Q_y)	or	w_0	(5.2.27)

Eqs. (5.2.24) can be rewritten in terms of the displacements only by substituting Eqs. (5.2.4) and (5.2.5) into Eqs. (5.2.24). These formulations are, however, not necessary for an impact analysis. Since a transient analysis at a given point on the plate is the focus of this investigation, Lagrangian equations of motion are sufficient.

5.2.3 Plate Equations of Motion for Transient Analysis

Plate equations of motion at a given point are obtained by applying the Lagrangian equations of motion and the Rayleigh-Ritz method in conjunction with assumed mode shapes to the energy equations obtained in Section 5.2.2.

Assumed Mode Shapes

For spatial discretization of the displacements as functions of x and y, let,

$$\psi_x(x,y,t)=\sum_{\varsigma}\sum_{\mu}A_{\varsigma\mu}(t)f_{\varsigma}(x)g_{\mu}(y) \tag{5.2.28a}$$

$$\psi_y(x,y,t)=\sum_{\varsigma}\sum_{\mu}B_{\varsigma\mu}(t)h_{\varsigma}(x)l_{\mu}(y) \tag{5.2.28b}$$

$$u(x,y,t)=\sum_{\varsigma}\sum_{\mu}C_{\varsigma\mu}(t)m_{\varsigma}(x)n_{\mu}(y) \tag{5.2.28c}$$

$$v(x,y,t)=\sum_{\varsigma}\sum_{\mu}D_{\varsigma\mu}(t)o_{\varsigma}(x)p_{\mu}(y) \tag{5.2.28d}$$

$$w(x,y,t)=\sum_{\varsigma}\sum_{\mu}E_{\varsigma\mu}(t)q_{\varsigma}(x)r_{\mu}(y) \tag{5.2.28e}$$

or, using single summation instead of double summation yields,

$$\psi_x(x,y,t)=\sum_{i}A_i(t)f_{\varsigma}(x)g_{\mu}(y) \tag{5.2.29a}$$

$$\psi_y(x,y,t)=\sum_{i}B_i(t)h_{\varsigma}(x)l_{\mu}(y) \tag{5.2.29b}$$

$$u(x,y,t)=\sum_{i}C_i(t)m_{\varsigma}(x)n_{\mu}(y) \tag{5.2.29c}$$

$$v(x,y,t)=\sum_{i}D_i(t)o_{\varsigma}(x)p_{\mu}(y) \tag{5.2.29d}$$

$$w(x,y,t)=\sum_{i}E_i(t)q_{\varsigma}(x)r_{\mu}(y) \tag{5.2.29e}$$

where A_i, B_i, C_i, D_i, E_i are modal amplitudes to be determined from the analysis and the index numbers, i, ς, μ, are related by some organized scheme as previously shown in Table 2.1.† Beam functions, $f, g, h, l, m, n, o, p, q, r$ representing mode shapes are discussed in Section 5.2.4 after a reduction of the system of equations.

† In this case, ς and μ are replaced by r and s shown in Table 2.1.

Lagrangian Equations of Motion

The Lagrangian function L, is defined to be,

$$L = T - U \tag{5.2.30}$$

The Lagrangian equations of motion [31] can be expressed as,

$$\frac{d}{dt}\left(\frac{\partial L}{\partial \dot{q}_j}\right) - \frac{\partial L}{\partial q_j} = Q_j \qquad j = 1, 2, \ldots, M \tag{5.2.31}$$

where M denotes the number of degrees of freedom, and q_j denotes the generalized coordinates. In this analysis, q_j are A_i, B_i, C_i, D_i, E_i, and the number of degrees of freedom would be $j = 5 \times i = 5 \times \varsigma \times \mu$. Since the kinetic energy is a function of $\dot{q}_j$ only and the potential energy is a function of q_j only, Eq. (5.2.31) can be expanded to the following forms.

$$\begin{aligned}
\frac{d}{dt}\left(\frac{\partial T}{\partial \dot{A}_i}\right) + \frac{\partial U}{\partial A_i} &= P_{ai} \\
\frac{d}{dt}\left(\frac{\partial T}{\partial \dot{B}_i}\right) + \frac{\partial U}{\partial B_i} &= P_{bi} \\
\frac{d}{dt}\left(\frac{\partial T}{\partial \dot{C}_i}\right) + \frac{\partial U}{\partial C_i} &= P_{ci} \\
\frac{d}{dt}\left(\frac{\partial T}{\partial \dot{D}_i}\right) + \frac{\partial U}{\partial D_i} &= P_{di} \\
\frac{d}{dt}\left(\frac{\partial T}{\partial \dot{E}_i}\right) + \frac{\partial U}{\partial E_i} &= P_{ei}
\end{aligned} \tag{5.2.32}$$

where $P_{ai}, P_{bi}, P_{ci}, P_{di}, P_{ei}$ indicate the work done by the external forces.

Substituting Eqs. (5.2.11), (5.2.18), and (5.2.29) into Eqs. (5.2.32) yields the following system of equations,

$$[\underline{M}]\begin{Bmatrix}\ddot{\underline{A}}_i\\ \ddot{\underline{B}}_i\\ \ddot{\underline{C}}_i\\ \ddot{\underline{D}}_i\\ \ddot{\underline{E}}_i\end{Bmatrix}+[\underline{K}_{\mathrm{I}}]\begin{Bmatrix}\underline{A}_i\\ \underline{B}_i\\ \underline{C}_i\\ \underline{D}_i\\ \underline{E}_i\end{Bmatrix}+[\underline{K}_{\mathrm{II}}]\begin{Bmatrix}\underline{A_kE_l}\\ \underline{B_kE_l}\\ \underline{C_kE_l}\\ \underline{D_kE_l}\\ \underline{E_kE_l}\end{Bmatrix}+[\underline{K}_{\mathrm{III}}]\begin{Bmatrix}\underline{A_kE_lE_m}\\ \underline{B_kE_lE_m}\\ \underline{C_kE_lE_m}\\ \underline{D_kE_lE_m}\\ \underline{E_kE_lE_m}\end{Bmatrix}=-F\{\underline{R}\} \tag{5.2.33}$$

where,

$$[\underline{M}]=\begin{bmatrix}\underline{I_a} & \underline{0} & \underline{I_b} & \underline{0} & \underline{0}\\ \underline{0} & \underline{I_c} & \underline{0} & \underline{I_d} & \underline{0}\\ \underline{I_b}^{\mathrm{T}} & \underline{0} & \underline{I_e} & \underline{0} & \underline{0}\\ \underline{0} & \underline{I_d}^{\mathrm{T}} & \underline{0} & \underline{I_f} & \underline{0}\\ \underline{0} & \underline{0} & \underline{0} & \underline{0} & \underline{m}\end{bmatrix} \tag{5.2.34a}$$

$$[\underline{K}_{\mathrm{I}}]=\begin{bmatrix}\underline{K}_{\mathrm{I}aa} & \underline{K}_{\mathrm{I}ab} & \underline{K}_{\mathrm{I}ac} & \underline{K}_{\mathrm{I}ad} & \underline{K}_{\mathrm{I}ae}\\ \underline{K}_{\mathrm{I}ab}^{\mathrm{T}} & \underline{K}_{\mathrm{I}bb} & \underline{K}_{\mathrm{I}bc} & \underline{K}_{\mathrm{I}bd} & \underline{K}_{\mathrm{I}be}\\ \underline{K}_{\mathrm{I}ac}^{\mathrm{T}} & \underline{K}_{\mathrm{I}bc}^{\mathrm{T}} & \underline{K}_{\mathrm{I}cc} & \underline{K}_{\mathrm{I}cd} & \underline{0}\\ \underline{K}_{\mathrm{I}ad}^{\mathrm{T}} & \underline{K}_{\mathrm{I}bd}^{\mathrm{T}} & \underline{K}_{\mathrm{I}cd}^{\mathrm{T}} & \underline{K}_{\mathrm{I}dd} & \underline{0}\\ \underline{K}_{\mathrm{I}ae}^{\mathrm{T}} & \underline{K}_{\mathrm{I}be}^{\mathrm{T}} & \underline{0} & \underline{0} & \underline{K}_{\mathrm{I}ee}\end{bmatrix} \tag{5.2.34b}$$

$$[\underline{K}_{\mathrm{II}}]=\begin{bmatrix}\underline{0} & \underline{0} & \underline{0} & \underline{0} & \underline{K}_{\mathrm{II}ae}\\ \underline{0} & \underline{0} & \underline{0} & \underline{0} & \underline{K}_{\mathrm{II}be}\\ \underline{0} & \underline{0} & \underline{0} & \underline{0} & \underline{K}_{\mathrm{II}ce}\\ \underline{0} & \underline{0} & \underline{0} & \underline{0} & \underline{K}_{\mathrm{II}de}\\ \underline{K}_{\mathrm{II}ea} & \underline{K}_{\mathrm{II}eb} & \underline{K}_{\mathrm{II}ec} & \underline{K}_{\mathrm{II}ed} & \underline{0}\end{bmatrix} \tag{5.2.34c}$$

$$[\underline{K}_{III}] = \begin{bmatrix} \underline{0} & \underline{0} & \underline{0} & \underline{0} & \underline{0} \\ \underline{0} & \underline{0} & \underline{0} & \underline{0} & \underline{0} \\ \underline{0} & \underline{0} & \underline{0} & \underline{0} & \underline{0} \\ \underline{0} & \underline{0} & \underline{0} & \underline{0} & \underline{0} \\ \underline{0} & \underline{0} & \underline{0} & \underline{0} & \underline{K}_{III_{ee}} \end{bmatrix} \tag{5.2.34d}$$

$$\{\underline{R}\} = \begin{Bmatrix} \underline{R}_{ai} \\ \underline{R}_{bi} \\ \underline{R}_{ci} \\ \underline{R}_{di} \\ \underline{R}_{ei} \end{Bmatrix} \tag{5.2.34e}$$

F denotes an external applied force. Each element of the inertia matrix, stiffness matrices for the linear and nonlinear terms, and the generalized force vector is given in terms of assumed mode shapes as follows.

Inertia Matrix $[\underline{M}]$:

$$\underline{I}_a = \int_0^b \int_0^a I_3 (f_i g_i)(f_j g_j)\, dx\, dy \tag{5.2.35a}$$

$$\underline{I}_b = \int_0^b \int_0^a I_2 (f_i g_i)(m_j n_j)\, dx\, dy \tag{5.2.35b}$$

$$\underline{I}_c = \int_0^b \int_0^a I_3 (h_i l_i)(h_j l_j)\, dx\, dy \tag{5.2.35c}$$

$$\underline{I}_d = \int_0^b \int_0^a I_2 (h_i l_i)(o_j p_j)\, dx\, dy \tag{5.2.35d}$$

$$\underline{I}_e = \int_0^b \int_0^a I_1 (m_i n_i)(m_j n_j)\, dx\, dy \tag{5.2.35e}$$

$$\underline{I}_f = \int_0^b \int_0^a I_1 (o_i p_i)(o_j p_j)\, dx\, dy \tag{5.2.35f}$$

$$\underline{m} = \int_0^b \int_0^a I_1 (q_i r_i)(q_j r_j)\, dx\, dy \qquad (5.2.35g)$$

Stiffness Matrix $[\underline{K}_I]$:

$$\underline{K}_{Iaa} = \int_0^b \int_0^a \begin{bmatrix} D_{11}(f_i' g_i)(f_j' g_j) + D_{16}(f_i' g_i)(f_j g_j') + D_{16}(f_i g_i')(f_j' g_j) \\ + D_{66}(f_i g_i')(f_j g_j') + G_{55}(f_i g_i)(f_j g_j) \end{bmatrix} dx\, dy \qquad (5.3.36a)$$

$$\underline{K}_{Iab} = \int_0^b \int_0^a \begin{bmatrix} D_{12}(f_i' g_i)(h_j l_j') + D_{16}(f_i' g_i)(h_j' l_j) + D_{26}(f_i g_i')(h_j l_j') \\ + D_{66}(f_i g_i')(h_j' l_j) + G_{45}(f_i g_i)(h_j l_j) \end{bmatrix} dx\, dy \qquad (5.2.36b)$$

$$\underline{K}_{Iac} = \int_0^b \int_0^a \begin{bmatrix} B_{11}(f_i' g_i)(m_j' n_j) + B_{16}(f_i g_i')(m_j' n_j) + B_{16}(f_i' g_i)(m_j n_j') \\ + B_{66}(f_i g_i')(m_j n_j') \end{bmatrix} dx\, dy \qquad (5.2.36c)$$

$$\underline{K}_{Iad} = \int_0^b \int_0^a \begin{bmatrix} B_{12}(f_i' g_i)(o_j p_j') + B_{16}(f_i' g_i)(o_j' p_j) + B_{26}(f_i g_i')(o_j p_j') \\ + B_{66}(f_i g_i')(o_j' p_j) \end{bmatrix} dx\, dy \qquad (5.2.36d)$$

$$\underline{K}_{Iae} = \int_0^b \int_0^a \left[G_{55}(f_i g_i)(q_j' r_j) + G_{45}(f_i g_i)(q_j r_j') \right] dx\, dy \qquad (5.2.36e)$$

$$\underline{K}_{Ibb} = \int_0^b \int_0^a \begin{bmatrix} D_{22}(h_i l_i')(h_j l_j') + D_{26}(h_i' g_i)(h_j l_j') + D_{26}(h_i l_i')(h_j' l_j) \\ + D_{66}(h_i' l_i)(h_j' l_j) + G_{44}(h_i l_i)(h_j l_j) \end{bmatrix} dx\, dy \qquad (5.2.36f)$$

$$\underline{K}_{Ibc} = \int_0^b \int_0^a \begin{bmatrix} B_{12}(h_i l_i')(m_j' n_j) + B_{16}(h_i' l_i)(m_j' n_j) + B_{26}(h_i l_i')(m_j n_j') \\ + B_{66}(h_i' l_i)(m_j n_j') \end{bmatrix} dx\, dy \qquad (5.2.36g)$$

$$\underline{K}_{\mathrm{I}bd} = \int_0^b \int_0^a \begin{bmatrix} B_{22}(h_i l_i')(o_j p_j') + B_{26}(h_i' l_i)(o_j p_j') + B_{26}(h_i l_i')(o_j' p_j) \\ + B_{66}(h_i' l_i)(o_j' p_j) \end{bmatrix} dx\,dy \qquad (5.2.36h)$$

$$\underline{K}_{\mathrm{I}be} = \int_0^b \int_0^a \left[G_{45}(h_i l_i)(q_j' r_j) + G_{44}(h_i l_i)(q_j r_j') \right] dx\,dy \qquad (5.2.36i)$$

$$\underline{K}_{\mathrm{I}cc} = \int_0^b \int_0^a \begin{bmatrix} A_{11}(m_i' n_i)(m_j' n_j) + A_{16}(m_i n_i')(m_j' n_j) + A_{16}(m_i' n_i)(m_j n_j') \\ + A_{66}(m_i n_i')(m_j n_j') \end{bmatrix} dx\,dy \qquad (5.2.36j)$$

$$\underline{K}_{\mathrm{I}cd} = \int_0^b \int_0^a \begin{bmatrix} A_{12}(m_i' n_i)(o_j p_j') + A_{16}(m_i' n_i)(o_j' p_j) + A_{26}(m_i n_i')(o_j p_j') \\ + A_{66}(m_i n_i')(o_j' p_j) \end{bmatrix} dx\,dy \qquad (5.2.36k)$$

$$\underline{K}_{\mathrm{I}dd} = \int_0^b \int_0^a \begin{bmatrix} A_{22}(o_i p_i')(o_j p_j') + A_{26}(o_i' p_i)(o_j p_j') + A_{26}(o_i p_i')(o_j' p_j) \\ + A_{66}(o_i' p_i)(o_j' p_j) \end{bmatrix} dx\,dy \qquad (5.2.36l)$$

$$\underline{K}_{\mathrm{I}ee} = \int_0^b \int_0^a \begin{bmatrix} G_{55}(q_i' r_i)(q_j' r_j) + G_{45}(q_i' r_i)(q_j r_j') \\ + G_{45}(q_i r_i')(q_j' r_j) + G_{44}(q_i r_i')(q_j r_j') \end{bmatrix} dx\,dy \qquad (5.2.36m)$$

Stiffness Matrix $[\underline{K}_{\mathrm{II}}]$:

$$\underline{K}_{\mathrm{II}ae} = \int_0^b \int_0^a \begin{bmatrix} \frac{1}{2} B_{11}(f_i' g_i)(q_k' r_k)(q_l' r_l) + \frac{1}{2} B_{12}(f_i' g_i)(q_k r_k')(q_l r_l') \\ + \frac{1}{2} B_{16}(f_i g_i')(q_k' r_k)(q_l' r_l) + B_{16}(f_i' g_i)(q_k' r_k)(q_l r_l') \\ + \frac{1}{2} B_{26}(f_i g_i')(q_k r_k')(q_l r_l') + B_{66}(f_i g_i')(q_k' r_k)(q_l r_l') \end{bmatrix} dx\,dy \qquad (5.2.37a)$$

$$\underline{K}_{\Pi be} = \int_0^b \int_0^a \begin{bmatrix} \frac{1}{2} B_{12}(h_i l_i')(q_k' r_k)(q_l' r_l) + \frac{1}{2} B_{16}(h_i' l_i)(q_k' r_k)(q_l' r_l) \\ + \frac{1}{2} B_{22}(h_i l_i')(q_k r_k')(q_l r_l') + \frac{1}{2} B_{26}(h_i' l_i)(q_k r_k')(q_l r_l') \\ + B_{26}(h_i l_i')(q_k' r_k)(q_l r_l') + B_{66}(h_i' l_i)(q_k' r_k)(q_l r_l') \end{bmatrix} dx\,dy \qquad (5.2.37b)$$

$$\underline{K}_{\Pi ce} = \int_0^b \int_0^a \begin{bmatrix} \frac{1}{2} A_{11}(m_i' n_i)(q_k' r_k)(q_l' r_l) + \frac{1}{2} A_{12}(m_i' n_i)(q_k r_k')(q_l r_l') \\ + A_{16}(m_i' n_i)(q_k' r_k)(q_l r_l') + \frac{1}{2} A_{16}(m_i n_i')(q_k' r_k)(q_l' r_l) \\ + \frac{1}{2} A_{26}(m_i n_i')(q_k r_k')(q_l r_l') + A_{66}(m_i n_i')(q_k' r_k)(q_l r_l') \end{bmatrix} dx\,dy \qquad (5.2.37c)$$

$$\underline{K}_{\Pi de} = \int_0^b \int_0^a \begin{bmatrix} \frac{1}{2} A_{12}(o_i p_i')(q_k' r_k)(q_l' r_l) + \frac{1}{2} A_{22}(o_i p_i')(q_k r_k')(q_l r_l') \\ + \frac{1}{2} A_{16}(o_i' p_i)(q_k' r_k)(q_l' r_l) + A_{26}(o_i p_i')(q_k' r_k)(q_l r_l') \\ + \frac{1}{2} A_{26}(o_i' p_i)(q_k r_k')(q_l r_l') + A_{66}(o_i' p_i)(q_k' r_k)(q_l r_l') \end{bmatrix} dx\,dy \qquad (5.2.37d)$$

$$\underline{K}_{\Pi ea} = \int_0^b \int_0^a \begin{bmatrix} B_{11}(q_i' r_i)(f_k' g_k)(q_l' r_l) + B_{12}(q_i r_i')(f_k' g_k)(q_l r_l') \\ + B_{16}(q_i' r_i)(f_k g_k')(q_l' r_l) + B_{16}(q_i' r_i)(f_k' g_k)(q_l r_l') \\ + B_{16}(q_i r_i')(f_k' g_k)(q_l' r_l) + B_{26}(q_i r_i')(f_k g_k')(q_l r_l') \\ + B_{66}(q_i' r_i)(f_k g_k')(q_l r_l') + B_{66}(q_i r_i')(f_k g_k')(q_l' r_l) \end{bmatrix} dx\,dy \qquad (5.2.37e)$$

$$\underline{K}_{\Pi eb} = \int_0^b \int_0^a \begin{bmatrix} B_{12}(q_i' r_i)(h_k l_k')(q_l' r_l) + B_{16}(q_i' r_i)(h_k' l_k)(q_l' r_l) \\ + B_{22}(q_i r_i')(h_k l_k')(q_l r_l') + B_{26}(q_i r_i')(h_k' l_k)(q_l r_l') \\ + B_{26}(q_i' r_i)(h_k l_k')(q_l r_l') + B_{26}(q_i r_i')(h_k l_k')(q_l' r_l) \\ + B_{66}(q_i' r_i)(h_k' l_k)(q_l r_l') + B_{66}(q_i r_i')(h_k' l_k)(q_l' r_l) \end{bmatrix} dx\,dy \qquad (5.2.37f)$$

$$\underline{K}_{\Pi ec} = \int_0^b \int_0^a \begin{bmatrix} A_{11}(q_i' r_i)(m_k' n_k)(q_l' r_l) + A_{12}(q_i r_i')(m_k' n_k)(q_l r_l') \\ +A_{16}(q_i' r_i)(m_k' n_k)(q_l r_l') + A_{16}(q_i r_i')(m_k' n_k)(q_l' r_l) \\ +A_{16}(q_i' r_i)(m_k n_k')(q_l' r_l) + A_{26}(q_i r_i')(m_k n_k')(q_l r_l') \\ +A_{66}(q_i' r_i)(m_k n_k')(q_l r_l') + A_{66}(q_i r_i')(m_k n_k')(q_l' r_l) \end{bmatrix} dx\,dy \qquad (5.2.37g)$$

$$\underline{K}_{\Pi ed} = \int_0^b \int_0^a \begin{bmatrix} A_{12}(q_i' r_i)(o_k p_k')(q_l' r_l) + A_{22}(q_i r_i')(o_k p_k')(q_l r_l') \\ +A_{16}(q_i' r_i)(o_k' p_k)(q_l' r_l) + A_{26}(q_i' r_i)(o_k p_k')(q_l r_l') \\ +A_{26}(q_i r_i')(o_k p_k')(q_l' r_l) + A_{26}(q_i r_i')(o_k' p_k)(q_l r_l') \\ +A_{66}(q_i' r_i)(o_k' p_k)(q_l r_l') + A_{66}(q_i r_i')(o_k' p_k)(q_l' r_l) \end{bmatrix} dx\,dy \qquad (5.2.37h)$$

Stiffness Matrix $[\underline{K}_{III}]$:

$$\underline{K}_{III_{ee}} = \int_0^b \int_0^a \begin{bmatrix} \frac{1}{2}A_{11}(q_i' r_i)(q_k' r_k)(q_l' r_l)(q_m' r_m) \\ +\frac{1}{2}A_{12}(q_i' r_i)(q_k' r_k)(q_l r_l')(q_m r_m') \\ +\frac{1}{2}A_{12}(q_i r_i')(q_k' r_k)(q_l' r_l)(q_m r_m') \\ +\frac{1}{2}A_{22}(q_i r_i')(q_k r_k')(q_l r_l')(q_m r_m') \\ +\frac{3}{2}A_{16}(q_i' r_i)(q_k' r_k)(q_l' r_l)(q_m r_m') \\ +\frac{1}{2}A_{16}(q_i r_i')(q_k' r_k)(q_l' r_l)(q_m' r_m) \\ +\frac{1}{2}A_{26}(q_i' r_i)(q_k r_k')(q_l r_l')(q_m r_m') \\ +\frac{3}{2}A_{26}(q_i r_i')(q_k' r_k)(q_l r_l')(q_m r_m') \\ +A_{66}(q_i' r_i)(q_k' r_k)(q_l r_l')(q_m r_m') \\ +A_{66}(q_i r_i')(q_k' r_k)(q_l' r_l)(q_m r_m') \end{bmatrix} dx\,dy \qquad (5.2.38)$$

Generalized Force Vector † $\{\underline{R}\}$:

$$\{\underline{R}\} = \begin{Bmatrix} \underline{R}_{ai} \\ \underline{R}_{bi} \\ \underline{R}_{ci} \\ \underline{R}_{di} \\ \underline{R}_{ei} \end{Bmatrix} = \begin{Bmatrix} \underline{0} \\ \underline{0} \\ \underline{0} \\ \underline{0} \\ [q_i(\xi_c) r_i(\eta_c)] \end{Bmatrix} \qquad (5.2.39)$$

† The transverse impact force is assumed to act at (ξ_c, η_c) as shown in Figure 2.1.

The index systems used in Eq. (5.2.33) are organized as in the following examples.

Index "i" system:

$$\left\{\underline{\ddot{A}}_i\right\} = \begin{Bmatrix} \ddot{A}_1 \\ \ddot{A}_2 \\ \ddot{A}_3 \\ \vdots \\ \vdots \end{Bmatrix} \tag{5.2.40a}$$

Index "k & l" system:

$$\left\{\underline{A_k E_l}\right\} = \begin{Bmatrix} A_1E_1 \\ A_1E_2 \\ A_1E_3 \\ \vdots \\ A_2E_1 \\ A_2E_2 \\ A_2E_3 \\ \vdots \\ A_3E_1 \\ A_3E_2 \\ A_3E_3 \\ \vdots \end{Bmatrix} \tag{5.2.40b}$$

Index "k, l, & m" system:

$$\left\{\underline{E_k E_l E_m}\right\} = \begin{Bmatrix} E_1E_1E_1 \\ E_1E_1E_2 \\ E_1E_1E_3 \\ \vdots \\ E_1E_2E_1 \\ E_1E_2E_2 \\ E_1E_2E_3 \\ \vdots \\ E_1E_3E_1 \\ E_1E_3E_2 \\ E_1E_3E_3 \\ \vdots \\ E_2E_1E_1 \\ E_2E_1E_2 \\ E_2E_1E_3 \\ \vdots \\ E_2E_2E_1 \\ E_2E_2E_2 \\ E_2E_2E_3 \\ \vdots \end{Bmatrix} \qquad (5.2.40c)$$

Note that for $\varsigma \times \mu = 3 \times 3$ mode case in Eq. (5.2.29), the sizes of the matrices in Eq. (5.2.33) are, 45×45 for $[\underline{M}]$ and $[\underline{K}_{\mathrm{I}}]$, 45×405 for $[\underline{K}_{\mathrm{II}}]$, and $45 \times 3{,}645$ for $[\underline{K}_{\mathrm{III}}]$. For the case of $\varsigma \times \mu = 7 \times 7$ mode, the sizes of the matrices increase geometrically to 245×245 for $[\underline{M}]$ and $[\underline{K}_{\mathrm{I}}]$, $245 \times 12{,}005$ for $[\underline{K}_{\mathrm{II}}]$, and $245 \times 588{,}245$ for $[\underline{K}_{\mathrm{III}}]$.

5.2.4 Reduction of the Plate Equations of Motion

The plate equations of motion (5.2.33) are reduced by making additional assumptions in order to minimize the computational intensity. These assumptions are as follows.

i) symmetric laminate is assumed ($B_{ij}=0$).

ii) in-plane displacements are neglected compared to the out-of-plane displacement.

Assumption i) was also made in Chapter 2 and is appropriate since many of the practical laminated composite plates take symmetrical stacking sequences. Assumption ii) is based on the assumption that the influence of in-plane displacement is negligible for the particular impact problem studied here as evidenced from the nonlinear beam study in Section 4.4.

By assuming symmetric laminates, $B_{ij}=0$, and neglecting all the in-plane displacements, u and v, as well as the corresponding assumed mode shapes, $m_\varsigma(x), n_\mu(y), o_\varsigma(x), p_\mu(y)$, representing the u, v terms, Eq. (5.2.33) can be reduced to the following form.

$$[\underline{M}]\begin{Bmatrix}\ddot{\underline{A}}_i\\ \ddot{\underline{B}}_i\\ \ddot{\underline{E}}_i\end{Bmatrix}+[\underline{K}_{\mathrm{I}}]\begin{Bmatrix}\underline{A}_i\\ \underline{B}_i\\ \underline{E}_i\end{Bmatrix}+[\underline{K}_{\mathrm{III}}]\begin{Bmatrix}\underline{A_kE_lE_m}\\ \underline{B_kE_lE_m}\\ \underline{E_kE_lE_m}\end{Bmatrix}=-F_z\{\underline{R}\} \tag{5.2.41}$$

where,

$$[\underline{M}]=\begin{bmatrix} \underline{I}_a & \underline{0} & \underline{0} \\ \underline{0} & \underline{I}_b & \underline{0} \\ \underline{0} & \underline{0} & \underline{m} \end{bmatrix} \tag{5.2.42a}$$

$$[\underline{K}_{\mathrm{I}}]=\begin{bmatrix} \underline{K}_{\mathrm{I}aa} & \underline{K}_{\mathrm{I}ab} & \underline{K}_{\mathrm{I}ae} \\ \underline{K}_{\mathrm{I}ab}{}^{\mathrm{T}} & \underline{K}_{\mathrm{I}bb} & \underline{K}_{\mathrm{I}be} \\ \underline{K}_{\mathrm{I}ae}{}^{\mathrm{T}} & \underline{K}_{\mathrm{I}be}{}^{\mathrm{T}} & \underline{K}_{\mathrm{I}ee} \end{bmatrix} \tag{5.2.42b}$$

$$[\underline{K}_{\mathrm{III}}]=\begin{bmatrix} \underline{0} & \underline{0} & \underline{0} \\ \underline{0} & \underline{0} & \underline{0} \\ \underline{0} & \underline{0} & \underline{K}_{\mathrm{III}ee} \end{bmatrix} \tag{5.2.42c}$$

$$\{\underline{R}\}=\begin{Bmatrix} \underline{R}_{ai} \\ \underline{R}_{bi} \\ \underline{R}_{ei} \end{Bmatrix} \tag{5.2.42d}$$

Since there is no coupling involved in the $[\underline{K}_{\mathrm{III}}]$ term, the plate equations of motion (5.2.41) are simplified further by static condensation†. Neglecting rotary inertia terms, while retaining the influence of shearing deformation, results in the following equations in terms of out-of-plane modal amplitude only.

$$[\underline{m}]\{\ddot{\underline{E}}_i\}+[\underline{K}_{\mathrm{I}}]\{\underline{E}_i\}+[\underline{K}_{\mathrm{III}ee}]\{\underline{E_k E_l E_m}\}=-F_z\{\underline{R}_{ei}\} \tag{5.2.43}$$

where,

$$\underline{K}_{\mathrm{I}}=\underline{K}_{\mathrm{I}ee}-\begin{bmatrix} \underline{K}_{\mathrm{I}ae}{}^{\mathrm{T}} & \underline{K}_{\mathrm{I}be}{}^{\mathrm{T}} \end{bmatrix}\begin{bmatrix} \underline{K}_{\mathrm{I}aa} & \underline{K}_{\mathrm{I}ab} \\ \underline{K}_{\mathrm{I}ab}{}^{\mathrm{T}} & \underline{K}_{\mathrm{I}bb} \end{bmatrix}^{-1}\begin{bmatrix} \underline{K}_{\mathrm{I}ae} \\ \underline{K}_{\mathrm{I}be} \end{bmatrix} \tag{5.2.44}$$

† Discussion regarding the static condensation by neglecting rotary inertia terms are made in Section 2.2.3.

By using the beam shape functions for free-free boundary conditions in one direction, the inversed term in Eq. (5.2.44) becomes singular and can not be inversed without some rearrangement. Normally, some of the rows and columns are all zero's and those should be eliminated. Also, corresponding rows and columns in Eq. (5.2.42b) should be eliminated and compressed.

Since the in-plane displacements, u and v, and their corresponding assumed mode shapes are neglected, only the rotations, ψ_x and ψ_y, the out-of-plane displacement, w, and their corresponding assumed mode shapes should be considered. Following the procedure taken in Section 2.2.3, the beam functions representing mode shapes in Eqs. (5.2.29a,b,e) are assumed to have the relations described as,

$$\begin{aligned} f_\alpha(\xi) &= \frac{d}{d\xi}\left[q_\alpha(\xi)\right] \\ h_\alpha(\xi) &= q_\alpha(\xi) \\ g_\beta(\eta) &= r_\beta(\eta) \\ l_\beta(\eta) &= \frac{d}{d\eta}\left[r_\beta(\eta)\right] \end{aligned} \tag{5.2.45}$$

Each beam function takes a form depending on the boundary condition. In this analysis, Generalized Beam Functions (GBFs) studied by Dugundji [30] are employed.†

† See Appendix A for more detail concerning the Generalized Beam Functions.

5.2.5 System of Equations of Motion

The system of equations of motion including both the plate and rigid impactor equations of motion is now constructed. The impactor is assumed as a point mass whose equation of motion can be derived from Newton's second law of motion as,

$$m_I \ddot{u}_I = -F_z \tag{5.2.46}$$

where m_I is the mass of the impactor, u_I is the displacement of the impactor, and F_z is the impact force in the transverse direction. Eqs. (5.2.43) and (5.2.46) can be combined to give,

$$\underline{M}\ddot{\underline{\lambda}} + \underline{K}^* \underline{\lambda} + \underline{K}_{\text{III}}{}^* \underline{\lambda}^{[3]} = -F_z \underline{R} \tag{5.2.47}$$

where,

$$\begin{aligned} \underline{M} &= \begin{bmatrix} \underline{m} & \underline{0} \\ \underline{0} & m_I \end{bmatrix}, \qquad \underline{K}^* = \begin{bmatrix} \underline{K} & \underline{0} \\ \underline{0} & 0 \end{bmatrix}, \\ \underline{K}_{\text{III}}{}^* &= \begin{bmatrix} \underline{K}_{\text{III}_{ee}} & \underline{0} \\ \underline{0} & 0 \end{bmatrix}, \qquad \underline{R} = \begin{Bmatrix} \underline{R}_{ei} \\ 1 \end{Bmatrix} \end{aligned} \tag{5.2.48}$$

and the generalized coordinates are,

$$\ddot{\underline{\lambda}} = \begin{Bmatrix} \ddot{\underline{E}}_i \\ \ddot{u}_I \end{Bmatrix}, \qquad \underline{\lambda} = \begin{Bmatrix} \underline{E}_i \\ u_I \end{Bmatrix}, \qquad \underline{\lambda}^{[3]} = \begin{Bmatrix} \underline{E_k E_l E_m} \\ 0 \end{Bmatrix} \tag{5.2.49}$$

The plate midplane displacement, w, and the impactor displacement, u_I, are assumed to be coupled together by the Hertzian contact law which assumes a nonlinear local contact spring [14].† The

† The analytical contact law model [41] is summarized in Appendix B for isotropic material case.

schematic of the rigid impactor contact on a flexible plate is illustrated in Figure 2.3. The constitutive equation for the Hertzian stiffness relation can be written as,

$$F_z = F = k\alpha^n \tag{5.2.50}$$

where k is the local contact stiffness of the plate and n is the exponent value controlling the stiffening property of the contact spring. The indentation of the plate is modeled as,

$$\alpha = u_I + w = \underline{R}^{\mathrm{T}} \underline{\lambda} \tag{5.2.51}$$

The system of the equations of motion are expressed in terms of Eqs. (5.2.47), (5.2.50), and (5.2.51).

5.3 Solution Method

5.3.1 Solution Technique

Direction of Applying Geometrical Nonlinearity

The development of the plate equations of motion in Section 5.2 contains geometrical nonlinearities in both the x and y directions. Due to the reduction of the system of equations performed in Section 5.2.4 based on the assumption which neglects in-plane displacement behavior, the strain energy, U_{I}, as described in Eq. (5.2.13) is reduced and can be expressed in terms of out-of-plane displacement and in-plane stiffnesses, A_{11} and A_{22}, only. Now, A_{11} and A_{22} control the stiffening

effect in the x and y directions, respectively. If a boundary condition does not allow any constraint in either of the directions (i.e. free-free boundary conditions in the x or y direction), only one of the A_{11} and A_{22} terms should be included in order to apply the geometrical nonlinearity in one direction.

Time-Integration

Eqs. (5.2.47), (5.2.50), and (5.2.51) are solved together to produce the generalized coordinates, $\underline{\lambda}$, and impact force, F_z, as functions of time. The initial conditions for this particular impact analysis are,

$$\underline{\lambda}_{t=0} = \begin{Bmatrix} \underline{0} \\ 0 \end{Bmatrix}, \qquad \dot{\underline{\lambda}}_{t=0} = \begin{Bmatrix} \underline{0} \\ \dot{u}_0 \end{Bmatrix}, \qquad \ddot{\underline{\lambda}}_{t=0} = \begin{Bmatrix} \underline{0} \\ 0 \end{Bmatrix} \tag{5.3.1}$$

where $\dot{u}_0$ indicates the initial impactor velocity.

For the impact analysis using *linear* plate theory as discussed in Chapter 2, the Newmark (beta=1/4) time-integration scheme was applied to solve a system of second-order linear differential equations since the scheme is unconditionally stable for linear problems.† This scheme requires a Newton-Raphson method to find a root for a coupled nonlinear equation (Hertzian contact relation) for each time step. However, in order to apply the Newmark (beta=1/4) time-integration scheme to the impact analysis using *nonlinear* plate theory which deals with multiple coupled second-order nonlinear differential equations

† The Newmark (beta=1/4) numerical integration scheme, although unconditionally stable for linear problems, is not proven stable for nonlinear problems [21].

plus a coupled nonlinear Hertzian contact relation, all the roots of the plate equations need to be determined first. Also, apparently, these root findings have to be done for each time step. Since this computation using the Newmark (beta=1/4) time-integration involving root findings would be very costly, the standard fourth-order Runge-Kutta method [45] is employed for the present nonlinear analysis of the impacted plate.

To complete the discretization with respect to time, Eqs. (5.2.47), (5.2.50), and (5.2.51) can be combined and rewritten as,

$$\ddot{\underline{\lambda}}^{(j+1)} = -\underline{M}^{-1}\underline{K}^{*}\underline{\lambda}^{(j)} - \underline{M}^{-1}\underline{K}_{\mathrm{III}}{}^{*}\underline{\lambda}^{[3](j)} - k\left[\underline{R}^{\mathrm{T}}\underline{\lambda}^{(j)}\right]^{n}\underline{M}^{-1}\underline{R} \tag{5.3.2}$$

where the superscripts $(j+1)$ and (j) indicate the time steps.
Eq. (5.3.2) is now divided into two coupled first-order differential equations in order to apply the numerical integration.

$$\begin{aligned}
\dot{\underline{\chi}}^{(j+1)} &= -\underline{M}^{-1}\underline{K}^{*}\underline{\lambda}^{(j)} - \underline{M}^{-1}\underline{K}_{\mathrm{III}}{}^{*}\underline{\lambda}^{[3](j)} - k\left[\underline{R}^{\mathrm{T}}\underline{\lambda}^{(j)}\right]^{n}\underline{M}^{-1}\underline{R} \\
\dot{\underline{\lambda}}^{(j+1)} &= \underline{\chi}^{(j+1)}
\end{aligned} \tag{5.3.3}$$

Eqs. (5.3.3) are now ready for application of the fourth-order Runge-Kutta method.

5.3.2 Computational Issues

The impact model developed using nonlinear laminated plate theory with first-order shear deformation was implemented in a FORTRAN program called "*GLOBAL2*" and installed on MIT's CRAY

X-MP EA/464 supercomputer. The source code of the program is listed in Appendix D. Although *GLOBAL2*, which is an extended version of *GLOBAL*, has the capability to solve both linear and nonlinear problems, it encounters a problem due to the hardware constraint. *GLOBAL2* deals with a relatively large coefficient matrix for the nonlinear (cubic) term as shown in Eq. (5.2.38). For example, using 9×9 modes results in a 81×531,441 non-square $\underline{K}_{III}^{*}$ matrix. Because of its size, *GLOBAL2* requires much more memory (RAM) than *GLOBAL*; the maximum RAM on MIT's CRAY supercomputer limits the *GLOBAL2* to 10×7 (or 9×8) modes. Therefore, *GLOBAL2* has a option that only odd modes can be included, so that, for example, using the maximum of 9×8 modes yields up to 17×15 odd modes. Although it is understood that some laminates having non-zero bending-twisting coupling terms (i.e. $[\pm 45_2 / 0_2]_s$ laminate case) may not bend symmetrically, using odd modes may still provide an adequate response.

Computational time (CPU time) required for this nonlinear analysis is also one of the issues to be noted. The required CPU time seems to be strongly dependent on the number of modes used as input. Initial investigation using *GLOBAL2* indicated that using the 17×15 odd modes, which is the maximum capability of this investigation at this point, and 3,000 time steps requires more than 12 hours of CPU time on the CRAY supercomputer. However, using the 9×9 odd modes and the same number of time steps required less than 30 minutes. Increasing the number of modes leads to an increase of the CPU time at a geometrical rate.

5.4 Numerical Example

In the following numerical example, an impact problem for a 252 mm by 89 mm AS4/3501-6 graphite/epoxy plate in a $[\pm 45_2 / 0_2]_S$ configuration is analyzed. This is the same problem analyzed in Section 2.4 using the linear theory. The input data are summarized in Table 5.1. In Figure 5.1, the force-time histories of both linear analysis and nonlinear analysis are shown. Clearly, there is a notable difference between the results obtained by linear and nonlinear analysis. Peak impact force using nonlinear analysis is five times larger than the one using linear analysis and the impact duration using nonlinear analysis is one fifth of the one using the linear analysis. As claimed by Kant and Mallikarjuna [26], the nonlinear analysis predicts larger peak impact force and shorter impact duration than the linear analysis. In Figure 5.2, this force-time history obtained by nonlinear analysis is compared with experimental data obtained by Wolf [19]. The nonlinear analysis predicts a larger peak force and shorter impact duration than the experimental data.

Table 5.1 : Inputs for *GLOBAL2* Analysis – Example Problem

Laminate Material System :	AS4/3501-6 Graphite/Epoxy
Lay-up :	$[\pm 45_2/0_2]_s$
x-direction Boundary Condition :	Clamped-Clamped (Rigid)
y-direction Boundary Condition :	Free-Free
Plate Length (x-direction) :	252 mm
Plate Width (y-direction) :	89 mm
Plate Thickness :	1.608 mm
Plate Density :	1540 kg/m^3
A_{11} :	125,542,700 N/m
D_{1111} :	17.072 N-m
D_{1122} :	11.272 N-m
D_{1112} :	2.560 N-m
D_{2222} :	15.365 N-m
D_{2212} :	2.560 N-m
D_{1212} :	12.325 N-m
A_{44} :	6.92 MN/m
A_{45} :	0.00 MN/m
A_{55} :	8.06 MN/m
Shear Correction Factor :	0.833
Impactor Mass :	1.53 kg
Impactor Velocity :	3.0 m/s
Local Contact Stiffness :	0.5 GN/m$^{1.5}$
Local Contact Exponent Value :	1.5
Number of Modes in x-direction :	15 (odd modes only)
Number of Modes in y-direction :	15 (odd modes only)
Time Step Increment :	5.0 μs
Number of Time Steps :	3,000 time steps

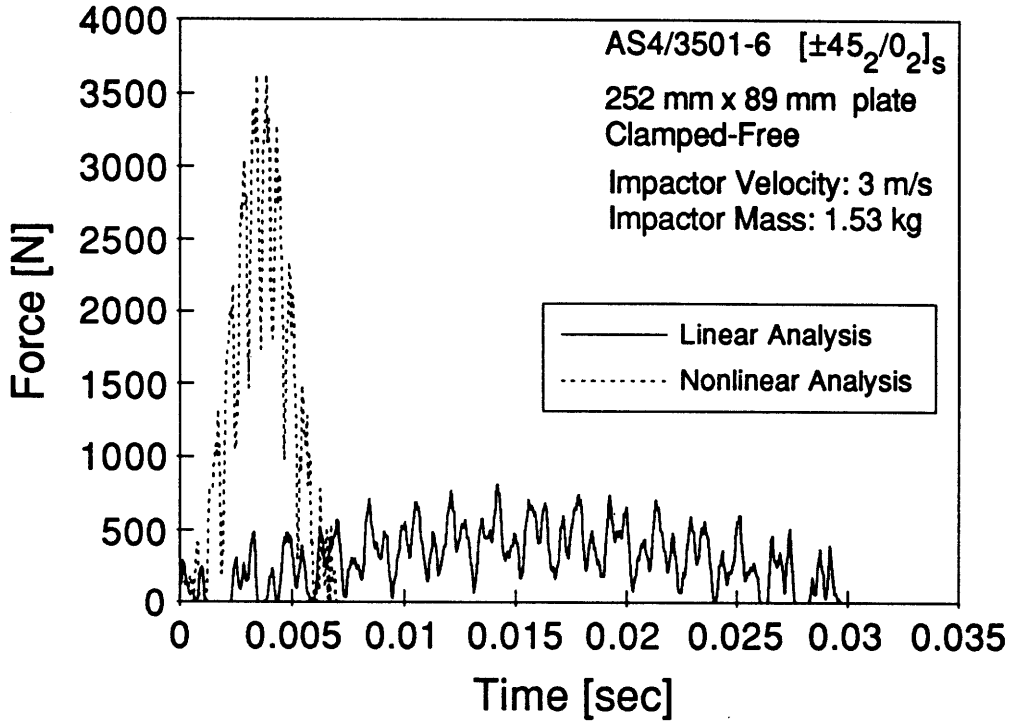

Figure 5.1 : Comparison of Impact Force-Time Histories – Linear Analysis and Nonlinear Analysis

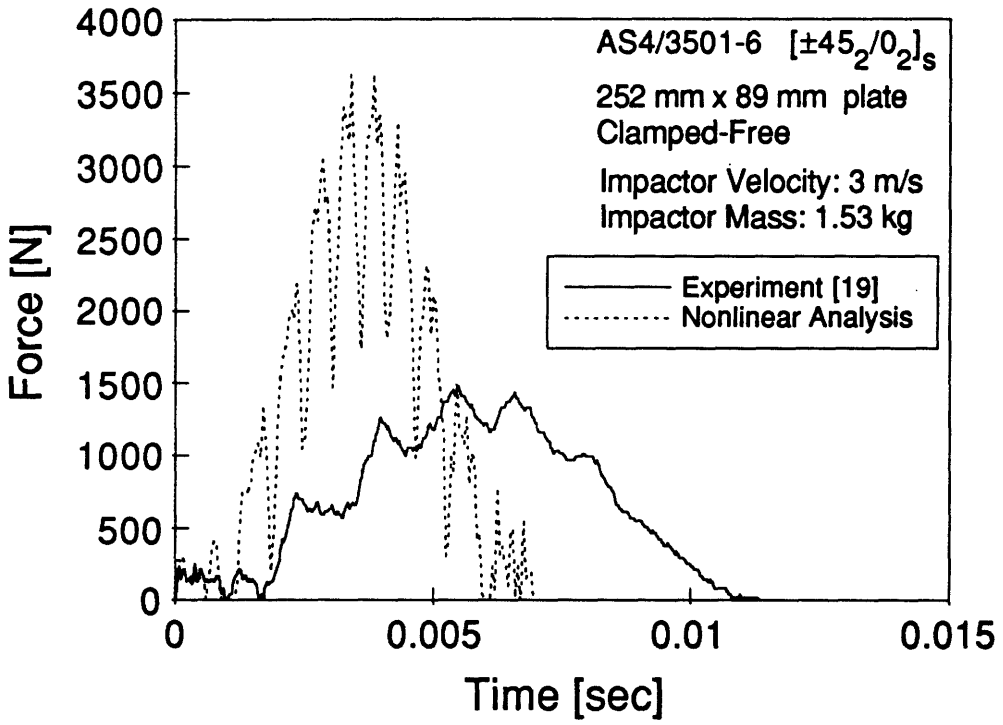

Figure 5.2 : Comparison of Impact Force-Time Histories – Nonlinear Analysis and Experiment

5.5 Summary

In this chapter, an impact model using nonlinear laminated plate theory with first-order shear deformation was developed. The energy equations were derived from the three-dimensional nonlinear theory of elasticity by combining Timoshenko-type theory and von Kármán nonlinear plate theory as described by Reddy [21]. Using the energy equations, a transient impact model was developed by means of Lagrangian equations of motion and the Rayleigh-Ritz method in conjunction with assumed mode shapes.

From the numerical example, the nonlinear analysis predicted a larger peak impact force and shorter impact duration than the linear analysis as expected; however, the nonlinear analysis also predicted a larger peak impact force and shorter impact duration than experiment showed. Some further investigations are discussed in Chapter 6 which provide insight into the usage of nonlinear analysis.

Chapter 6

Results and Discussion of Nonlinear Plate Impact Analysis

6.1 Parametric Studies Using Nonlinear Impact Analysis

The result of the numerical example in Section 5.4 showed that the nonlinear analysis predicted a larger peak impact force and shorter impact duration than the experimental data showed. In order to improve the ability of prediction using nonlinear analysis, there were several parametric studies performed. The parameters varied were the number of modes, the local contact stiffness, and the degree of the geometrical nonlinearity.

6.1.1 Number of Modes

The number of modes used in Section 5.4 was 15×15 modes

containing only odd modes due to the computer hardware constraint as discussed in Section 5.3.2. The validity of the assumption neglecting even modes can be checked by comparing the force-time history using 7×7 modes including both odd and even modes with the force-time history using 7×7 modes including only odd modes which lead to zero bending-twisting coupling terms as shown in Figure 6.1. There was no significant difference in the output which indicated that the bending-twisting coupling terms associated with the even modes in *GLOBAL2* nonlinear analysis were negligible.

Convergence was also checked for the force-time history by changing the number of modes. As can be seen from Figure 6.2, there was little change in the force-time history due to the change in the number of modes. The peak impact force gradually decreased as the number of modes increased, although the change in impact force was small. The assumption that 9×9 modes containing only odd modes was sufficient for convergence appears to be valid. All the following analyses were based on 9×9 modes containing only odd modes.

6.1.2 Local Contact Stiffness

In Figure 6.3, the force-time histories are shown for various values of the local contact stiffness. Unlike the linear analysis results shown in Section 3.3.1, the force-time history obtained by nonlinear analysis was sensitive to the change in the local contact stiffness. The reason for this can be explained using the simplified spring-mass model shown in Figure 3.9. For nonlinear analysis, the ratio of the two spring

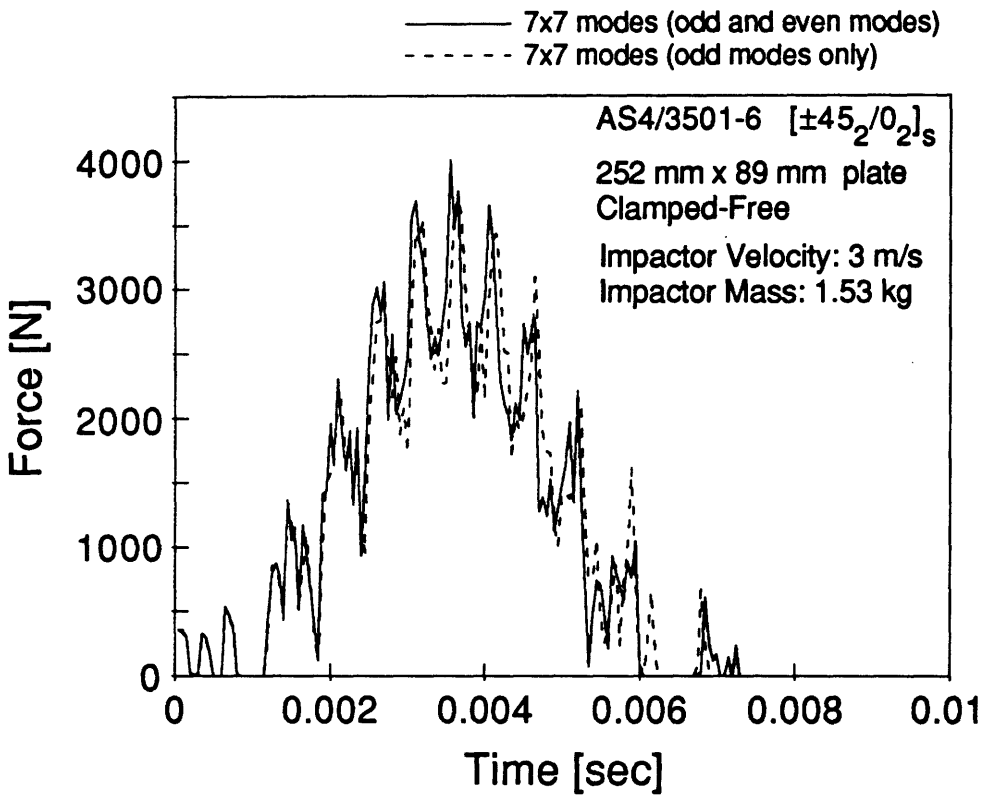

Figure 6.1 : Effect of Bending-Twisting Coupling in Nonlinear Analysis (Using only odd modes results in zero bending-twisting coupling.)

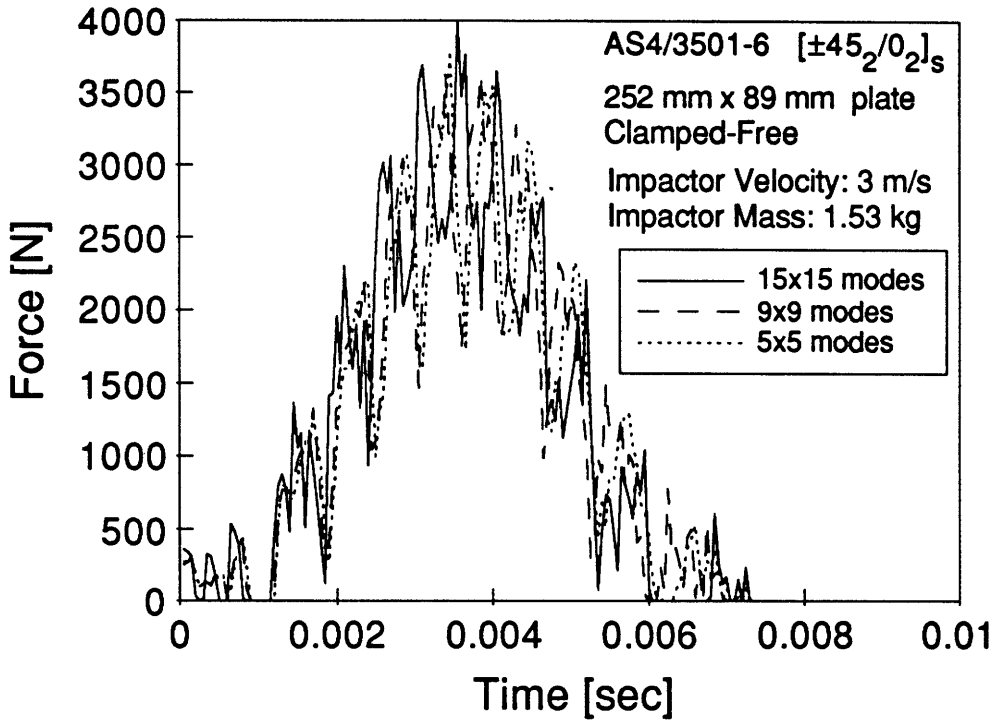

Figure 6.2 : Force-Time Histories for Various Number of Modes by Nonlinear Analysis Using *GLOBAL2*

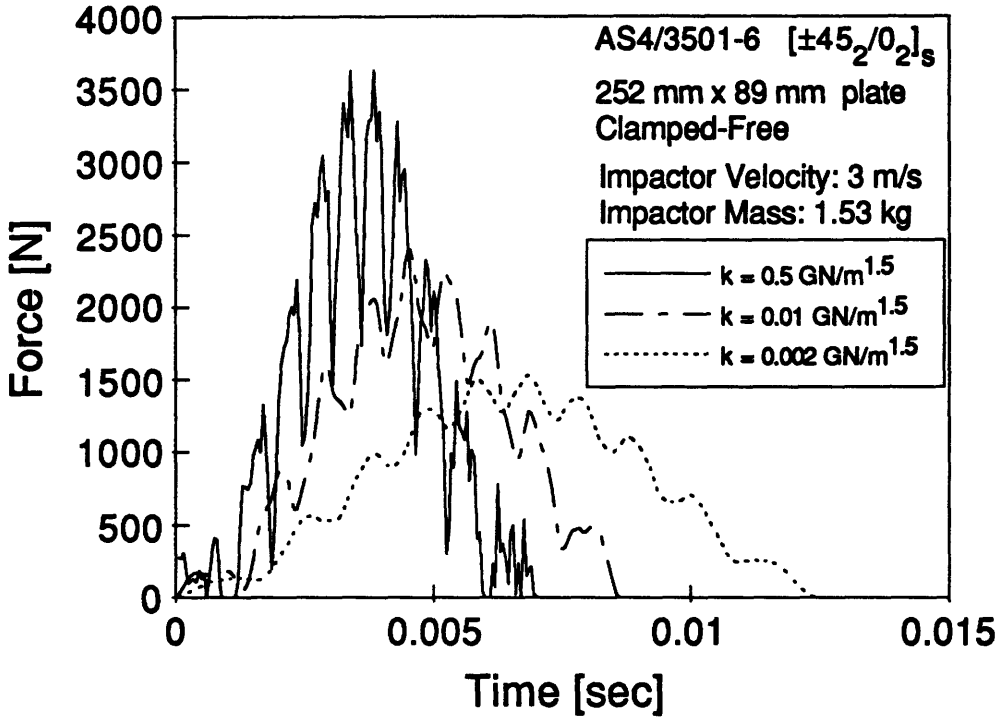

Figure 6.3 : Force-Time Histories for Various Local Contact Stiffnesses, k, by Nonlinear Analysis Using *GLOBAL2*

stiffnesses representing local contact stiffness and plate motion would be in the range that could influence one another due to the stiffening effect of the plate. By artificially adjusting the value of the local contact stiffness to 2×10^6 N/m$^{1.5}$, the force-time history approached to the one obtained experimentally by Wolf [19] in terms of the peak impact force and the impact duration as shown in Figure 6.4. However, as can be seen from Figure 6.5 showing the displacement-time history, the maximum indentation† was approximately 0.008 m which was five times larger than the plate thickness. Since this phenomenon is physically unrealistic, this artificially chosen number for the local stiffness constant should not be used.

6.1.3 Geometrical Nonlinearity

The impact model using nonlinear laminated plate theory with first-order shear deformation developed in Chapter 5 assumed that the clamped boundary condition in the numerical example currently discussed was *perfectly* rigid. However, in a realistic situation, the plate holding jig used in the experiment was made of aluminum [19] and would not be perfectly rigid. The plate holding jig might be flexible and allow some unexpected small displacement in the in-plane direction during an impact. As shown in Section 4.4, the effect of in-plane displacement for the beam analysis was negligible, although the effect of membrane force could not be neglected. This implies that the quantity of the in-plane displacement is very small but still contributes to the

† (*Indentation*) = (*Impactor Displacement*) – (*Plate Midplane Displacement*)

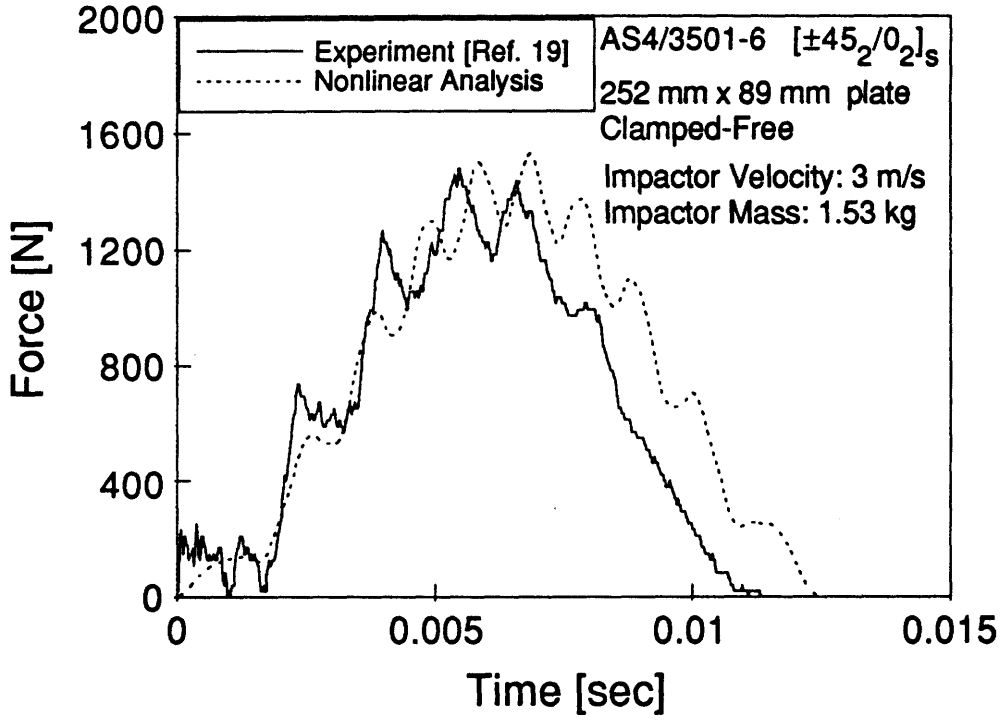

Figure 6.4 : Comparison of Force-Time Histories – Nonlinear Analysis Using $k = 2 \times 10^6$ N / m$^{1.5}$ and Experiment

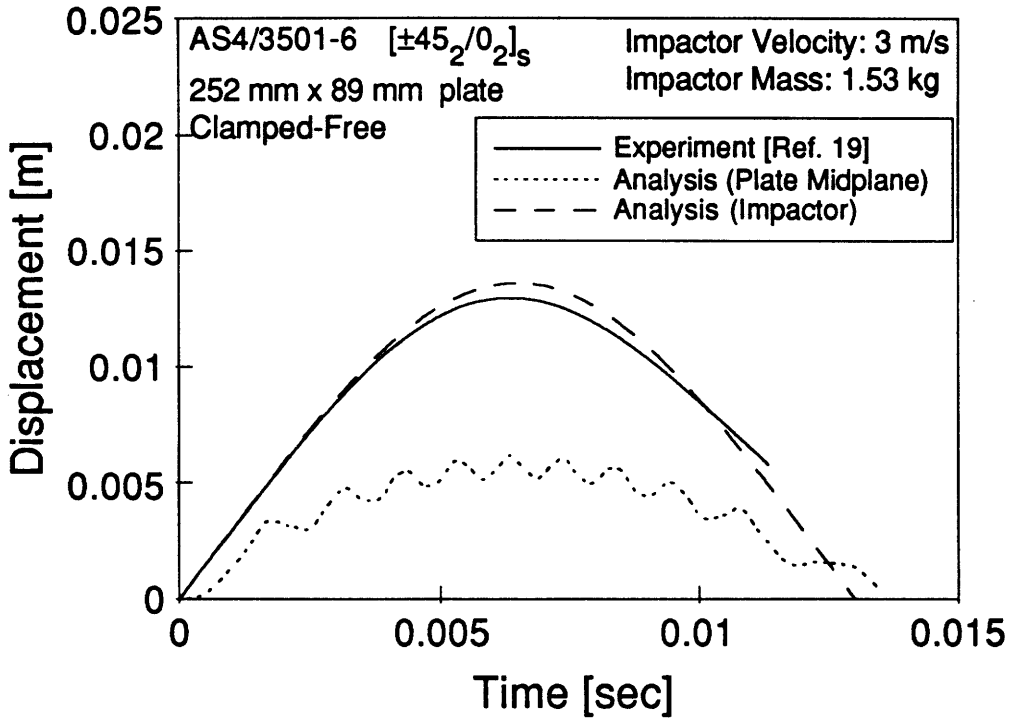

Figure 6.5 : Comparison of Displacement-Time Histories – Nonlinear Analysis Using $k = 2 \times 10^6$ N / m$^{1.5}$ and Experiment

membrane force effect. This observation can be applied to the nonlinear plate model. In other words, *small displacements due to the slightly flexible boundary condition can still cause a significant effect in membrane force*. For this reason, a study was performed using a nonlinear analysis which applied a geometrical nonlinearity *partially*. The system of equations of motion (5.2.47) was modified so that the nonlinear cubic stiffening term could be applied partially by multiplying by some factor, β, ranging from 0 to 1.†

Now, the modified system of equations of motion representing both the plate and the impactor can be expressed as,

$$\underline{M}\ddot{\underline{\lambda}} + \underline{K}^{*}\underline{\lambda} + \beta \underline{K}_{\mathrm{III}}{}^{*}\underline{\lambda}^{[3]} = -F_{z}\underline{R} \tag{6.1.1}$$

where,

for $\beta = 0$: loosely clamped boundary condition (equivalent to a linear analysis)

for $\beta = 1$: rigidly clamped boundary condition (equivalent to a nonlinear analysis)

In Figure 6.6, the force-time histories for various β values are presented. By decreasing the β value, a smaller peak force and longer impact duration can be obtained. The force-time history using $\beta = 0.05$ or 5% of the stiffening force effect is shown with experimental force-time history [19] in Figure 6.7. Although the analysis predicted a peak force approximately 30% larger than the experimental peak force, the overall trend of the signature or the primary frequency response of the force-time histories were close. The difference in peak forces was primarily due to the larger amplitudes in the secondary frequency response

† The factor, β, is defined as a *geometrical nonlinearity factor* in this investigation.

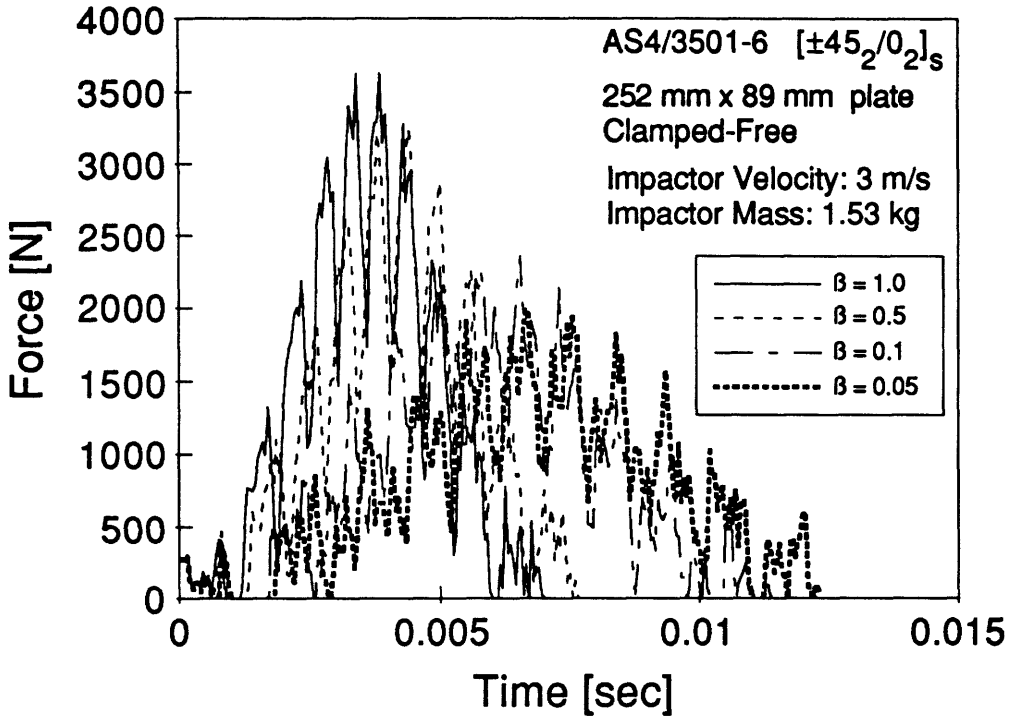

Figure 6.6 : Force-Time Histories for Various Geometrical Nonlinearity Factors, β

predicted by the nonlinear analysis. The displacement-time histories are shown in Figure 6.8. The analysis predicted the maximum plate midplane displacement approximately 15% larger than the experiment showed; however, again, the overall trends of the curve were very similar. Also, the analysis predicted a realistic indentation which was approximately one tenth of the plate thickness. Comparison between the nonlinear and the linear analysis shown in Figures 6.9 and 6.10 clearly shows that the effect of the geometrical nonlinearity of the membrane force is crucial, even though only 5% of the stiffening effect is accounted for.

6.2 Comparison of Nonlinear Analysis and Experiment

By assuming that the partially applied geometrical nonlinearity ($\beta = 0.05$) gives a sufficient prediction of impact response, six other impact cases were analyzed and compared with experimental data obtained by Wolf [19]. The material system, the stacking sequence, and the initial impactor velocity of each case are summarized in Table 6.1.

Two cases, Case 1 and Case 2, were performed based on the same material system and stacking sequence as described in Table 5.1 but using different initial impactor velocities. Case 1 used an initial velocity of 2 m/s and Case 2 used an initial velocity of 1 m/s. For Case 1, as can be seen in Figure 6.11, the analysis predicted a peak force approximately 30% larger than the experimental peak force. This was assumed due to the large amplitude in the secondary frequency response; however, the

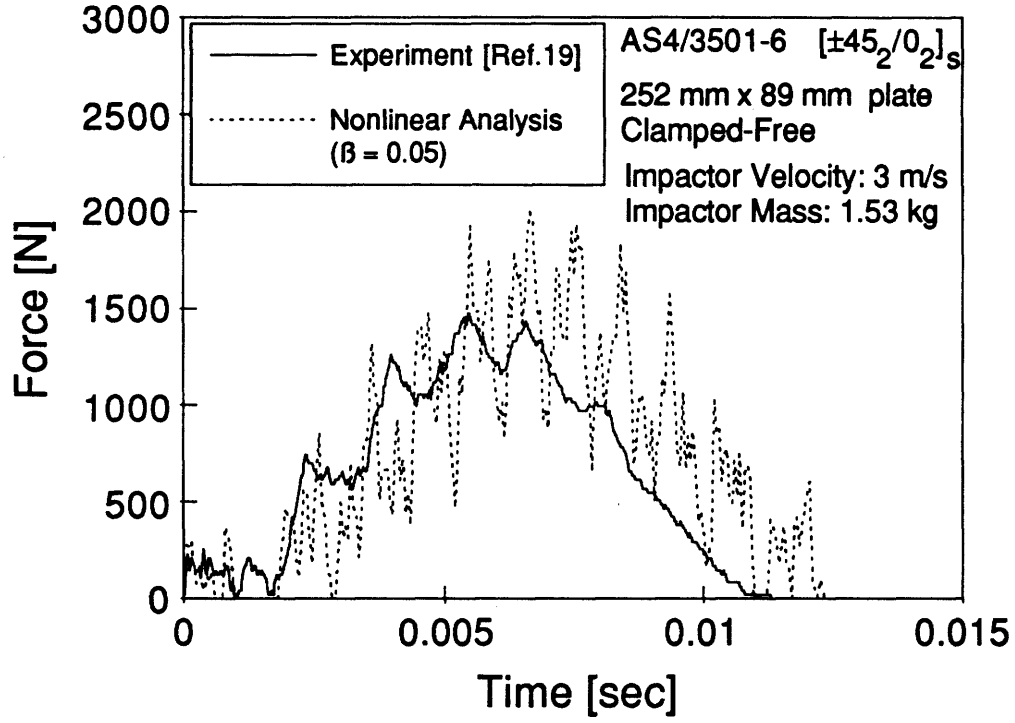

Figure 6.7 : Comparison of Force-Time Histories – Nonlinear Analysis ($\beta = 0.05$) and Experiment

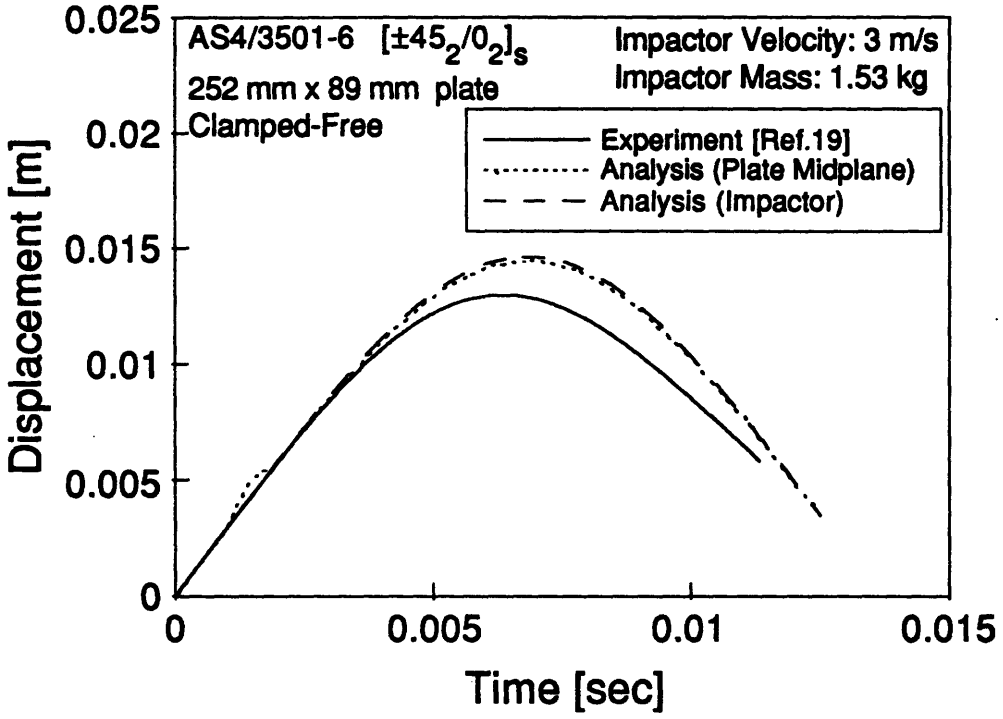

Figure 6.8 : Comparison of Displacement-Time Histories – Nonlinear Analysis ($\beta = 0.05$) and Experiment

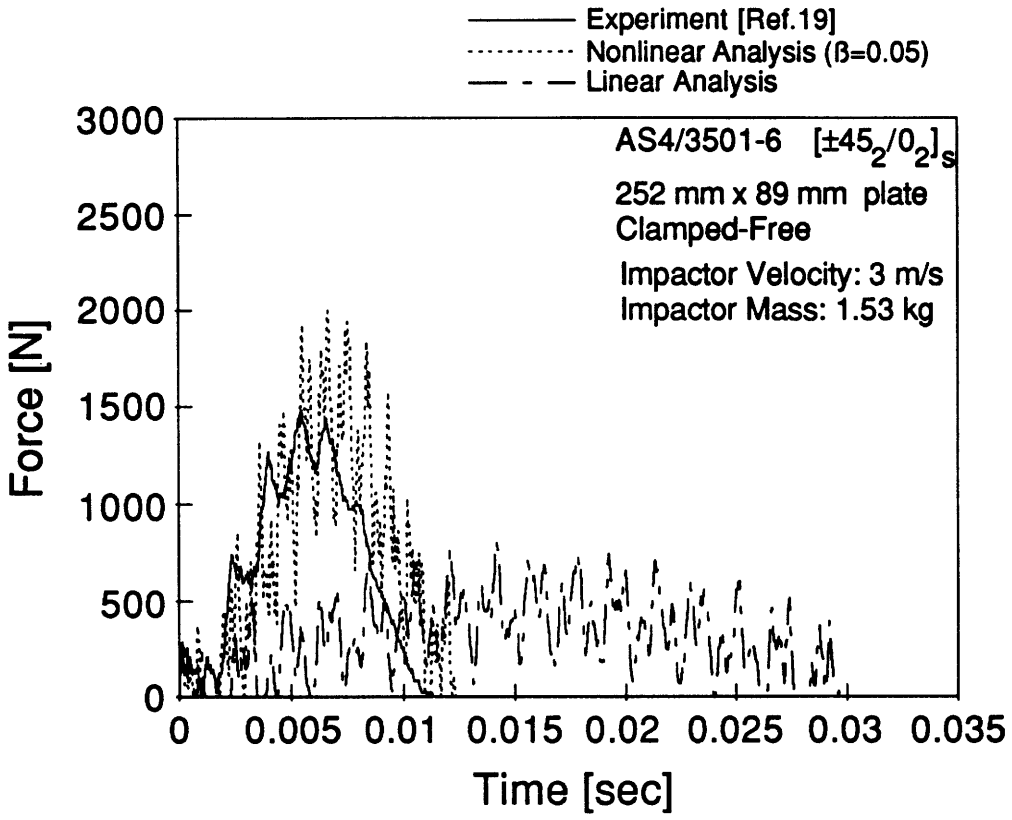

Figure 6.9 : Comparison of Force-Time Histories – Analyses (Linear and Nonlinear) and Experiment

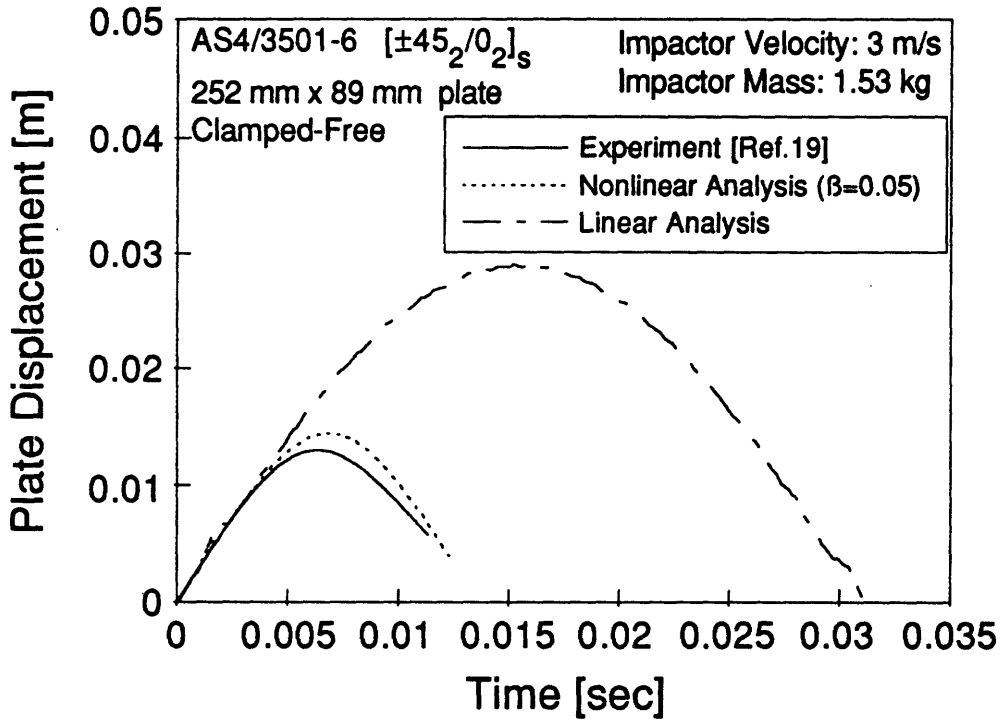

Figure 6.10 : Comparison of Displacement-Time Histories – Analyses (Linear and Nonlinear) and Experiment

overall trend of the force-time signature was close. Figure 6.12 shows a comparison of the displacement-time histories between the analysis and experiment. Although approximately 10% difference in the maximum displacements was observed, the overall trend of both displacement-time histories was similar. Force-time histories and displacement-time histories for Case 2 are shown in Figures 6.13 and 6.14, respectively. The analysis predicted 8% less peak force and approximately 50% longer impact duration. Using a value of β higher than 0.05 in the nonlinear analysis could perhaps give a better correlation with experimental data. This suggests that the geometrical nonlinearity factor might depend on the applied impact energy as well as the flexibility of the boundary region. Assuming that the mass of the impactor is fixed, the value of β would be influenced by the initial impactor velocity.

Case 3 used a stacking sequence of $[90_4/0_2]_s$ and an impactor velocity of 3 m/s. The input data used in the analysis is shown in Table 6.2. The comparisons of force-time histories and displacement-time histories are presented in Figures 6.15 and 6.16, respectively. There are relatively poor correlations compared to Cases 1 and 2. The analysis predicted longer impact duration, higher peak force, and larger displacement. For this case, varying β would not improve the impact response since a higher β value produces a higher peak force and a shorter impact duration and a lower β value produces a lower peak force and a longer impact duration as observed in Figure 6.6.

Case 4 used a stacking sequence of $[\pm 45_2/0_2/90_2]_s$ and an impactor velocity of 3 m/s and showed relatively good correlations as can be observed in Figures 6.17 and 18. The input data used for Case 4 is shown

Table 6.1 : Six Cases Investigated and Compared with Experiment

Case	Material System	Stacking Sequence	Initial Impactor Velocity
1	AS4/3501-6	$[\pm 45_2/0_2]_s$	2 m/s
2	AS4/3501-6	$[\pm 45_2/0_2]_s$	1 m/s
3	AS4/3501-6	$[90_4/0_2]_s$	3 m/s
4	AS4/3501-6	$[\pm 45_2/0_2/90_2]_s$	3 m/s
5	IM7G/X8553-50	$[\pm 45_2/0_2]_s$	3 m/s
6	IM7G/X8553-50	$[\pm 45_2/0_2]_s$	5 m/s

in Table 6.3. Although the peak force predicted by the analysis was approximately 60% higher than the experimental results, the primary frequency response or the overall trend of the curve produced by the analysis was similar to the experimental data. The displacement-time histories shown in Figure 6.18 present good correlations. The difference seen after the peak displacements might be due to the material nonlinearity induced by damage since the displacement obtained from the experiment never returned to zero.

Cases 5 and 6 used a different material system, IM7G/X8553-50, known as a "toughened" graphite/epoxy composite. The input data for the analysis is listed in Table 6.4. Cases 5 and 6 used initial impactor velocities of 3 m/s and 5 m/s, respectively. From the comparisons of force-time histories shown in Figures 6.19 and 6.20, the analyses predicted impact durations which were close to the experimental data; however, the analyses predicted more than 60% higher peak forces than experimental data showed, although the overall trends were still similar.

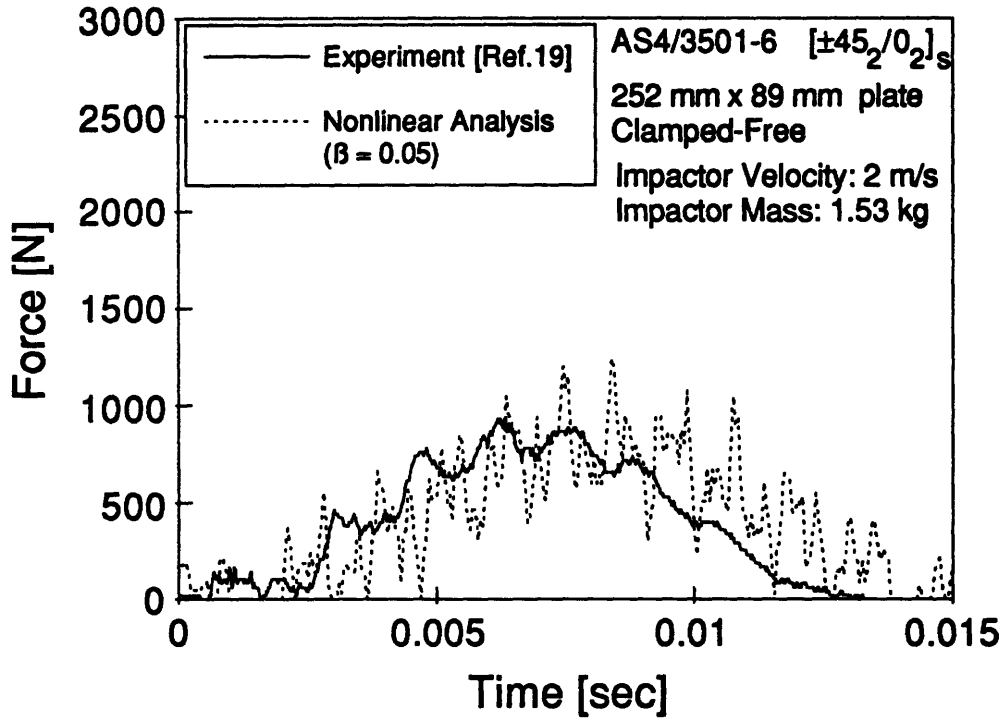

Figure 6.11 : Case 1 : Comparison of Force-Time Histories – Nonlinear Analysis ($\beta = 0.05$) and Experiment

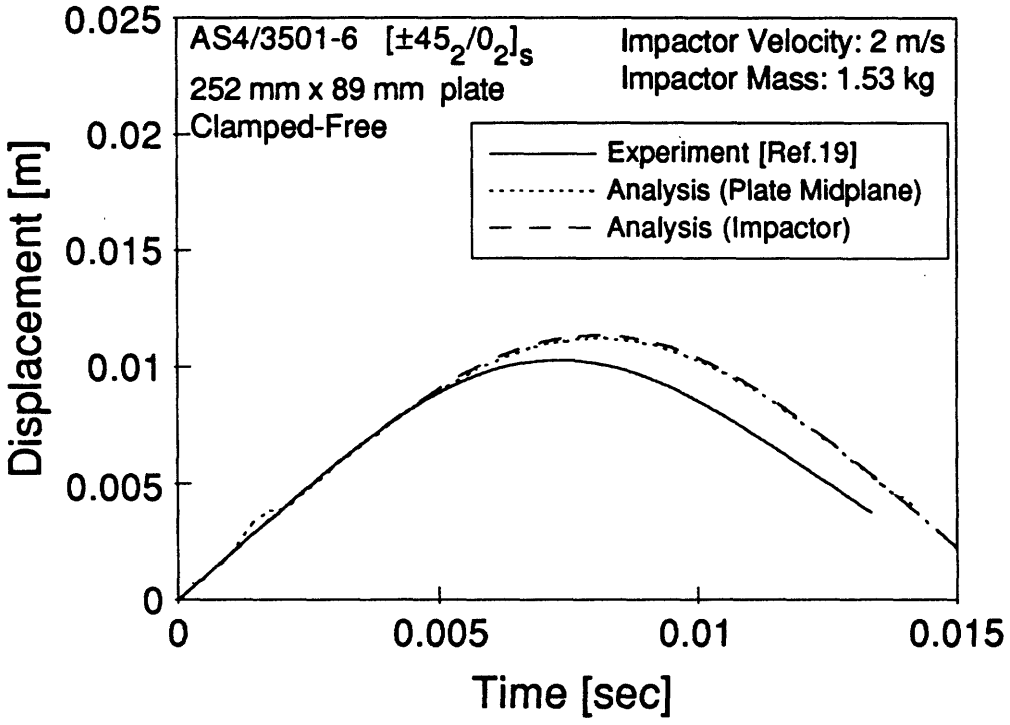

Figure 6.12 : Case 1 : Comparison of Displacement-Time Histories – Nonlinear Analysis ($\beta = 0.05$) and Experiment

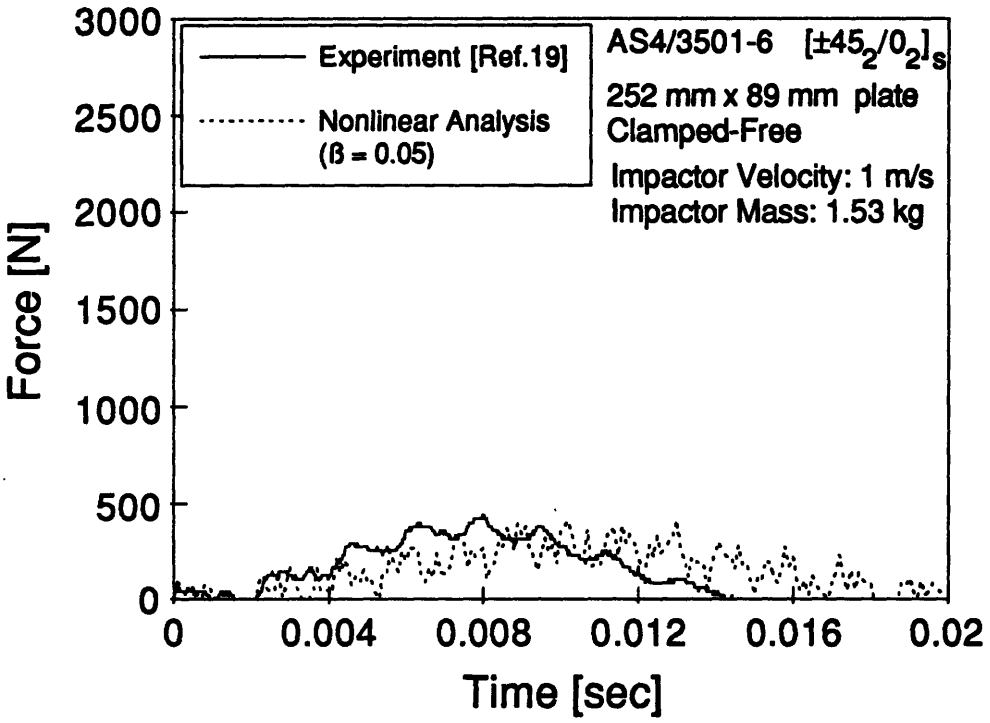

Figure 6.13 : Case 2 : Comparison of Force-Time Histories – Nonlinear Analysis ($\beta = 0.05$) and Experiment

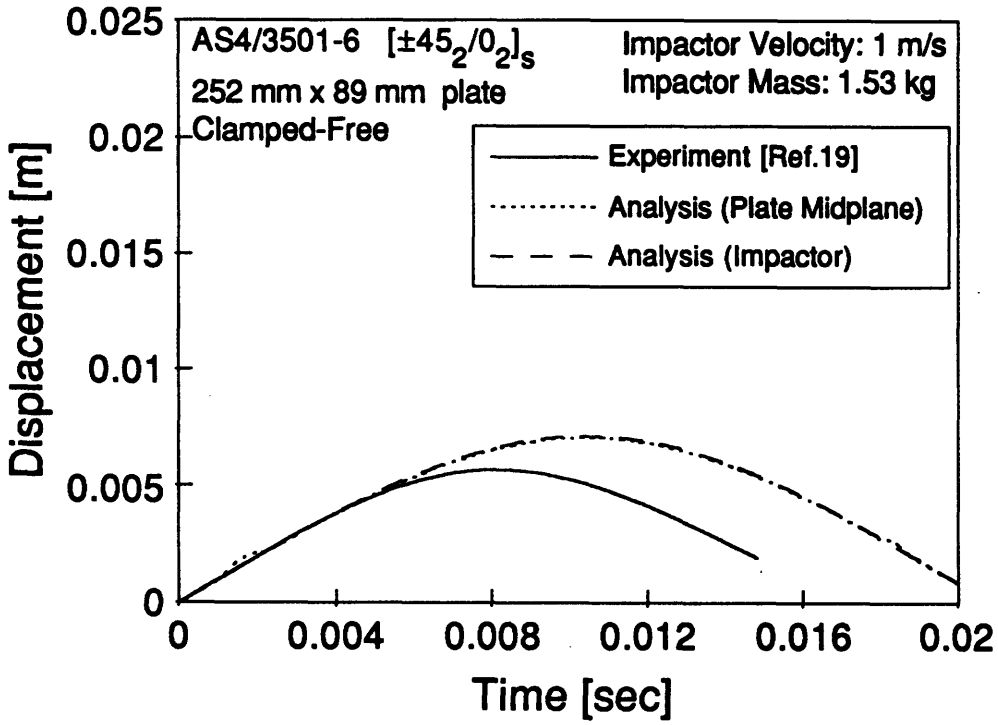

Figure 6.14 : Case 2 : Comparison of Displacement-Time Histories – Nonlinear Analysis ($\beta = 0.05$) and Experiment

Table 6.2 : Input Data for Case 3 Analysis

Laminate Material System :	AS4/3501-6 Graphite/Epoxy
Lay-up :	$[90_4/0_2]_s$
x-direction Boundary Condition :	Clamped-Clamped
Geometrical Nonlinearity Factor (β) :	0.05
y-direction Boundary Condition :	Free-Free
Plate Length (x-direction) :	252 mm
Plate Width (y-direction) :	89 mm
Plate Thickness :	1.608 mm
Plate Density :	1540 kg/m^3
A_{11} :	87,170,300 N/m
D_{1111} :	5.1272 N-m
D_{1122} :	1.0261 N-m
D_{1112} :	0.0 N-m
D_{2222} :	47.8009 N-m
D_{2212} :	0.0 N-m
D_{1212} :	2.0789 N-m
A_{44} :	8.06 MN/m
A_{45} :	0.00 MN/m
A_{55} :	6.92 MN/m
Shear Correction Factor :	0.833
Impactor Mass :	1.53 kg
Impactor Velocity :	3.0 m/s
Local Contact Stiffness :	0.5 GN/m$^{1.5}$
Local Contact Exponent Value :	1.5
Number of Modes in x-direction :	9 (odd modes only)
Number of Modes in y-direction :	9 (odd modes only)
Time Step Increment :	5.0 μs
Number of Time Steps :	3,000 time steps

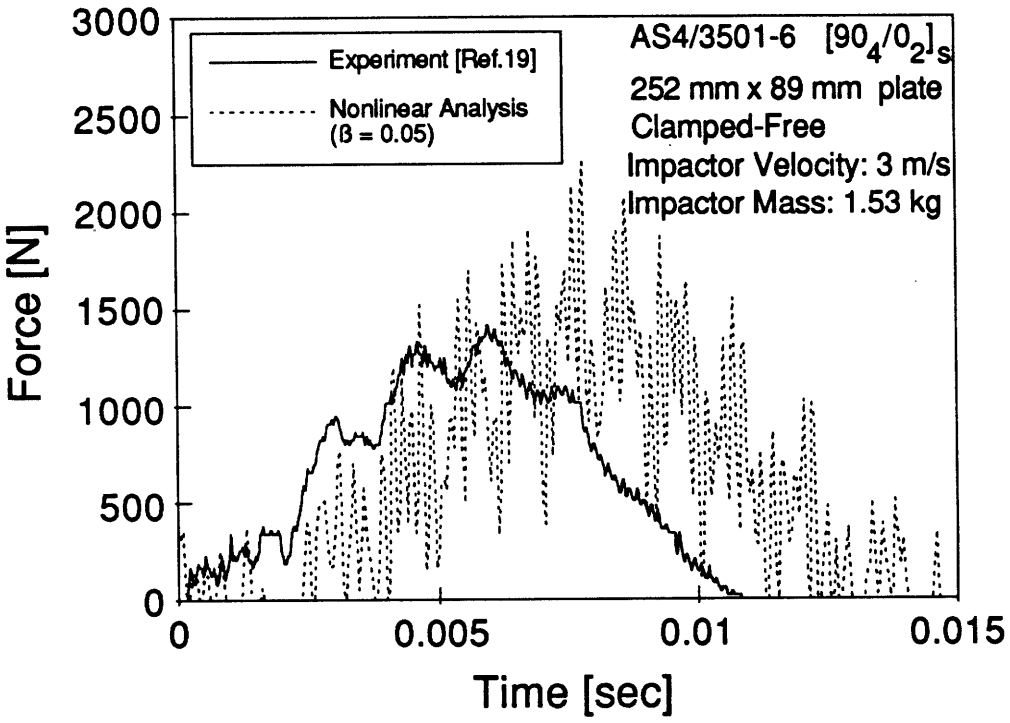

Figure 6.15 : Case 3 : Comparison of Force-Time Histories – Nonlinear Analysis ($\beta = 0.05$) and Experiment

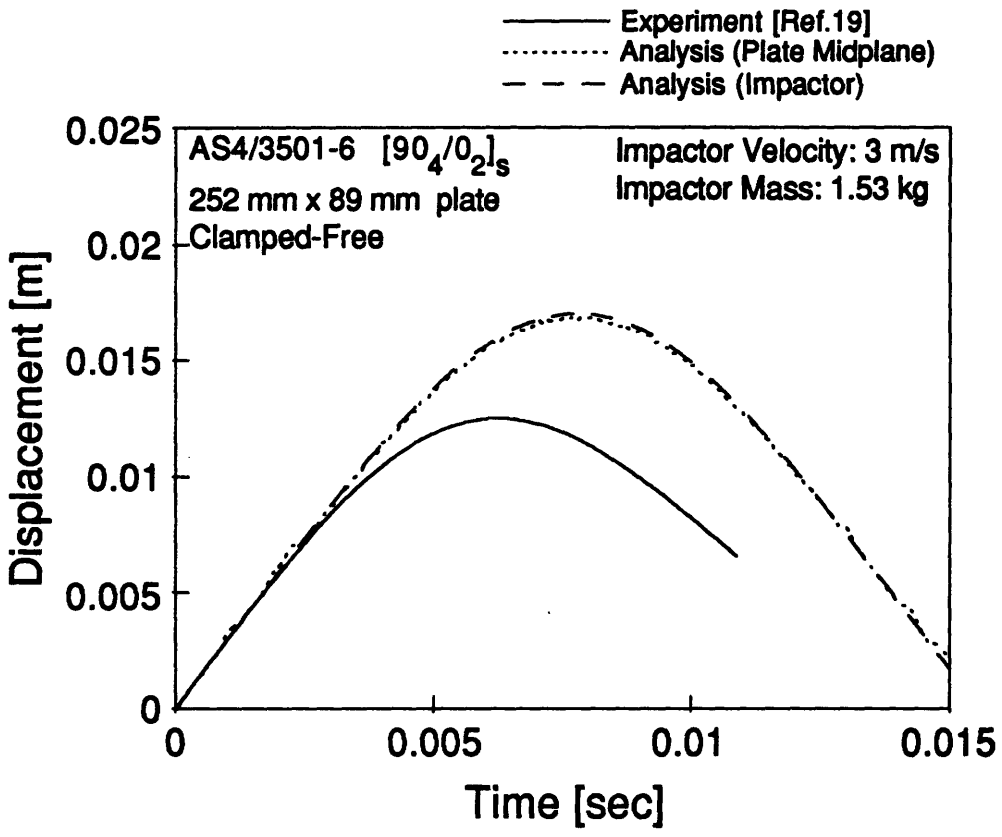

Figure 6.16 : Case 3 : Comparison of Displacement-Time Histories – Nonlinear Analysis ($\beta = 0.05$) and Experiment

Table 6.3 : Input Data for Case 4 Analysis

Laminate Material System :	AS4/3501-6 Graphite/Epoxy
Lay-up :	$[\pm 45_2/0_2\ /90_2]_S$
x-direction Boundary Condition :	Clamped-Clamped
Geometrical Nonlinearity Factor (β) :	0.05
y-direction Boundary Condition :	Free-Free
Plate Length (x-direction) :	252 mm
Plate Width (y-direction) :	89 mm
Plate Thickness :	2.144 mm
Plate Density :	1540 kg/m^3
A_{11} :	130,838,300 N/m
D_{1111} :	45.7821 N-m
D_{1122} :	35.5402 N-m
D_{1112} :	3.8406 N-m
D_{2222} :	35.5402 N-m
D_{2212} :	3.8406 N-m
D_{1212} :	26.9961 N-m
A_{44} :	9.93 MN/m
A_{45} :	0.00 MN/m
A_{55} :	9.93 MN/m
Shear Correction Factor :	0.833
Impactor Mass :	1.53 kg
Impactor Velocity :	3.0 m/s
Local Contact Stiffness :	0.5 GN/m$^{1.5}$
Local Contact Exponent Value :	1.5
Number of Modes in x-direction :	9 (odd modes only)
Number of Modes in y-direction :	9 (odd modes only)
Time Step Increment :	5.0 μs
Number of Time Steps :	3,000 time steps

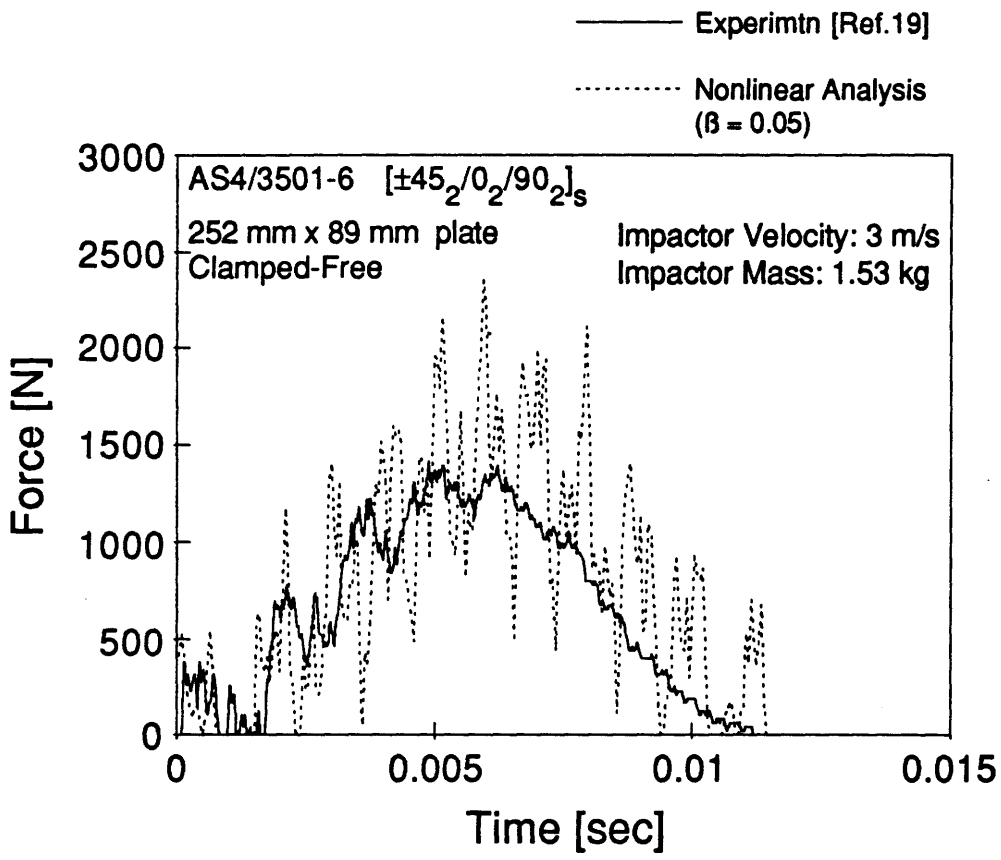

Figure 6.17 : Case 4 : Comparison of Force-Time Histories – Nonlinear Analysis ($\beta = 0.05$) and Experiment

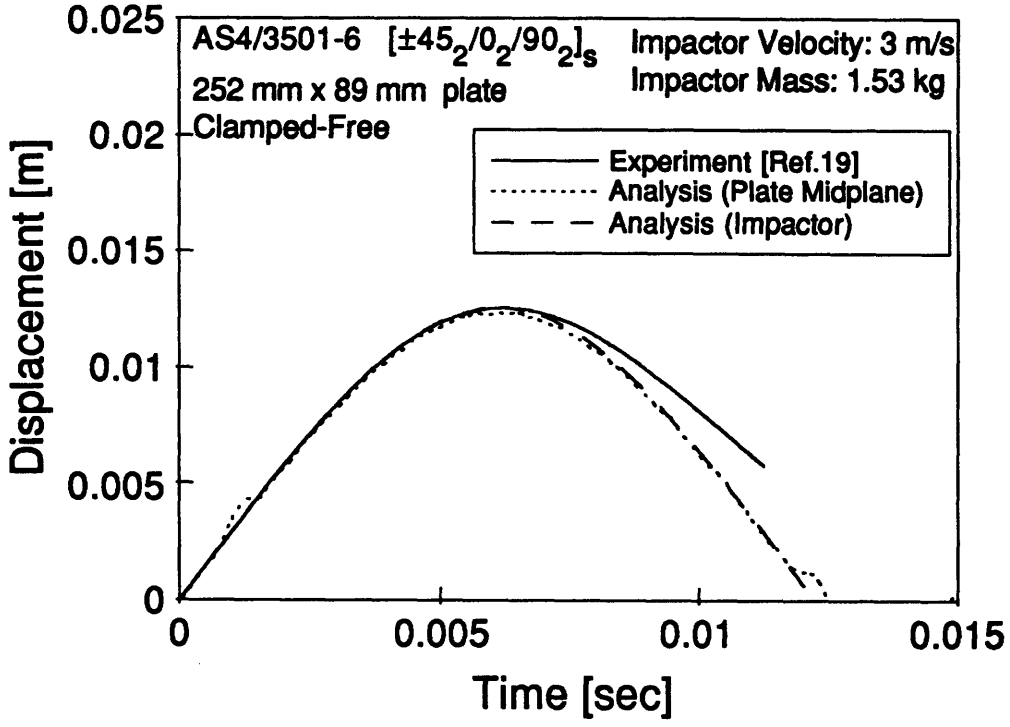

Figure 6.18 : Case 4 : Comparison of Displacement-Time Histories – Nonlinear Analysis ($\beta = 0.05$) and Experiment

Table 6.4 : Input Data for Case 5 and Case 6 Analysis

Laminate Material System :	IM7G/X8553-50
Lay-up :	$[\pm 45_2/0_2]_s$
x-direction Boundary Condition :	Clamped-Clamped
Geometrical Nonlinearity Factor (β) :	0.05
y-direction Boundary Condition :	Free-Free
Plate Length (x-direction) :	252 mm
Plate Width (y-direction) :	89 mm
Plate Thickness :	1.740 mm
Plate Density :	1540 kg/m^3
A_{11} :	143,591,000 N/m
D_{1111} :	22.5264 N-m
D_{1122} :	15.0949 N-m
D_{1112} :	3.5227 N-m
D_{2222} :	20.1778 N-m
D_{2212} :	3.5227 N-m
D_{1212} :	16.5905 N-m
A_{44} :	10.27 MN/m
A_{45} :	0.00 MN/m
A_{55} :	10.27 MN/m
Shear Correction Factor :	0.833
Impactor Mass :	1.53 kg
Impactor Velocity :	3.0 m/s (Case 5)
	5.0 m/s (Case 6)
Local Contact Stiffness :	0.5 GN/m$^{1.5}$
Local Contact Exponent Value :	1.5
Number of Modes in x-direction :	9 (odd modes only)
Number of Modes in y-direction :	9 (odd modes only)
Time Step Increment :	5.0 μs
Number of Time Steps :	3,000 time steps

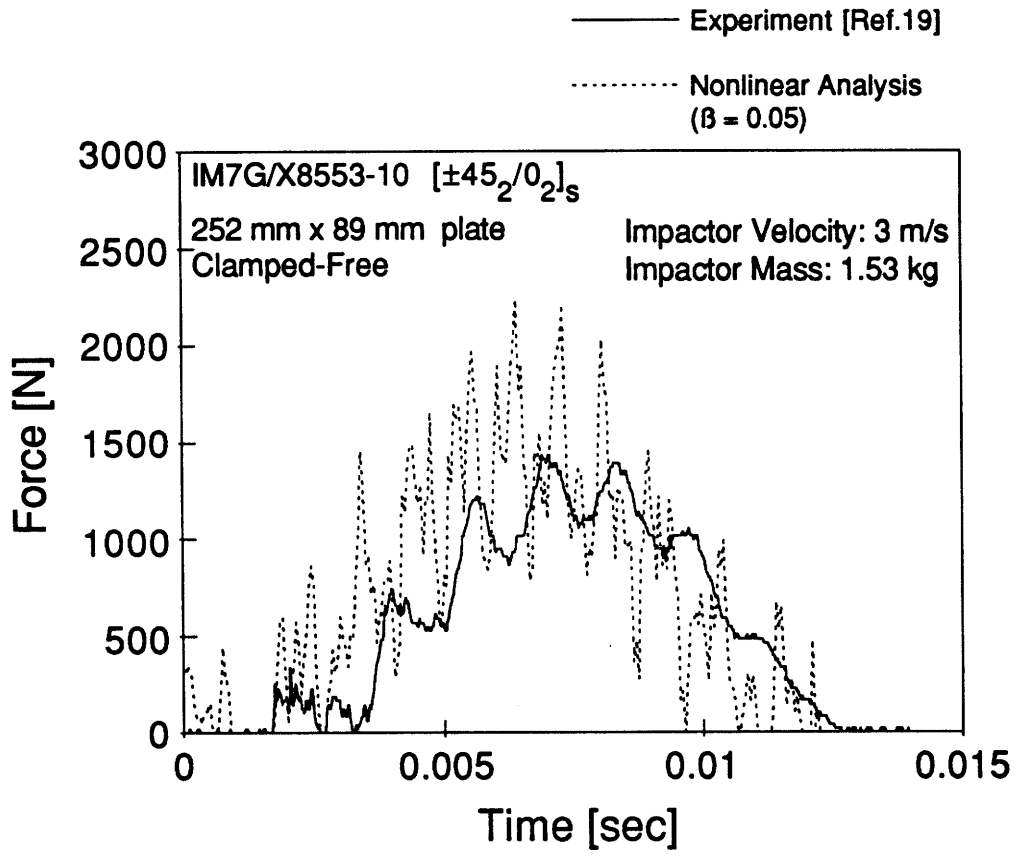

Figure 6.19 : Case 5 : Comparison of Force-Time Histories – Nonlinear Analysis ($\beta = 0.05$) and Experiment

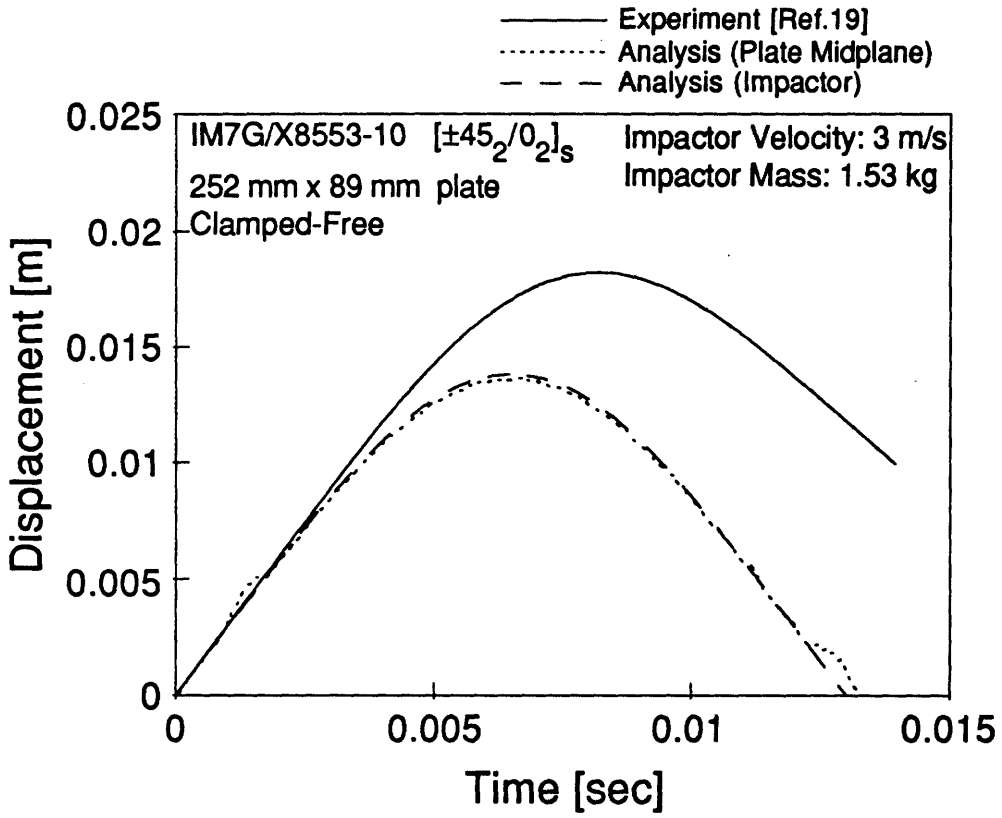

Figure 6.20: Case 5 : Comparison of Displacement-Time Histories – Nonlinear Analysis ($\beta = 0.05$) and Experiment

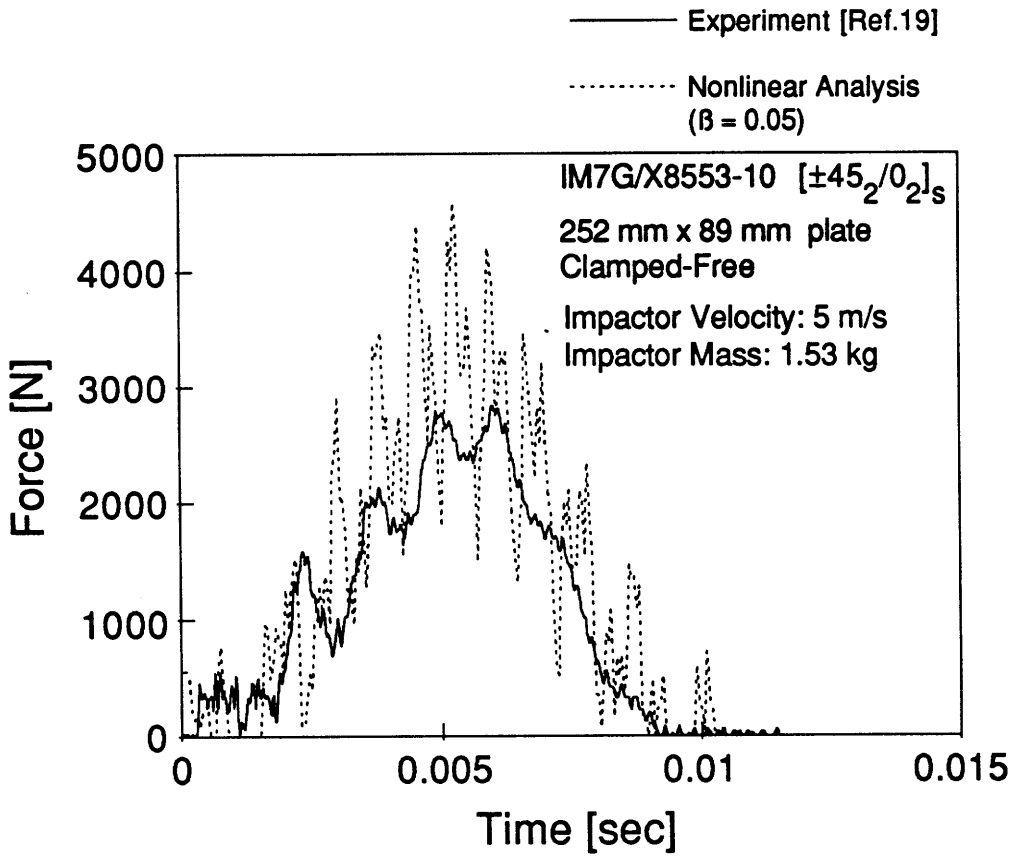

Figure 6.21 : Case 6 : Comparison of Force-Time Histories – Nonlinear Analysis ($\beta = 0.05$) and Experiment

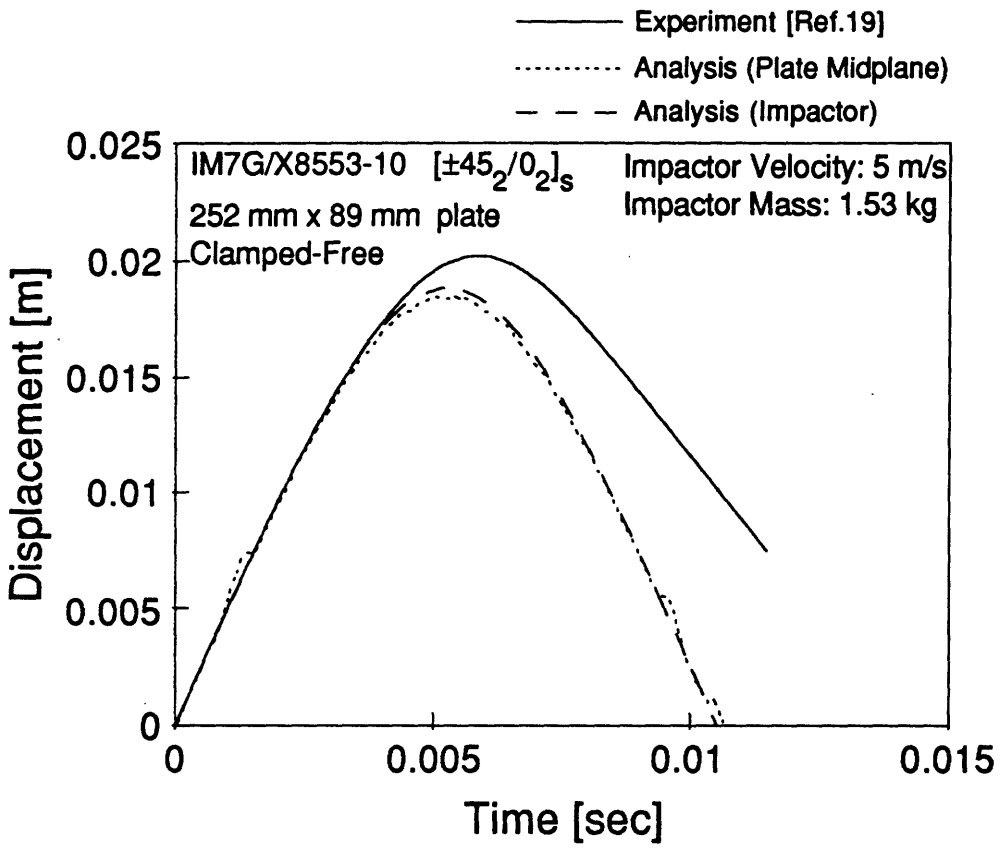

Figure 6.22 : Case 6 : Comparison of Displacement-Time Histories – Nonlinear Analysis ($\beta = 0.05$) and Experiment

6.3 Summary

In this chapter, parametric studies and comparisons with the existing experimental data were performed using the nonlinear plate impact analysis developed in Chapter 5. Parameters varied were the number of modes, the local contact stiffness, and the geometrical nonlinearity factor. The nonlinear plate impact model was relatively insensitive to the inclusion of the even modes which contribute to the bending-twisting coupling; however, the model was sensitive to the change in the local contact stiffness. A partial geometrical nonlinearity was applied to the nonlinear plate impact model using the geometrical nonlinearity factor, β. This factor was included after considering the flexible plate holding jig which might allow some unexpected displacement in the in-plane direction resulting in a reduction of membrane stiffening effect during an actual impact situation. Using $\beta = 0.05$ or 5% of the membrane stiffening effect gave a good correlation with experimental data in terms of the force- and displacement-time histories. Although the overall trends or the primary frequency responses of the force-time history were predicted well, there were significant differences in the secondary frequency responses between the analysis and the experiment. Further refinement needs to be done to bring this nonlinear plate impact response analysis into better agreement with the experimental data.

Chapter 7

Conclusions and Recommendations

7.1 Conclusions

Including geometrical nonlinearity in the shear deformable laminated plate impact analysis showed a significant effect in impact response compared to linear plate impact analysis.

Specific conclusions are drawn as follows.

1) The impact response predicted by the linear impact analysis did not agree with the impact response observed by experiment using a rigidly clamped boundary. Linear impact analysis produced a lower peak force and longer impact duration than the experiment showed.

2) Using a linear analysis, a large number of modes (i.e. more than 25x25 modes) would be necessary to converge for the impact problem investigated. Increasing the number of modes to more

than 15x15 modes gave essentially a "fine tuning" of the force-time history output and did not influence the overall trend of the force-time signature.

3) The linear impact response was insensitive to changes in certain combinations of the characteristics of the local nonlinear contact spring and the spring representing the plate stiffness.

4) The geometrical nonlinearity for a beam model could be included using two different approaches. One approach used a support stiffness which was a virtual spring, and the other approach was based on nonlinear strain-displacement relations. The first approach produced a nonlinear equation in terms of the out-of-plane displacement only and the second approach produced coupled nonlinear equations in terms of both the in-plane and the out-of-plane displacements.

5) The investigation using a beam model showed that the geometrical nonlinear effect of the membrane stiffening was significant in terms of the impact response. The nonlinear beam model produced a higher peak force and a shorter duration than the linear beam model.

6) The investigation using a beam model showed that the effect of the in-plane displacement on the beam equation of motion was negligible for the example problem studied.

7) The nonlinear impact model for the laminated plate produced a higher peak force and a shorter impact duration than the linear impact model.

8) The nonlinear impact model for the laminated plate produced a higher peak force and a shorter impact duration than the experiment showed.

9) The impact response produced by the nonlinear impact analysis was relatively sensitive to the change in the local contact spring characteristics. Using an unrealistically low value for the local stiffness constant gave a reasonable force-time history, but generated an indentation larger than the plate thickness, a physically unrealistic result.

10) The impact model which included the geometrical nonlinearity *partially* (i.e. 5% of the full nonlinearity) gave reasonable impact responses in terms of the primary frequency response compared to the experimental data. Typically, the analysis predicted larger amplitudes for the secondary frequency response.

7.2 Recommendations

Although the impact model which included the geometrical nonlinearity partially gave reasonable impact responses, there are still significant differences in the secondary frequency response observed by

comparisons with the experimental data. The recommendations for the future work are summarized as follows.

1) The membrane stiffening force during the impact needs to be obtained experimentally so that the geometrical nonlinearity factor (β) can be determined.

2) Since the nonlinear plate model is sensitive to the change in the local contact spring characteristics, sufficiently accurate values in local contact stiffness and the local nonlinearity exponent should be obtained.

3) Further simplification of the nonlinear analysis should be introduced in order to reduce the computational intensity so that more modes can be included.

4) The current analysis assumed a point loading. A distributed patch loading might improve the analysis.

5) The local modeling for the impacted region including fully three-dimensional effects should be coupled with the current nonlinear global model in order to properly include the influence of the local contact characteristics.

In particular, the focus should be to verify the influence of the membrane stiffening force due to the flexibility/rigidity in the boundary

region and the importance of the global-local interaction with respect to the impact response modeling.

Bibliography

[1] Tsai, S.W., and Hahn, H.T., *Introduction to Composite Materials*, Technomic Publishing Company, Westport, Conneticut, 1980.

[2] Cairns, D. S., "Impact and Post-Impact Response of Graphite/Epoxy and Kevlar/Epoxy Structures," Ph.D. Thesis, Department of Aeronautics and Astronautics, Massachusetts Institute of Technology, Cambridge, MA, August, 1987.

[3] Gosse, J. H., and Mori, P. B. Y., "Impact Damage Characterization of Graphite/Epoxy Laminates," *Proceedings of the American Society for Composites Third Technical Conference*, Seattle, 1988, pp. 344-353.

[4] O'Brian, T. K., "Toward a Damage Tolerance Philosophy for Composite Materials and Structures," *Composite Materials: Testing and Design*, Vol. 9, ASTM STP 1059, 1990, pp. 7-33.

[5] Yang, P. C., Norris, C. H., and Stavsky, Y., "Elastic Wave Propagation in Heterogeneous Plates," *International Journal of Solids and Structures*, Vol. 2, No. 4, 1966, pp. 665-684.

[6] Timoshenko, S. P., and Goodier, J. N., *Theory of Elasticity*, McGraw-Hill, New York, 1970.

[7] Greszczuk, L. B., "Response of Isotropic and Composite Materials to Particle Impact," *ASTM STP 568*, 1975, pp. 183-211.

[8] Timoshenko, S. P., "Zur frage nach der wirkung eines stosses auf einen balken," *ZAMP 62*, 1913, pp. 198-209.

[9] Karas, K., "Platten unter seitchem stoss," *Ing Arch 10*, 1939, pp. 237-250.

[10] Sun, C. T., and Chattopadhyay, S., "Dynamic Response of Anisotropic Laminates Under Initial Stress to Impact of a Mass," *Journal of Applied Mechanics*, Vol. 42, 1975, pp. 693-698.

[11] Whitney, J. M., and Pagano, N. J., "Shear Deformation in Heterogeneous Anisotropic Plates," *Journal of Applied Mechanics*, Vol. 37, No. 4, December 1970, pp. 1031-1036.

[12] Tan, T. M., and Sun, C. T., "Use of Statical Indentation Laws in the Impact Analysis of Laminated Composite Plates," *Journal of Applied Mechanics*, Vol. 52, No. 1, March 1985, pp. 6-12.

[13] Sun, C. T., and Chen, J. K., "On the Impact of Initially Stressed Composite Laminates," *Journal of Composite Materials*, Vol. 19, No. 6, November 1985, pp. 490-504.

[14] Yang, S. H., and Sun, C. T., "Indentation Law for Composite Laminates," *Composite Materials: Testing and Design*, ASTM STP 787, American Society for Testing and Materials, 1982, pp. 425-449.

[15] Wu, H. T., and Springer, G. S., "Impact Induced Stresses, Strains, and Delaminations in Composite Plates," *Journal of Composite Materials*, Vol. 22, No. 6, June 1988, pp. 533-560.

[16] Graves, M. J., and Koontz, J. S., "Initiation and Extent of Impact Damage in Graphite/Epoxy and Graphite/PEEK Composites," *Proceedings of AIAA/ASME/ASCE/AHS 29th Structures, Structural Dynamics, and Materials Conference*, Williamsburg, VA, April 18-20 1988, pp. 967-975.

[17] Cairns, D. S., and Lagace, P. A., "Transient Response of Graphite/Epoxy and Kevlar/Epoxy Laminates Subjected to Impact," *AIAA Journal*, Vol. 27, No. 11, November 1989, pp. 1590-1596.

[18] Ryan, K. F., "Dynamic Response of Graphite/Epoxy Plates Subjected to Impact Loading," S.M. Thesis, Department of Aeronautics and Astronautics, Massachusetts Institute of Technology, Cambridge, MA, September, 1989.

[19] Wolf, E., "Impact Damage Mechanisms in Several Laminated Material Systems," S.M. Thesis, Department of Aeronautics and Astronautics, Massachusetts Institute of Technology, Cambridge, MA, March, 1992.

[20] Qian, Y., and Swanson, R., "Experimental Measurement of Impact Response in Carbon/Epoxy Plates," *AIAA Journal*, Vol. 28, No. 6, June 1990, pp. 1069-1074.

[21] Reddy, J. N., "Geometrically Nonlinear Transient Analysis of Laminated Composite Plates," *AIAA Journal*, Vol. 21, No. 4, April 1983, pp. 621-629.

[22] Chen, J. K., and Sun, C. T., "Nonlinear Transient Responses of Initially Stressed Composite Plates," *Computational Structures*, Vol.21, 1985, pp. 513-520.

[23] Sun, C. T., and Shafey, N. A., "Wave Propagation in Heterogeneous Anisotropic Plates Involving Large Deflection," *International Journal of Solids and Structures*, Vol. 11, 1975, pp. 99-114.

[24] Reddy, J. N., "A Refined Nonlinear Theory of Plates with Transverse Shear Deformation," *International Journal of Solids and Structures*, Vol. 20, No. 9/10, 1984, pp. 881-896.

[25] Nosier, A., and Reddy, J. N., "A Study of Non-Linear Dynamic Equations of Higher-Order Shear Deformation Plate Theories," *International Journal of Non-Linear Mechanics*, Vol. 26, No. 2, 1991, pp. 233-249.

[26] Kant, T., and Mallikarjuna, "Non-Linear Dynamics of Laminated Plates with a Higher-Order Theory and C^0 Finite Elements," *International Journal of Non-Linear Mechanics*, Vol. 26, No. 3/4, 1991, pp. 335-343.

[27] Ren-Huai, L., and Ling-Hui, H., "A Simple Theory for Non-Linear Bending of Laminated Composite Rectangular Plates Including Higher-Order Effects," *International Journal of Non-Linear Mechanics*, Vol. 26, No. 5, 1991, pp. 537-545.

[28] Gu, Q., and Reddy, J. N., "Non-Linear Analysis of Free-Edge Effects in Composite Laminates Subjected to Axial Loads," *International Journal of Non-Linear Mechanics*, Vol. 27, No. 1, 1992, pp. 27-41.

[29] Tsang, P. H. W., "Impact Resistance of Graphite/Epoxy Sandwich Panels," S.M. Thesis, Department of Aeronautics and Astronautics, Massachusetts Institute of Technology, Cambridge, MA, September, 1989.

[30] Dugundji, J., "Simple Expression for Higher Vibration Modes of Uniform Euler Beams," *AIAA Journal*, Vol.26, No. 8, August 1988, pp. 1013-1014.

[31] Ginsberg, J. H., *Advanced Engineering Dynamics*, Harper & Row, Publishers, Inc., New York, NY, 1987.

[32] Bathe, K.-J., *Numerical Methods in Finite Element Analysis*, Prentice-Hall, Inc., 1982.

[33] Williamson, J. E., "Response Mechnisms in the Impact of Graphite/Epoxy Honeycomb Sandwich Panels," S.M. Thesis, Department of Aeronautics and Astronautics, Massachusetts Institute of Technology, Cambridge, MA, August, 1991.

[34] Qian, Y., and Swanson, S. R., "A Comparison of Solution Techniques for Impact Response of Composite Plates," *Composite Structures*, Vol. 14, 1990, pp. 177-192.

[35] Shivakumar, K. N., Elber, W., and Illg, W., "Prediction of Impact Force and Duration due to Low-Velocity Impact on Circular Composite Laminates", *Journal of Applied Mechanics*, Vol. 52, September 1985, pp. 674-680.

[36] Dugundji, J., *Oral Communication*, Department of Aeronautics and Astronautics, Massachusetts Institute of Technology, Cambridge, MA, January 1992.

[37] Reismann, H., *Elastic Plates: Theory and Application*, A Wiley-Interscience Publication, 1988.

[38] Chia, C. Y., *Nonlinear Analysis of Plates*, McGraw-Hill, Inc., 1980.

[39] Whitney, J. M., *Structural Analysis of Laminated Anisotropic Plates*, Technomic, Lancaster, PA, 1987.

[40] Minguet, P. J., "Buckling of Graphite/Epoxy Sandwich Plates," S.M. Thesis, Department of Aeronautics and Astronautics, Massachusetts Institute of Technology, Cambridge, MA, May, 1986.

[41] Goldsmith, W., *Impact*, Arnold, London, 1960.

[42] Dobyns, A. L., "Analysis of Simply-Supported Plates Subjected to Static and Dynamic Loads," *AIAA Journal*, Vol. 19, No. 5, 1980, pp. 642-650.

[43] Cook, R. D., Malkus, D. S., and Plesha, M. E., *Concepts and Applications of Finite Element Analysis*, John Wiley & Sons, Inc., 1989.

[44] Reddy, J. N., *Energy and Variational Methods in Applied Mechanics*, John Wiley & Sons, Inc., 1984.

[45] Hornbeck, R. W., Numerical Methods, Prentice-Hall, Inc., Englewood Cliffs, NJ, 1975.

[46] Dowell, E. H., "Nonlinear Oscillations of a Fluttering Plate," *AIAA Journal*, Vol. 4, No. 7, July, 1966.

[47] Abrate, S., "Impact on Laminated Composite Materials," *Applied Mechanics Review*, Vol. 44, No. 4, April, 1991.

[48] Chia, C. Y., "Geometrical Nonlinear Behavior of Composite Plates: A Review," *Applied Mechanics Review*, Vol. 41, No. 12, December, 1988.

Appendix A

Generalized Beam Functions (GBFs)

Dugundji [36] derived approximate beam shape functions (GBFs) for various boundary conditions. Although these GBFs are approximations to the traditional beam shape functions, the difference between the two becomes negligible when the mode number is greater than 2.

The GBFs are written in the form,

$$\phi_n(x) = \sqrt{2}\sin(\beta_n x + \theta) + Ae^{-\beta_n x} + Be^{-\beta_n(1-x)} \tag{A.1}$$

where the constants or shape parameters β_n, θ, A, and B are given in Table A.1 for some common boundary conditions. The corresponding frequencies for an isotropic beam are given by,

$$\omega_n = \beta_n^2\sqrt{EI/ml^4} \tag{A.2}$$

All modes are normalized such that the mode shape $\phi_n(x)$ satisfies the condition,

$$\int_0^1 \phi_n{}^2(x)\,dx = 1 \tag{A.3}$$

These modes also apply for $n = 1$ with less than a 1% error, except for the clamped-free case. The form of Eq. (A.1) has the advantage that GBFs can be written in one single parametric form and easily evaluated numerically. Also, Eq. (A.1) can be useful in performing large multimode Rayleigh-Ritz type analyses for beam, plates, and shells with different boundary conditions.

Table A.1 : Euler Beam Elastic Mode Shape Parameters

Boundary Condition†	β_n	θ	A	B
SS–SS	$n\pi$	0	0	0
CL–FR	$(n-1/2)\pi$	$-\pi/4$	1	$(-1)^{n+1}$
CL–CL	$(n+1/2)\pi$	$-\pi/4$	1	$(-1)^{n+1}$
FR–FR	$(n+1/2)\pi$	$+3\pi/4$	1	$(-1)^{n+1}$
SS–CL	$(n+1/2)\pi$	0	0	$(-1)^{n+1}$
SS–FR	$(n+1/2)\pi$	0	0	$(-1)^{n}$

† SS = simply supported, CL = clamped, and FR = free.

Appendix B

Analytical Contact Law Model for Response of an Isotropic Plate to Impact Loading

In this analytical development, a contact law model for response of a plate to impact loading is considered. The problem of low velocity impact on laminated composites is idealized using the classical Hertzian contact law. For a detailed discussion of the origins of the law and limiting assumptions, see the work by Goldsmith [41]. The law as applied to composite plates has been investigated by a number of researchers such as Tan and Sun [12], Yang and Sun [14], and Dobyns [42]. The essential feature of this contact law is given below (Eq. B.1) in the relationship between the force generated between two colliding elastic bodies and their relative displacement. The geometry of the colliding bodies is illustrated in Figure B.1.

$$F(t) = k\alpha_o^{3/2} = k\left(w_s - w_p\right)^{3/2} \tag{B.1}$$

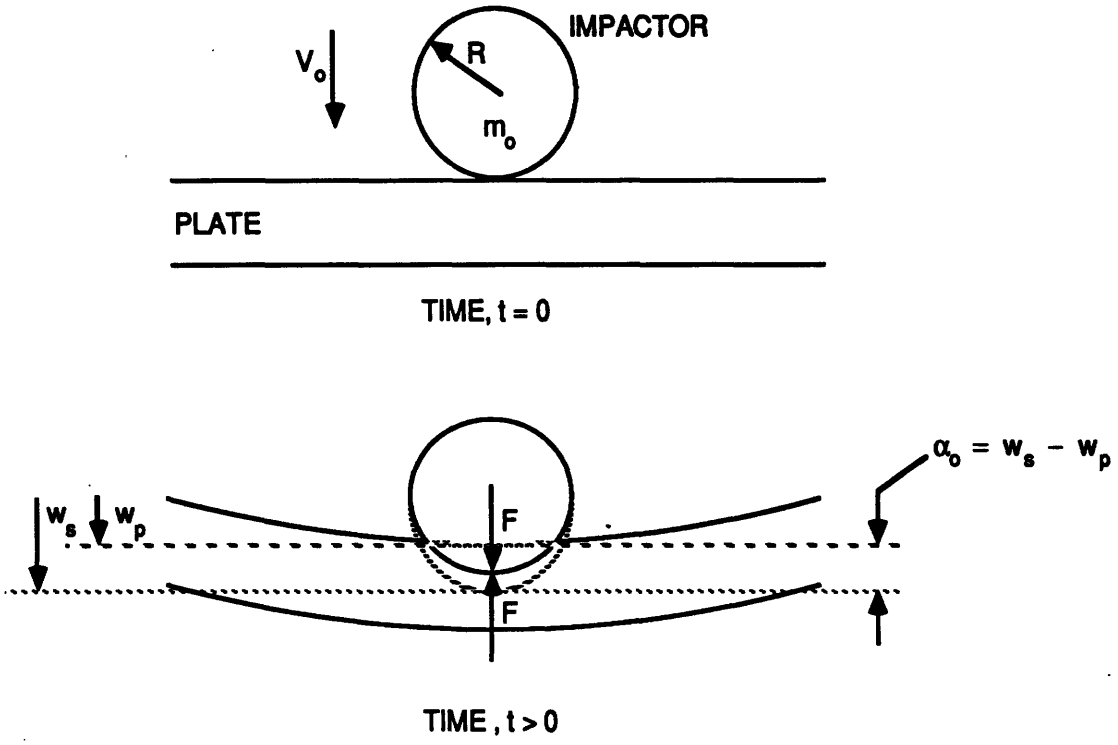

GEOMETRY OF COLLIDING BODIES

where,

R : radius of impactor
m_o : mass of impactor
V_o : velocity of impactor at $t = 0$
w_p : structural deflection of plate at center of contact
w_s : displacement of impactor relative to position at $t = 0$
F : force generated between the colliding bodies
α_o : relative displacement or approach of the colliding bodies

Figure B.1 : Geometry of Colliding Bodies

To determine the force, $F(t)$, the following procedure is used. First, the proportionality constant or local stiffness constant, k, can be found either experimentally [14] or analytically using the Hertzian contact theory [41]. The present discussion uses the analytical constant describing a spherical body contacting a plane surface and can be written as,

$$k = \frac{4}{3\pi} \frac{\sqrt{R}}{(\delta_1 + \delta_2)} \tag{B.2a}$$

where,

$$\delta_1 = \frac{1 - \nu_1^2}{\pi E_1} \quad ; \quad \text{impactor} \tag{B.2b}$$

$$\delta_2 = \frac{1 - \nu_2^2}{\pi E_2} \quad ; \quad \text{plate} \tag{B.2c}$$

and

E_1 : modulus of impactor
ν_1 : Poisson's ratio of impactor
E_2 : transverse modulus of plate
ν_2 : transverse Poisson's ratio of plate

Second, the displacement, w_s, can be determined from Newton's second law if the contact force is assumed to cause the impactor to decelerate. Taking the initial velocity as V_o, the expression for w_s becomes,

$$w_s = V_o t - \frac{1}{m_o} \int_0^t F(\tau)(t - \tau)\, d\tau \tag{B.3}$$

The approach, α_o, can then be written as,

$$\alpha_o = V_o t - \frac{1}{m_o} \int_0^t F(\tau)(t - \tau)\, d\tau - w_p \tag{B.4}$$

Substituting the Hertzian contact law equation (B.1) for α_o, the Eq. (B.4) becomes,

$$\left(\frac{F}{k}\right)^{2/3} = V_o t - \frac{1}{m_o}\int_0^t F(\tau)(t-\tau)\,d\tau - w_p \tag{B.5}$$

which is the governing nonlinear integral equation in terms of the contact force, $F(t)$, and the plate displacement, w_p, which can be expressed in terms of $F(t)$ for a four-sides simply supported boundary condition case [10] as,

$$w_p(x,y,t) = \frac{4}{abm_p}\sum\sum\frac{1}{\omega_{mn}}\left[\int_0^t F(\tau)\sin\omega_{mn}(t-\tau)d\tau\right] \times \sin\left(\frac{m\pi}{2}\right)\sin\left(\frac{n\pi}{2}\right)\sin\left(\frac{m\pi x}{a}\right)\sin\left(\frac{n\pi y}{b}\right) \tag{B.6}$$

where, m_p, a, and b denote a plate mass of unit area, dimensions of a plate in the x and y directions, respectively.

Appendix C1

NLBEAM FORTRAN Source Code

NLBEAM is the FORTRAN program analyzing both linear and nonlinear transient response of an isotropic beam due to an impact loading used in Section 4.3. The program algorithm is based on solving Eqs. (4.2.9), (4.2.11), and (4.2.12) using a fourth-order Runge-Kutta numerical integration method.

Sample input data file "beam.dat" and output data file "beam.out" are also listed.

```
C=======================================================================
      PROGRAM NLBEAM
C=======================================================================
C
C Program developed by Hiroto Matsuhashi,
C Technology Laboratory for Advanced Composites,
C Department of Aeronautics and Astronautics, MIT, 1992.
C
C
C Copyright c1992 Massachusetts Institute of Technology
C
C
C Permission to use, copy, and modify this software and its
C documentation for internal purposes only and without fee is hereby
C granted provided that the above copyright notice and this
C permission appear on all copies of the code and supporting
C documentation.  For any other use of this software, in original or
C modified form, including but not limited to, adaptation as the
C basis of a commercial software or hardware product, or distribution
C in whole or in part, specific prior permission and/or the
C appropriate licenses must be obtained from MIT.
C
C This software is provided "as is" without any warranties
C whatsoever, either express or implied, including but not limited to
C the implied warranties of marchantability and fitness for a
C particular purpose.
C
C This software is a research program, and MIT does not represent
C that it is free of errors or bugs or suitable for any particular
C task.
C
C=======================================================================
C
C     This test program computes transient response of impact force
C     and displacement of the rigidly clamped beam using nonlinearity
C     effect which produces stiffening effect.
C
C     The governing equation of the beam used in this program is,
C
C     q" + C1*q + C2*(q**3) = C3*P
C
C     where,
C         q  :  Modal amplitude for the transverse displacement ( w )
C         P  :  Impact force
C        (") :  Second derivative with respect to time
C         C1, C2, C3 : Constants due to given mode and other
C                      conditions.
C
C     This equation and also impactor equation of motion can be
C     solved by numerical time integration (this program uses 4th-
C     order Runge-Kutta method).
C
C     Note that in-plane displacement ( u ) is not considered in this
C     analysis.
C=======================================================================
```

```
C
C
C     [ VARIABLES ]
      IMPLICIT DOUBLE PRECISION (A-H, O-Z)
      DOUBLE PRECISION mB,L,k,n,mI
      INTEGER ts
C
C
      CALL INPUT(E,aI,aA,mB,L,beta,k,n,vI,mI,dt,ts,ITI)
C
      OPEN( UNIT=11, FILE='beam.out', STATUS='NEW' )
C
C
      C1 = 500.6*E*aI/(mB*(L**4))
      C2 = 75.6*beta*E*aA/(mB*(L**4))
      C3 = 1.588/(mB*L)
C
C
C     -------------------------
C     * VARIABLE INITIALIZATION
C     -------------------------
C
      time= 0.
      y   = 0.
      q   = 0.
      z   = vI
      u   = 0.
      P   = 0.
      P1  = 0.
      IT  = 0
C
C
C
C     ------------------------------------------------------
C     * TIME INTEGRATION USING 4th-ORDER RUNGE-KUTTA METHOD
C     ------------------------------------------------------
C
      DO 10 I=1,ts
C
         IT = IT+1
C
         CALL RK4(C1,C2,C3,mI,y,q,z,u,P,dt)
C
         alpha = u+1.588*q
         IF(alpha .LT. 0.) THEN
            P = k*(-alpha)**n
            P = 0.
            P0= 0.
         ELSE
            P = -k*(alpha)**n
            P0= -P
         ENDIF
C
         w = -1.588*q
         time = time+dt
```

```
C
         IF(IT .EQ. ITI) THEN
            WRITE(11,40)time,P0,w
 40         FORMAT(3F16.8)
            IT = 0
         ENDIF
C
 10   CONTINUE
C
C
C
      CLOSE( UNIT=11 )
C
C
      STOP
      END
C
C
C=====================================================================
C
C---------------------------------------------------------------------
C
C
C     SUBROUTINE LIBRARIES
C
C
C---------------------------------------------------------------------
      SUBROUTINE INPUT(E,aI,aA,mB,L,beta,k,n,vI,mI,dt,ts,ITI)
C---------------------------------------------------------------------
C
C     [ VARIABLES ]
      IMPLICIT DOUBLE PRECISION (A-H, O-Z)
      DOUBLE PRECISION mB, L, k, n, mI
      INTEGER ts
C
C
      OPEN( UNIT=10, FILE='beam.dat', STATUS='OLD' )
C
      READ(10,*) E, aI, aA, mB, L
      READ(10,*) beta, k, n
      READ(10,*) vI, mI, dt, ts, ITI
C
      CLOSE( UNIT=10 )
C
      RETURN
      END
C
C
C---------------------------------------------------------------------
C
C---------------------------------------------------------------------
      SUBROUTINE RK4(C1,C2,C3,mI,y,q,z,u,P,dt)
C---------------------------------------------------------------------
C
C     [ VARIABLES ]
```

```
      IMPLICIT DOUBLE PRECISION (A-H, O-Z)
      DOUBLE PRECISION mI
C
C
      FUN1(C1,C2,C3,P,q) = C3*P - C1*q - C2*(q**3)
C
      ak1 = dt * FUN1(C1,C2,C3,P,q)
      bk1 = dt * y
      ak2 = dt * FUN1(C1,C2,C3,P,q+.5*bk1)
      bk2 = dt * (y+.5*ak1)
      ak3 = dt * FUN1(C1,C2,C3,P,q+.5*bk2)
      bk3 = dt * (y+.5*ak2)
      ak4 = dt * FUN1(C1,C2,C3,P,q+bk3)
      bk4 = dt * (y+ak3)
      y   = y + (ak1+2.*ak2+2.*ak3+ak4)/6.
      q   = q + (bk1+2.*bk2+2.*bk3+bk4)/6.
C
      ck1 = dt * (P/mI)
      dk1 = dt * z
      ck2 = ck1
      dk2 = dt * (z+.5*ck1)
      ck3 = ck1
      dk3 = dt * (z+.5*ck2)
      ck4 = ck1
      dk4 = dt * (z+ck3)
      z   = z + (ck1+2.*ck2+2.*ck3+ck4)/6.
      u   = u + (dk1+2.*dk2+2.*dk3+dk4)/6.
C
C
      RETURN
      END
C
C
C-----------------------------------------------------------------------
```

Sample Input Data File "beam.dat"

```
70.E+9      3.084E-11  0.000143112      0.22  0.252
1.0   1.0E+6      1.5
3.0   1.53  0.000001   30000       50
```

Each input number represents (in order);

First Line :
- Young's Modulus of Elasticity of Beam [Pa]
- Area Moment of Inertia of Beam Cross Section [m^4]
- Cross Sectional Area [m^2]
- Mass of Beam for Unit Length [kg/m]
- Length of the Beam [m]

Second Line :
- Geometrical Nonlinearity Factor, β [range from 0 to 1]
- k: Local Contact Stiffness [N/m^n]
- n: Local Nonlinearity Exponent

Third Line :
- Initial Velocity of Impactor [m/s]
- Mass of Impactor [kg]
- Time Increment for Numerical Integration [sec]
- Time Steps
- Time Steps to be skipped for Reduction of the Output

Sample Output Data File "beam.dat"

First Column	Second Column	Third Column
Time [sec]	Impact Force [N]	Plate Midplane Displacement [m]
0.00005000	1.83668781	0.00000002
0.00010000	5.18916491	0.00000027
0.00015000	9.51042019	0.00000110
0.00020000	14.58464281	0.00000302
0.00025000	20.26597376	0.00000658
0.00030000	26.43471571	0.00001243
0.00035000	32.98214768	0.00002124
0.00040000	39.80411433	0.00003373
0.00045000	46.79826615	0.00005063
0.00050000	53.86313209	0.00007270
0.00055000	60.89823773	0.00010065
0.00060000	67.80487145	0.00013522
0.00065000	74.48726969	0.00017707
0.00070000	80.85407277	0.00022683
0.00075000	86.81994612	0.00028508
0.00080000	92.30728863	0.00035229
0.00085000	97.24796853	0.00042888
0.00090000	101.58504245	0.00051514
0.00095000	105.27442534	0.00061125
0.00100000	108.28648802	0.00071726
0.00105000	110.60756402	0.00083307
0.00110000	112.24134631	0.00095841
0.00115000	113.21014790	0.00109284
⋮	⋮	⋮
⋮	⋮	⋮
⋮	⋮	⋮

Appendix C2

NLBEAM2 FORTRAN Source Code

NLBEAM2 is the FORTRAN program analyzing both linear and nonlinear transient response of an isotropic beam due to an impact loading used in Section 4.3. The program algorithm is based on solving Eqs. (4.2.9), (4.2.11), and (4.2.12) using a fourth-order Runge-Kutta numerical integration method. Both an in-plane and out-of-plane displacements are considered in this program.

Input data file "beam.dat" and output data file "beam.out" take the same formats as listed in Appendix C1.

```
C=======================================================================
      PROGRAM NLBEAM2
C=======================================================================
C
C Program developed by Hiroto Matsuhashi,
C Technology Laboratory for Advanced Composites,
C Department of Aeronautics and Astronautics, MIT, 1992.
C
C
C Copyright c1992 Massachusetts Institute of Technology
C
C
C Permission to use, copy, and modify this software and its
C documentation for internal purposes only and without fee is hereby
C granted provided that the above copyright notice and this
C permission appear on all copies of the code and supporting
C documentation.  For any other use of this software, in original or
C modified form, including but not limited to, adaptation as the
C basis of a commercial software or hardware product, or distribution
C in whole or in part, specific prior permission and/or the
C appropriate licenses must be obtained from MIT.
C
C This software is provided "as is" without any warranties
C whatsoever, either express or implied, including but not limited to
C the implied warranties of marchantability and fitness for a
C particular purpose.
C
C This software is a research program, and MIT does not represent
C that it is free of errors or bugs or suitable for any particular
C task.
C
C=======================================================================
C
C     This test program computes transient response of impact force
C     and displacement of the rigidly clamped beam using nonlinearity
C     effect which produces stiffening effect.  Also, in-plane
C     displacement ( u ) is considered in this analysis.
C
C     The governing equations of the beam used in this program are,
C
C     q" + C1*q + C2*(q**3) + C6*p*q = C3*P
C     p" + C4*p + C5*(q**2) = 0
C
C     where,
C         q  :  Modal amplitude for the transverse displacement ( w )
C         P  :  Impact force
C         p  :  Modal amplitude for the inplane displacement ( u )
C        (") :  Second derivative with respect to time
C         C1, C2, C3,
C         C4, C5, C6 : Constants due to given mode and other
C                      conditions.
C
C     These coupled equations and also impactor equation of motion
C     can be solved by numerical time integration (this program uses
C     4th-order Runge-Kutta method).
```

```
C
C=============================================================
C
C     [ VARIABLES ]
      IMPLICIT DOUBLE PRECISION (A-H, O-Z)
      DOUBLE PRECISION mB,L,k,n,mI
      INTEGER ts
C
C
      CALL INPUT(E,aI,aA,mB,L,beta,k,n,vI,mI,dt,ts,ITI)
C
      OPEN( UNIT=11, FILE='beam.out', STATUS='NEW' )
C
C
      CALL INTEGRL(L,D1,D2,D3)
C
C
      C1 = 500.6*E*aI/(mB*(L**4))
      C2 = 75.6*beta*E*aA/(mB*(L**4))
      C3 = 1.588/(mB*L)
      C4 = D2/D1*E*aA/mB
      C5 = D3/D1*E*aA/mB
      C6 = D3*E*aA/(mB*L)
C
C
C     -------------------------
C     * VARIABLE INITIALIZATION
C     -------------------------
C
      time= 0.
      y   = 0.
      q   = 0.
      z   = vI
      u   = 0.
      P   = 0.
      P1  = 0.
      IT  = 0
      s   = 0.
      r   = 0.
      P1  = 0.
C
C
C
C     ------------------------------------------------------
C     * TIME INTEGRATION USING 4th-ORDER RUNGE-KUTTA METHOD
C     ------------------------------------------------------
C
      DO 10 I=1,ts
C
         IT = IT+1
C
         CALL RK4(C1,C2,C3,C4,C5,C6,mI,y,q,z,u,P,dt,s,r)
C
         alpha = u+1.588*q
         IF(alpha .LT. 0.) THEN
```

```
            P = k*(-alpha)**n
            P0= 0.
         ELSE
            P = -k*(alpha)**n
            P0= -P
         ENDIF
C
         w = -1.588*q
         time = time+dt
C
         IF(IT .EQ. ITI) THEN
            WRITE(11,40)time,P0,w
 40         FORMAT(4F16.8)
            IT = 0
         ENDIF
C
 10   CONTINUE
C
C
C
      CLOSE( UNIT=11 )
C
C
      STOP
      END
C
C
C=======================================================================
C
C-----------------------------------------------------------------------
C
C
C     SUBROUTINE LIBRARIES
C
C
C-----------------------------------------------------------------------
      SUBROUTINE INPUT(E,aI,aA,mB,L,beta,k,n,vI,mI,dt,ts,ITI)
C-----------------------------------------------------------------------
C
C     [ VARIABLES ]
      IMPLICIT DOUBLE PRECISION (A-H, O-Z)
      DOUBLE PRECISION mB, L, k, n, mI
      INTEGER ts
C
C
      OPEN( UNIT=10, FILE='beam.dat', STATUS='OLD' )
C
      READ(10,*) E, aI, aA, mB, L
      READ(10,*) beta, k, n
      READ(10,*) vI, mI, dt, ts, ITI
C
      CLOSE( UNIT=10 )
C
      RETURN
      END
```

```
C
C
C-----------------------------------------------------------------
C


C-----------------------------------------------------------------
      SUBROUTINE INTEGRL(L,D1,D2,D3)
C-----------------------------------------------------------------
C
C     [ VARIABLES ]
      IMPLICIT DOUBLE PRECISION (A-H, O-Z)
      DOUBLE PRECISION L
C
C
C
      SI(x,L) =SIN(2.*3.14159*x/L)
      DSI(x,L)=2.*3.14159/L*COS(2.*3.14159*x/L)
      DPI(x,L)=1.5*3.14159/L*SQRT(2.)*
     &        COS(1.5*3.14159*x/L-(3.14159/4.))
     &       +(-1.5*3.14159/L)*EXP(-1.5*3.14159*x/L)
     &       +(1.5*3.14159/L)*EXP(-1.5*3.14159+1.5
     &       *3.14159*x/L)
C
C
      D1 = (L/5.)*(0.5*(SI(L/5.,L)**2) + SI(2.*L/5.,L)**2
     &    + SI(3.*L/5.,L)**2 + SI(4.*L/5.,L)**2
     &    + 0.5*(SI(5.*L/5.,L)**2))
C
      D2 = (L/5.)*(0.5*(DSI(L/5.,L)**2) + DSI(2.*L/5.,L)**2
     &    + DSI(3.*L/5.,L)**2 + DSI(4.*L/5.,L)**2
     &    + 0.5*(DSI(5.*L/5.,L)**2))
C
      D3 = (L/5.)*(0.5*(SI(L/5.,L)*(DPI(L/5.,L)**2))
     &    + SI(2.*L/5.,L)*(DPI(2.*L/5.,L)**2)
     &    + SI(3.*L/5.,L)*(DPI(3.*L/5.,L)**2)
     &    + SI(4.*L/5.,L)*(DPI(4.*L/5.,L)**2)
     &    + 0.5*SI(5.*L/5.,L)*(DPI(5.*L/5.,L)**2))
C
C
      RETURN
      END
C
C
C-----------------------------------------------------------------
C
C-----------------------------------------------------------------
      SUBROUTINE RK4(C1,C2,C3,C4,C5,C6,mI,y,q,z,u,P,dt,s,r)
C-----------------------------------------------------------------
C
C     [ VARIABLES ]
      IMPLICIT DOUBLE PRECISION (A-H, O-Z)
      DOUBLE PRECISION mI
C
C
```

```
      FUN1(C1,C2,C3,C6,P,s,q) = C3*P - C1*q - C2*(q**3) - C6*s*q
      FUN2(C4,C5,s,q) = - C4*s - C5*(q**2)
C
C
         ek1 = dt * FUN2(C4,C5,s,q)
         fk1 = dt * r
         ek2 = dt * FUN2(C4,C5,s+.5*fk1,q)
         fk2 = dt * (r+.5*ek1)
         ek3 = dt * FUN2(C4,C5,s+.5*fk2,q)
         fk3 = dt * (r+.5*ek2)
         ek4 = dt * FUN2(C4,C5,s+.5*fk3,q)
         fk4 = dt * (r+ek3)
         r   = r + (ek1+2.*ek2+2.*ek3+ek4)/6.
         s   = s + (fk1+2.*fk2+2.*fk3+fk4)/6.
C
         ak1 = dt * FUN1(C1,C2,C3,C6,P,s,q)
         bk1 = dt * y
         ak2 = dt * FUN1(C1,C2,C3,C6,P,s,q+.5*bk1)
         bk2 = dt * (y+.5*ak1)
         ak3 = dt * FUN1(C1,C2,C3,C6,P,s,q+.5*bk2)
         bk3 = dt * (y+.5*ak2)
         ak4 = dt * FUN1(C1,C2,C3,C6,P,s,q+bk3)
         bk4 = dt * (y+ak3)
         y   = y + (ak1+2.*ak2+2.*ak3+ak4)/6.
         q   = q + (bk1+2.*bk2+2.*bk3+bk4)/6.
C
C
      ck1 = dt * (P/mI)
      dk1 = dt * z
      ck2 = ck1
      dk2 = dt * (z+.5*ck1)
      ck3 = ck1
      dk3 = dt * (z+.5*ck2)
      ck4 = ck1
      dk4 = dt * (z+ck3)
      z   = z + (ck1+2.*ck2+2.*ck3+ck4)/6.
      u   = u + (dk1+2.*dk2+2.*dk3+dk4)/6.
C
C
      RETURN
      END
C
C
C-----------------------------------------------------------------------
```

Appendix D

GLOBAL2 FORTRAN Source Code

GLOBAL2 is the FORTRAN program analyzing both linear and nonlinear transient response of a shear deformable composite laminated plate due to an impact loading used in Chapters 5 and 6. The program algorithm is based on solving Eqs. (6.1.1), (5.2.50), and (5.2.51) using a fourth-order Runge-Kutta numerical integration method.

Sample input data files "global2.dat" and output data file "global2.out" are also listed.

```
C=======================================================================
      PROGRAM GLOBAL2
C=======================================================================
C
C Program developed by Hiroto Matsuhashi,
C Technology Laboratory for Advanced Composites,
C Department of Aeronautics and Astronautics, MIT, 1992.
C
C
C Copyright c1992 Massachusetts Institute of Technology
C
C
C Permission to use, copy, and modify this software and its
C documentation for internal purposes only and without fee is hereby
C granted provided that the above copyright notice and this
C permission appear on all copies of the code and supporting
C documentation.  For any other use of this software, in original or
C modified form, including but not limited to, adaptation as the
C basis of a commercial software or hardware product, or distribution
C in whole or in part, specific prior permission and/or the
C appropriate licenses must be obtained from MIT.
C
C This software is provided "as is" without any warranties
C whatsoever, either express or implied, including but not limited to
C the implied warranties of marchantability and fitness for a
C particular purpose.
C
C This software is a research program, and MIT does not represent
C that it is free of errors or bugs or suitable for any particular
C task.
C
C=======================================================================
C
C  This program analyzes the both linear and nonlinear global
C  transient response (i.e. force- and displacement-time histories)
C  of shear deformable composite laminated plates subjected to impact
C  loading.
C
C=======================================================================
C
C
C     [ Variables ]
C
      IMPLICIT DOUBLE PRECISION (A-H, O-Z)
      DOUBLE PRECISION mI,k,n,M1,M2,M3,
     &                 K1aa,K1ab,K1ae,K1bb,K1be,K1ee,K3ee,
     &                 KI,KIII
      INTEGER Ibx,Iby,IBCX,IBCY,NX,NY,IBC,ts
C
      PARAMETER ( N1=10, N2=N1*7, N4=N2**3 )
C
      DIMENSION BETAX(N1),BETAY(N1),BX(N1),BY(N1)
      DIMENSION CX(N1),CY(N1),DX(N1),DY(N1),EX(N1),EY(N1)
      DIMENSION M1(N2),M2(N2),M3(N2)
      DIMENSION K1aa(N2,N2),K1ab(N2,N2),K1ae(N2,N2)
```

```
      DIMENSION Klbb(N2,N2),Klbe(N2,N2),Klee(N2,N2)
      DIMENSION KI(N2,N2),KIII(N2,N4),Ri(N2),Rii(N2)
C
C
C     ================
C     * Main Program
C     ================
C
C
      CALL INPUT(IEO,Ibx,Iby,beta,IBCX,IBCY,NX,NY,XL,YL,
     &           A11,A22,A12,A16,A26,A66,
     &           D11,D22,D12,D16,D26,D66,
     &           G44,G55,G45,z1,z3,
     &           mI,vI,cf,
     &           k,n,dt,ts,ITI)
C
C
C
      IF(IEO .EQ. 0) THEN
C
         CALL BOUND(IBCX,NX,AX,THETAX,BETAX,BX,CX,DX,EX)
C
         CALL BOUND(IBCY,NY,AY,THETAY,BETAY,BY,CY,DY,EY)
C
      ENDIF
C
C
      IF(IEO .EQ. 1) THEN
C
         CALL BOUND1(IBCX,NX,AX,THETAX,BETAX,BX,CX,DX,EX)
C
         CALL BOUND1(IBCY,NY,AY,THETAY,BETAY,BY,CY,DY,EY)
C
      ENDIF
C
C
      CALL INTGRL1(NX,NY,AX,AY,THETAX,THETAY,IEO,
     &             BETAX,BETAY,BX,BY,
     &             CX,CY,DX,DY,EX,EY,
     &             D11,D22,D12,D16,D26,D66,
     &             G44,G55,G45,z1,z3,XL,YL,
     &             M1,M2,M3,Ri,cf,Rii,
     &             K1aa,K1ab,K1ae,K1bb,K1be,K1ee)
C
C
      CALL ARRANGE(NX,NY,iKaa,iKab,jKab,iKae,iKbb,iKbe,
     &             M1,M2,K1aa,K1ab,K1ae,K1bb,K1be)
C
C
      CALL CONDENS(NX,NY,iKaa,iKab,jKab,iKae,iKbb,iKbe,
     &             K1aa,K1ab,K1ae,K1bb,K1be,K1ee,KI)
C
C
      IF((Ibx .EQ. 0) .AND. (Iby .EQ. 0)) GOTO 100
C
```

```
C
      CALL INTGRL2(Ibx,Iby,beta,NX,NY,AX,AY,THETAX,THETAY,IEO,
     &             BETAX,BETAY,BX,BY,
     &             CX,CY,DX,DY,EX,EY,
     &             A11,A22,A12,A16,A26,A66,
     &             XL,YL,KIII)
C
C
 100  CONTINUE
C
C
      OPEN( UNIT=11, FILE='global2.out', STATUS='NEW' )
C
C
      IF(cf .EQ. 0.)THEN
C
         CALL SOLVE(NX,NY,M3,KI,KIII,Ri,vI,mI,k,n,dt,ts,ITI,
     &              Ibx,Iby,XL,YL,BETAX,BETAY,THETAX,THETAY,
     &              AX,AY,BX,BY,CX,CY,DX,DY,EX,EY)
C
      ELSE
C
         CALL SOLVE2(NX,NY,M3,KI,KIII,Ri,vI,mI,k,n,dt,ts,ITI,
     &               Ibx,Iby,XL,YL,BETAX,BETAY,THETAX,THETAY,
     &               AX,AY,BX,BY,CX,CY,DX,DY,EX,EY,Rii)
C
      ENDIF
C
C
      CLOSE( UNIT=11 )
C
C
      STOP
      END
C
C
C=======================================================================
C
C
C     SUBROUTINE LIBRARIES
C
C
C=======================================================================
C
C
C-----------------------------------------------------------------------
      SUBROUTINE  INPUT(IEO,Ibx,Iby,beta,IBCX,IBCY,NX,NY,XL,YL,
     &                  A11,A22,A12,A16,A26,A66,
     &                  D11,D22,D12,D16,D26,D66,
     &                  G44,G55,G45,z1,z3,
     &                  mI,vI,cf,
     &                  k,n,dt,ts,ITI)
C-----------------------------------------------------------------------
C
C
```

```
C  This subroutine reads data from existing input data file called
C  "global2.dat".  The format of the "global2.dat" is described as
C  follows;
C
C  line 1-5: comment line (program does not read)
C  line 5  : Ibx, Iby, beta
C  line 6  : IBCX, IBCY, NX, NY
C  line 7  : IEO
C  line 8  : XL, YL, THICK, ROU
C  line 9  : A11, A22, A12, A16, A26, A66
C  line 10 : D11, D22, D12, D16, D26, D66
C  line 11 : G44, G55, G45, sc
C  line 12 : mI, vI, cf, k, n
C  line 13 : dt, ts, ITI
C
C
C  where,
C
C
C     Ibx, Iby  : nonlinearity index numbers (integer) in the x and y
C                 direction
C                   1   =>  include nonlinear effect
C                   0   =>  do not include nonlinear effect (linear)
C
C     beta      : geometrical nonlinearity factor ranging from 0.0 to
C                 1.0
C                 0.0 =>  linear case
C                 1.0 =>  perfectly nonlinear case
C
C     IBCX, IBCY: index numbers for the boundary conditions in x and
C                 y directions
C                   1   =>  simply supported - simply supported
C                   2   =>  clamped - free
C                   3   =>  clamped - clamped
C                   4   =>  free - free
C                   5   =>  simply supported - clamped
C                   6   =>  simply supported - free
C
C     NX, NY    : number of modes in the x and y directions
C
C     IEO       : switch for turning off even modes
C                   0   =>  both odd and even modes
C                   1   =>  odd modes only
C
C     XL, YL    : dimensions of plate in the x and y directions (m)
C
C     THICK, ROU: thickness of the plate (m), density of the plate
C                 (kg/m^3)
C
C     A's       : tensor components of A matrix (N/m)
C     D's       : tensor components of D matrix (N-m)
C     G's       : shear stiffness components (N/m)
C     sc        : shear correction factor
C
C     mI, vI    : mass of impactor, initial impactor velocity
```

```
C
C     cf        : dimension of the square shape of the patched
C                 loading for point loading, let cf = 0.0
C                 (This program is capable of dealing with double-
C                  cosine type distributed patch loading, although
C                  there has not been verified, yet.)
C
C     k, n      : local contact stiffness (N/m^n), nonlinearity
C                 exponent
C
C     dt, ts    : time increment (sec), number of time steps
C
C     ITI       : number of time steps to be skipped for reducing the
C                 output results.  (i.e. for ITI=10, every 10th data
C                 will be recorded in the output data file.)
C
C-----------------------------------------------------------------------
C
C
C     [ Variables ]
C
      IMPLICIT DOUBLE PRECISION (A-H, O-Z)
      DOUBLE PRECISION mI,k,n
      INTEGER ts
C
C
C
      OPEN( UNIT=10, FILE='global2.dat', STATUS='OLD' )
C
C
      READ(10,*)
      READ(10,*)
      READ(10,*)
      READ(10,*)
      READ(10,*)
      READ(10,*) Ibx,Iby,beta
      READ(10,*) IBCX,IBCY,NX,NY
      READ(10,*) IEO
      READ(10,*) XL,YL,THICK,ROU
      READ(10,*) A11,A22,A12,A16,A26,A66
      READ(10,*) D11,D22,D12,D16,D26,D66
      READ(10,*) G44,G55,G45,sc
      READ(10,*) mI,vI,cf,k,n
      READ(10,*) dt,ts,ITI
C
C
      z1 = ROU*THICK
      z3 = ROU*(THICK**3)/12.
C
      G44 = sc*sc*G44
      G55 = sc*sc*G55
      G45 = sc*sc*G45
C
C
      CLOSE( UNIT=10 )
```

```
C
C
C
      RETURN
      END
C
C
C
C-----------------------------------------------------------------------
C
C-----------------------------------------------------------------------
      SUBROUTINE BOUND(IBC,N,A,THETA,BETA,B,C,D,E)
C-----------------------------------------------------------------------
C
C  This subroutine determines the the euler beam elastic mode shape
C  parameters depending on the boundary condition of each x and y
C  direction based on the Generalized Beam Functions described in
C  Appendix A.
C
C-----------------------------------------------------------------------
C
C
C     [ Variables ]
C
      IMPLICIT DOUBLE PRECISION (A-H, O-Z)
      INTEGER IBC,N
C
      PARAMETER ( N1=10 )
C
      DIMENSION BETA(N1),B(N1),C(N1),D(N1),E(N1)
C
C
C
      PI = 3.14159265
C
C
C
      IF(IBC .EQ. 1) THEN
         A = 0.
         THETA = 0.
         DO 201 I=1,N
            BETA(I) = (1.*I)*PI
            B(I) = 0.
            C(I) = 1.
            D(I) = 0.
            E(I) = 0.
 201     CONTINUE
      ENDIF
C
C
      IF(IBC .EQ. 2) THEN
         A = 1.
         THETA = -PI/4.
         DO 202 I=1,N
            BETA(I) = (1.*I-0.5)*PI
```

```
            B(I) = (-1.)**(I+1)
            C(I) = 1.
            D(I) = 0.
            E(I) = 0.
 202     CONTINUE
      ENDIF
C
C
      IF(IBC .EQ. 3) THEN
         A = 1.
         THETA = -PI/4.
         DO 203 I=1,N
            BETA(I) = (1.*I+0.5)*PI
            B(I) = (-1.)**(I+1)
            C(I) = 1.
            D(I) = 0.
            E(I) = 0.
 203     CONTINUE
      ENDIF
C
C
      IF(IBC .EQ. 4) THEN
         A = 1.
         THETA = 3.*PI/4.
         C(1) = 0.
         C(2) = 0.
         D(1) = 0.
         D(2) = 1.
         E(1) = 1.
         E(2) = 1.
         DO 204 I=3,N
            BETA(I) = (1.*I+0.5)*PI
            B(I) = (-1.)**(I+1)
            C(I) = 1.
            D(I) = 0.
            E(I) = 0.
 204     CONTINUE
      ENDIF
C
C
      IF(IBC .EQ. 5) THEN
         A = 0.
         THETA = 0.
         DO 205 I=1,N
            BETA(I) = (1.*I+0.25)*PI
            B(I) = (-1.)**(I+1)
            C(I) = 1.
            D(I) = 0.
            E(I) = 0.
 205     CONTINUE
      ENDIF
C
C
      IF(IBC .EQ. 6) THEN
         A = 0.
```

```
         THETA = 0.
         DO 206 I=1,N
            BETA(I) = (1.*I+0.25)*PI
            B(I) = (-1.)**(I)
            C(I) = 1.
            D(I) = 0.
            E(I) = 0.
 206     CONTINUE
      ENDIF
C
C
C
      RETURN
      END
C
C
C
C-----------------------------------------------------------------------
C
C-----------------------------------------------------------------------
      SUBROUTINE BOUND1(IBC,N,A,THETA,BETA,B,C,D,E)
C-----------------------------------------------------------------------
C
C  This subroutine determines the the euler beam elastic mode shape
C  parameters for odd modes only case depending on the boundary
C  condition of each x and y direction based on the  Generalized Beam
C  Functions described in Appendix A.
C
C-----------------------------------------------------------------------
C
C
C     [ Variables ]
C
      IMPLICIT DOUBLE PRECISION (A-H, O-Z)
      INTEGER IBC,N
C
      PARAMETER ( N1=10 )
C
      DIMENSION BETA(N1),B(N1),C(N1),D(N1),E(N1)
C
C
C
      PI = 3.14159265
C
C
C
      IF(IBC .EQ. 1) THEN
         A = 0.
         THETA = 0.
         DO 201 I=1,N
            BETA(I) = ((I*2.)-1.)*PI
            B(I) = 0.
            C(I) = 1.
            D(I) = 0.
            E(I) = 0.
```

```
 201     CONTINUE
      ENDIF
C
C
      IF(IBC .EQ. 2) THEN
         A = 1.
         THETA = -PI/4.
         DO 202 I=1,N
            BETA(I) = (1.*((I*2.)-1.)-0.5)*PI
            B(I) = (-1.)**(((I*2)-1)+1)
            C(I) = 1.
            D(I) = 0.
            E(I) = 0.
 202     CONTINUE
      ENDIF
C
C
      IF(IBC .EQ. 3) THEN
         A = 1.
         THETA = -PI/4.
         DO 203 I=1,N
            BETA(I) = ((I*2.-1.)+0.5)*PI
            B(I) = (-1.)**((I*2-1)+1)
            C(I) = 1.
            D(I) = 0.
            E(I) = 0.
 203     CONTINUE
      ENDIF
C
C
      IF(IBC .EQ. 4) THEN
         A = 1.
         THETA = 3.*PI/4.
         C(1) = 0.
         D(1) = 0.
         E(1) = 1.
         DO 204 I=2,N
            BETA(I) = (((I*2.-1.))+0.5)*PI
            B(I) = (-1.)**(((I*2-1))+1)
            C(I) = 1.
            D(I) = 0.
            E(I) = 0.
 204     CONTINUE
      ENDIF
C
C
      IF(IBC .EQ. 5) THEN
         A = 0.
         THETA = 0.
         DO 205 I=1,N
            BETA(I) = ((I*2.-1.)+0.25)*PI
            B(I) = (-1.)**((I*2-1)+1)
            C(I) = 1.
            D(I) = 0.
            E(I) = 0.
```

```
 205     CONTINUE
      ENDIF
C
C
      IF(IBC .EQ. 6) THEN
         A = 0.
         THETA = 0.
         DO 206 I=1,N
            BETA(I) = (1.*I+0.25)*PI
            B(I) = (-1.)**(I)
            C(I) = 1.
            D(I) = 0.
            E(I) = 0.
 206     CONTINUE
      ENDIF
C
C
C
      RETURN
      END
C
C
C
C-----------------------------------------------------------------------
C
C-----------------------------------------------------------------------
      SUBROUTINE INTGRL1(NX,NY,AX,AY,THETAX,THETAY,IEO,
     &                   BETAX,BETAY,BX,BY,
     &                   CX,CY,DX,DY,EX,EY,
     &                   D11,D22,D12,D16,D26,D66,
     &                   G44,G55,G45,z1,z3,XL,YL,
     &                   M1,M2,M3,Ri,cf,Rii,
     &                   K1aa,K1ab,K1ae,K1bb,K1be,K1ee)
C-----------------------------------------------------------------------
C
C  This subroutine computes the each matrix component for the
C  stiffness matrix [K] for linear term.
C
C-----------------------------------------------------------------------
C
C
C     [ Variables ]
C
      IMPLICIT DOUBLE PRECISION (A-H, O-Z)
      DOUBLE PRECISION l,M1,M2,M3,
     &                 Kaa,Kab,Kae,Kbb,Kbe,Kee,
     &                 K1aa,K1ab,K1ae,K1bb,K1be,K1ee
      INTEGER NX,NY,NXY,i,j
C
      PARAMETER ( N1=10, N2=N1*7, N4=N2**3 )
C
      DIMENSION BETAX(N1),BETAY(N1),BX(N1),BY(N1)
      DIMENSION CX(N1),CY(N1),DX(N1),DY(N1),EX(N1),EY(N1)
      DIMENSION M1(N2),M2(N2),M3(N2)
      DIMENSION K1aa(N2,N2),K1ab(N2,N2),K1ae(N2,N2)
```

```
      DIMENSION Klbb(N2,N2),Klbe(N2,N2),Klee(N2,N2)
      DIMENSION Ri(N2),Rii(N2)
      DIMENSION DUMMY(N2)
C
C
C
C     ------------------------------------------------------------
C     * Defining Beam Functions & Derivatives of Beam Functions
C     ------------------------------------------------------------
C
C
      f(i,x)   = (BETAX(i)*SQRT(2.)*COS(BETAX(i)*x+THETAX)
     &           -BETAX(i)*AX*EXP(-BETAX(i)*x)
     &           +BETAX(i)*BX(i)*EXP(-BETAX(i)*(1.-x)))*CX(i)
     &           +DX(i)*(-2.)
C
C
      df(i,x) =((-(BETAX(i)**2)*SQRT(2.)*SIN(BETAX(i)
     &                                       *x+THETAX)
     &           +(BETAX(i)**2)*AX*EXP(-BETAX(i)*x)
     &           +(BETAX(i)**2)*BX(i)*EXP(-BETAX(i)
     &                                    *(1.-x)))
     &           *CX(i))/XL
C
C
      g(i,y)   = (SQRT(2.)*SIN(BETAY(i)*y+THETAY)
     &           +AY*EXP(-BETAY(i)*y)
     &           +BY(i)*EXP(-BETAY(i)*(1.-y)))*CY(i)
     &           +2.*EY(i)*(DY(i)*(-y)+0.5)
C
C
      dg(i,y) =((BETAY(i)*SQRT(2.)*COS(BETAY(i)*y+THETAY)
     &           -BETAY(i)*AY*EXP(-BETAY(i)*y)
     &           +BETAY(i)*BY(i)*EXP(-BETAY(i)*(1.-y)))
     &           *CY(i)+DY(i)*(-2.))/YL
C
C
      h(i,x)   = (SQRT(2.)*SIN(BETAX(i)*x+THETAX)
     &           +AX*EXP(-BETAX(i)*x)
     &           +BX(i)*EXP(-BETAX(i)*(1.-x)))*CX(i)
     &           +2.*EX(i)*(DX(i)*(-x)+0.5)
C
C
      dh(i,x) =((BETAX(i)*SQRT(2.)*COS(BETAX(i)*x+THETAX)
     &           -BETAX(i)*AX*EXP(-BETAX(i)*x)
     &           +BETAX(i)*BX(i)*EXP(-BETAX(i)*(1.-x)))
     &           *CX(i)+DX(i)*(-2.))/XL
C
C
      l(i,y)   = (BETAY(i)*SQRT(2.)*COS(BETAY(i)*y+THETAY)
     &           -BETAY(i)*AY*EXP(-BETAY(i)*y)
     &           +BETAY(i)*BY(i)*EXP(-BETAY(i)*(1.-y)))
     &           *CY(i)+DY(i)*(-2.)
C
C
```

```
      dl(i,y) =((-(BETAY(i)**2)*SQRT(2.)*SIN(BETAY(i)
     &                                        *y+THETAY)
     &          +(BETAY(i)**2)*AY*EXP(-BETAY(i)*y)
     &          +(BETAY(i)**2)*BY(i)*EXP(-BETAY(i)
     &                                    *(1.-y)))
     &          *CY(i))/YL
C
C
      q(i,x)  = (SQRT(2.)*SIN(BETAX(i)*x+THETAX)
     &          +AX*EXP(-BETAX(i)*x)
     &          +BX(i)*EXP(-BETAX(i)*(1.-x)))*CX(i)
     &          +2.*EX(i)*(DX(i)*(-x)+0.5)
C
C
      dq(i,x) =((BETAX(i)*SQRT(2.)*COS(BETAX(i)*x+THETAX)
     &          -BETAX(i)*AX*EXP(-BETAX(i)*x)
     &          +BETAX(i)*BX(i)*EXP(-BETAX(i)*(1.-x)))
     &          *CX(i)+DX(i)*(-2.))/XL
C
C
      r(i,y)  = (SQRT(2.)*SIN(BETAY(i)*y+THETAY)
     &          +AY*EXP(-BETAY(i)*y)
     &          +BY(i)*EXP(-BETAY(i)*(1.-y)))*CY(i)
     &          +2.*EY(i)*(DY(i)*(-y)+0.5)
C
C
      dr(i,y) =((BETAY(i)*SQRT(2.)*COS(BETAY(i)*y+THETAY)
     &          -BETAY(i)*AY*EXP(-BETAY(i)*y)
     &          +BETAY(i)*BY(i)*EXP(-BETAY(i)*(1.-y)))
     &          *CY(i)+DY(i)*(-2.))/YL
C
C
C
      xunit = XL/20.
      yunit = YL/20.
C
C
C
C     ------------------------------------------------------
C     * Calculating inertia matrix components by numerical
C       integration using "Extended Trapezoidal Rule"
C     ------------------------------------------------------
C
C
C
      i = 0
      DO 310 ix = 1, NX
         DO 311 iy = 1, NY
            i = i+1
C
            j = 0
            DO 312 jx = 1, NX
               DO 313 jy = 1, NY
                  j = j+1
C
                  xM1 = 0.
```

```
                xM2 = 0.
                xM3 = 0.
C
                yM1 = 0.
                yM2 = 0.
                yM3 = 0.
C
                x = -0.05
                y = -0.05
C
                IF(IEO .EQ. 1) NNN = 11
                IF(IEO .EQ. 0) NNN = 21
C
C
                DO 314 II = 1, NNN
C
                   x = x+0.05
                   y = y+0.05
C
                   rc    = 1.
                   IF((II .EQ. 1) .OR. (II .EQ. 21)) rc = 2.
                   IF(IEO .EQ. 1) THEN
                      IF((II .EQ. 1) .OR. (II .EQ. 11)) rc=2.
                   ENDIF
C
C
                   xM1 = xM1+f(ix,x)*f(jx,x)*xunit/rc
C
                   xM2 = xM2+h(ix,x)*h(jx,x)*xunit/rc
C
                   xM3 = xM3+q(ix,x)*q(jx,x)*xunit/rc
C
C
                   yM1 = yM1+g(iy,y)*g(jy,y)*yunit/rc
C
                   yM2 = yM2+l(iy,y)*l(jy,y)*yunit/rc
C
                   yM3 = yM3+r(iy,y)*r(jy,y)*yunit/rc
C
 314            CONTINUE
C
C
                IF(i .EQ. j) THEN
                   M1(i) = z3 * xM1 * yM1
                   M2(i) = z3 * xM2 * yM2
                   M3(i) = z1 * xM3 * yM3
                ENDIF
C
C
                IF(IEO .EQ. 1) THEN
                   IF(i .EQ. j) THEN
                      M1(i) = z3 * xM1 * yM1 * 4.
                      M2(i) = z3 * xM2 * yM2 * 4.
                      M3(i) = z1 * xM3 * yM3 * 4.
                   ENDIF
```

```
                  ENDIF
C
C
 313           CONTINUE
 312         CONTINUE
C
 311      CONTINUE
 310  CONTINUE
C
C
C
C     ------------------------------------------------------
C     * Calculating stiffness matrix components by numerical
C       integration using "Extended Trapezoidal Rule"
C     ------------------------------------------------------
C
C
      i = 0
      DO 300 ix = 1, NX
         DO 301 iy = 1, NY
            i = i+1
C
            j = 0
            DO 302 jx = 1, NX
               DO 303 jy = 1, NY
                  j = j+1
C
                  xKaa1 = 0.
                  xKaa2 = 0.
                  xKaa3 = 0.
                  xKaa4 = 0.
                  xKab1 = 0.
                  xKab2 = 0.
                  xKab3 = 0.
                  xKab4 = 0.
                  xKae1 = 0.
                  xKae2 = 0.
                  xKbb1 = 0.
                  xKbb2 = 0.
                  xKbb3 = 0.
                  xKbb4 = 0.
                  xKbe1 = 0.
                  xKbe2 = 0.
                  xKee1 = 0.
                  xKee2 = 0.
                  xKee3 = 0.
                  xKee4 = 0.
C
                  yKaa1 = 0.
                  yKaa2 = 0.
                  yKaa3 = 0.
                  yKaa4 = 0.
                  yKab1 = 0.
                  yKab2 = 0.
                  yKab3 = 0.
```

```
      yKab4 = 0.
      yKae1 = 0.
      yKae2 = 0.
      yKbb1 = 0.
      yKbb2 = 0.
      yKbb3 = 0.
      yKbb4 = 0.
      yKbe1 = 0.
      yKbe2 = 0.
      yKee1 = 0.
      yKee2 = 0.
      yKee3 = 0.
      yKee4 = 0.
C
      x = -0.05
      y = -0.05
C
      NNN = 21
      IF(IEO .EQ. 1) NNN = 11
C
      DO 304 II = 1, NNN
         x = x+0.05
         y = y+0.05
C
         rc    = 1.
         IF((II .EQ. 1) .OR. (II .EQ. 21)) rc = 2.
C
         IF(IEO .EQ. 1) THEN
            IF((II .EQ. 1) .OR. (II .EQ. 11)) rc=2.
         ENDIF
C
         xKaa1 = xKaa1+df(ix,x)*df(jx,x)*xunit/rc
         xKaa2 = xKaa2+df(ix,x)*f(jx,x)*xunit/rc
         xKaa3 = xKaa3+f(ix,x)*df(jx,x)*xunit/rc
         xKaa4 = xKaa4+f(ix,x)*f(jx,x)*xunit/rc
C
         xKab1 = xKab1+df(ix,x)*h(jx,x)*xunit/rc
         xKab2 = xKab2+df(ix,x)*dh(jx,x)*xunit/rc
         xKab3 = xKab3+f(ix,x)*h(jx,x)*xunit/rc
         xKab4 = xKab4+f(ix,x)*dh(jx,x)*xunit/rc
C
         xKae1 = xKae1+f(ix,x)*dq(jx,x)*xunit/rc
         xKae2 = xKae2+f(ix,x)*q(jx,x)*xunit/rc
C
         xKbb1 = xKbb1+h(ix,x)*h(jx,x)*xunit/rc
         xKbb2 = xKbb2+dh(ix,x)*h(jx,x)*xunit/rc
         xKbb3 = xKbb3+h(ix,x)*dh(jx,x)*xunit/rc
         xKbb4 = xKbb4+dh(ix,x)*dh(jx,x)*xunit/rc
C
         xKbe1 = xKbe1+h(ix,x)*dq(jx,x)*xunit/rc
         xKbe2 = xKbe2+h(ix,x)*q(jx,x)*xunit/rc
C
         xKee1 = xKee1+dq(ix,x)*dq(jx,x)*xunit/rc
         xKee2 = xKee2+dq(ix,x)*q(jx,x)*xunit/rc
         xKee3 = xKee3+q(ix,x)*dq(jx,x)*xunit/rc
```

```
                  xKee4 = xKee4+q(ix,x)*q(jx,x)*xunit/rc
C
C
                  yKaa1 = yKaa1+g(iy,y)*g(jy,y)*yunit/rc
                  yKaa2 = yKaa2+g(iy,y)*dg(jy,y)*yunit/rc
                  yKaa3 = yKaa3+dg(iy,y)*g(jy,y)*yunit/rc
                  yKaa4 = yKaa4+dg(iy,y)*dg(jy,y)*yunit/rc
C
                  yKab1 = yKab1+g(iy,y)*dl(jy,y)*yunit/rc
                  yKab2 = yKab2+g(iy,y)*l(jy,y)*yunit/rc
                  yKab3 = yKab3+dg(iy,y)*dl(jy,y)*yunit/rc
                  yKab4 = yKab4+dg(iy,y)*l(jy,y)*yunit/rc
C
                  yKae1 = yKae1+g(iy,y)*r(jy,y)*yunit/rc
                  yKae2 = yKae2+g(iy,y)*dr(jy,y)*yunit/rc
C
                  yKbb1 = yKbb1+dl(iy,y)*dl(jy,y)*yunit/rc
                  yKbb2 = yKbb2+l(iy,y)*dl(jy,y)*yunit/rc
                  yKbb3 = yKbb3+dl(iy,y)*l(jy,y)*yunit/rc
                  yKbb4 = yKbb4+l(iy,y)*l(jy,y)*yunit/rc
C
                  yKbe1 = yKbe1+l(iy,y)*r(jy,y)*yunit/rc
                  yKbe2 = yKbe2+l(iy,y)*dr(jy,y)*yunit/rc
C
                  yKee1 = yKee1+r(iy,y)*r(jy,y)*yunit/rc
                  yKee2 = yKee2+r(iy,y)*dr(jy,y)*yunit/rc
                  yKee3 = yKee3+dr(iy,y)*r(jy,y)*yunit/rc
                  yKee4 = yKee4+dr(iy,y)*dr(jy,y)*yunit/rc
C
 304              CONTINUE
C
C
                  asm=1.
                  IF(IEO .EQ. 1) asm=4.
C
C
                  K1aa(i,j) =(D11 * xKaa1 * yKaa1
     &                       +D16 * xKaa2 * yKaa2
     &                       +D16 * xKaa3 * yKaa3
     &                       +D66 * xKaa4 * yKaa4
     &                       +G55 * xKaa4 * yKaa1)*asm
C
C
                  K1ab(i,j) =(D12 * xKab1 * yKab1
     &                       +D16 * xKab2 * yKab2
     &                       +D26 * xKab3 * yKab3
     &                       +D66 * xKab4 * yKab4
     &                       +G45 * xKab3 * yKab2)*asm
C
C
                  K1ae(i,j) =(G55 * xKae1 * yKae1
     &                       +G45 * xKae2 * yKae2)*asm
C
C
                  K1bb(i,j) =(D22 * xKbb1 * yKbb1
```

```
     &                          +D26 * xKbb2 * yKbb2
     &                          +D26 * xKbb3 * yKbb3
     &                          +D66 * xKbb4 * yKbb4
     &                          +G44 * xKbb1 * yKbb4)*asm
C
C
                  Klbe(i,j) =(G45 * xKbe1 * yKbe1
     &                          +G44 * xKbe2 * yKbe2)*asm
C
C
                  Klee(i,j) =(G55 * xKee1 * yKee1
     &                          +G45 * xKee2 * yKee2
     &                          +G45 * xKee3 * yKee3
     &                          +G44 * xKee4 * yKee4)*asm
C
C
 303           CONTINUE
 302        CONTINUE
C
 301     CONTINUE
 300  CONTINUE
C
C
C
C
C     ------------------------------------------------------
C     * Compute force vector terms for concentrated loading
C     ------------------------------------------------------
C
C
      x = 0.5
      y = 0.5
C
      i = 0
C
      DO 330 ix = 1, NX
         DO 331 iy = 1, NY
            i = i+1
            Ri(i) = q(ix,x)*r(iy,y)
 331     CONTINUE
 330  CONTINUE
C
C
      IF(cf .EQ. 0.) GOTO 345
C
C
C
C     ------------------------------------------------------------
C     * Compute force vector terms for cosine distributed patch
C       loading
C     ------------------------------------------------------------
C
C
      Pi = 3.14159265
C
```

```
      af = cf/XL
      bf = cf/YL
C
      aunit = cf*cf/100.
C
      p0 = (Pi**2)/(4.*cf*cf)
C
      ij = 0
C
C
      DO 335 ix = 1, NX
         DO 336 iy = 1, NY
C
            x = 0.5-af/2.
            SUM = 0.
C
            DO 340 I = 1, 10
               y = 0.5-bf/2.
               x = x+af/10.
C
               DO 341 J = 1, 10
                  y = y+bf/10.
C
                  PR = COS(Pi/af*(x-0.5))*COS(Pi/bf*(y-0.5))
     &                 *q(ix,x)*r(iy,y)*aunit
C
                  SUM = SUM+PR
C
 341           CONTINUE
 340        CONTINUE
C
            ij = ij+1
            Rii(ij) = p0*SUM
C
 336     CONTINUE
 335  CONTINUE
C
C
 345  CONTINUE
C
C
      RETURN
      END
C
C
C
C-----------------------------------------------------------------------
C
C-----------------------------------------------------------------------
      SUBROUTINE ARRANGE(NX,NY,iKaa,iKab,jKab,iKae,iKbb,iKbe,
     &                   M1,M2,K1aa,K1ab,K1ae,K1bb,K1be)
C-----------------------------------------------------------------------
C
C  This subroutine rearrange the stiffness matrix [K], if there is
C  any singularity due to the free-free beam boundary condition used.
```

```
C
C-----------------------------------------------------------------------
C
C     [ Variables ]
C
      IMPLICIT DOUBLE PRECISION (A-H, O-Z)
      DOUBLE PRECISION M1,M2,
     &                 K1aa,K1ab,K1ae,K1bb,K1be
      INTEGER NX,NY,NXY
C
      PARAMETER ( N1=10, N2=N1*7 )
C
      DIMENSION M1(N2),M2(N2)
      DIMENSION NM1(N2),NM2(N2)
      DIMENSION K1aa(N2,N2),K1ab(N2,N2),K1ae(N2,N2)
      DIMENSION K1bb(N2,N2),K1be(N2,N2)
C
C
      NXY = NX*NY
C
      DO 250 i = 1, NXY
C
         NM1(i) = 0
         IF(M1(i) .EQ. 0.) NM1(i) = 1
C
         NM2(i) = 0
         IF(M2(i) .EQ. 0.) NM2(i) = 1
C
 250  CONTINUE
C
C
      iKaa = NXY
      iKab = NXY
      jKab = NXY
      iKae = NXY
      iKbb = NXY
      iKbe = NXY
C
C
      ii = 0
      DO 251 i = 1, NXY
         iKaa = iKaa-1
         iKab = iKab-1
         iKae = iKae-1
         IF(NM1(i) .EQ. 1) GOTO 251
         ii = ii+1
         iKaa = iKaa+1
         iKab = iKab+1
         iKae = iKae+1
         DO 252 j = 1, NXY
            K1aa(ii,j) = K1aa(i,j)
            K1ab(ii,j) = K1ab(i,j)
            K1ae(ii,j) = K1ae(i,j)
 252     CONTINUE
 251  CONTINUE
```

```
C
C
      IF(iKaa .EQ. NXY) GOTO 253
C
      jj = 0
      DO 254 j = 1, NXY
         IF(NM1(i) .EQ. 1) GOTO 254
         jj = jj+1
         DO 255 i = 1, iKaa
            Klaa(i,jj) = Klaa(i,j)
 255     CONTINUE
 254  CONTINUE
C
C
 253  CONTINUE
C
C
C
      ii = 0
      DO 256 i = 1, NXY
         iKbb = iKbb-1
         iKbe = iKbe-1
         IF(NM2(i) .EQ. 1) GOTO 256
         ii = ii+1
         iKbb = iKbb+1
         iKbe = iKbe+1
         DO 257 j = 1, NXY
            Klbb(ii,j) = Klbb(i,j)
            Klbe(ii,j) = Klbe(i,j)
 257     CONTINUE
 256  CONTINUE
C
C
      IF(iKbb .EQ. NXY) GOTO 260
C
      jj = 0
      DO 258 j = 1, NXY
         jKab = jKab-1
         IF(NM2(j) .EQ. 1) GOTO 258
         jKab = jKab+1
         jj = jj+1
         DO 259 i = 1, iKbb
            Klbb(i,jj) = Klbb(i,j)
 259     CONTINUE
         DO 261 i = 1, iKab
            Klab(i,jj) = Klab(i,j)
 261     CONTINUE
 258  CONTINUE
C
C
 260  CONTINUE
C
C
C
      RETURN
```

```
      END
C
C
C
C-----------------------------------------------------------------------
C
C-----------------------------------------------------------------------
      SUBROUTINE CONDENS(NX,NY,iKaa,iKab,jKab,iKae,iKbb,iKbe,
     &                   Klaa,Klab,Klae,Klbb,Klbe,Klee,KI)
C-----------------------------------------------------------------------
C
C  This subroutine performs the static condensation in order to
C  reduce the system of equation.
C
C-----------------------------------------------------------------------
C
C     [ Variables ]
C
      IMPLICIT DOUBLE PRECISION (A-H, O-Z)
      DOUBLE PRECISION Klaa,Klab,Klae,Klba,Klbb,Klbe,
     &                 Klea,Kleb,Klee,
     &                 Kl,KK,KI
      INTEGER NX,NY,NXY
C
      PARAMETER ( N1=10, N2=N1*7, N3=N2**2, N4=N2**3, N5=N2*2 )
C
      DIMENSION Klaa(N2,N2),Klab(N2,N2),Klae(N2,N2)
      DIMENSION Klba(N2,N2),Klbb(N2,N2),Klbe(N2,N2),Klee(N2,N2)
      DIMENSION Klea(N2,N2),Kleb(N2,N2),Kl(N5,N5),KK(N2,N5)
      DIMENSION KI(N2,N2),Ri(N2),A(N5,N5)
      DIMENSION DUM(N2)
C
C
      NXY    = NX*NY
C
C
C
C     ----------------------------
C     * Obtain transpose of matrix
C     ----------------------------
C
C
      DO 404 I = 1, iKab
         DO 405 J = 1, jKab
            Klba(J,I) = Klab(I,J)
 405     CONTINUE
 404  CONTINUE
C
C
      DO 406 I = 1, iKae
         DO 407 J = 1, NXY
            Klea(J,I) = Klae(I,J)
 407     CONTINUE
 406  CONTINUE
C
```

```
C
      DO 408 I = 1, iKbe
         DO 409 J = 1, NXY
            K1eb(J,I) = K1be(I,J)
 409     CONTINUE
 408  CONTINUE
C
C
C
C     ---------------------------------
C     * Compute inverse of [ K ] matrix
C     ---------------------------------
C
C
      DO 424 I = 1, iKaa
         DO 425 J = 1, iKaa
            A(I,J) = K1aa(I,J)
 425     CONTINUE
         DO 426 J = 1, jKab
            A(I,iKaa+J) = K1ab(I,J)
 426     CONTINUE
 424  CONTINUE
C
      DO 427 I = 1, iKbb
         DO 428 J = 1, iKab
            A(iKaa+I,J) = K1ba(I,J)
 428     CONTINUE
         DO 429 J = 1, iKbb
            A(iKaa+I,iKab+J) = K1bb(I,J)
 429     CONTINUE
 427  CONTINUE
C
      NN = iKaa+iKbb
C
C
      CALL INVERSE(A,NN)
C
C
      DO 430 I = 1, NN
         DO 431 J = 1, NN
            K1(I,J) = A(I,J)
 431     CONTINUE
 430  CONTINUE
C
C
C
C     ---------------------------------------
C     * Static condensation for [ K* ] matrix
C     ---------------------------------------
C
C
      DO 440 I = 1, NXY
         DO 441 J = 1, NN
            SUM = 0.
            DO 442 JJ = 1, iKaa
```

```
                PR = K1ea(I,JJ)*K1(JJ,J)
                SUM = SUM+PR
 442          CONTINUE
              DO 443 JJ = 1, iKbb
                PR = K1eb(I,JJ)*K1(JJ+iKaa,J)
                SUM = SUM+PR
 443          CONTINUE
              KK(I,J) = SUM
 441       CONTINUE
 440   CONTINUE
C
C
       DO 444 I = 1, NXY
          DO 445 J = 1, NXY
             SUM = 0.
             DO 446 JJ = 1, iKaa
                PR = KK(I,JJ)*K1ae(JJ,J)
                SUM = SUM+PR
 446         CONTINUE
             DO 447 JJ = 1, iKbb
                PR = KK(I,JJ+iKaa)*K1be(JJ,J)
                SUM = SUM+PR
 447         CONTINUE
             K1(I,J) = SUM
 445       CONTINUE
 444   CONTINUE
C
C
       DO 448 I = 1, NXY
          DO 449 J = 1, NXY
             KI(I,J) = K1ee(I,J) - K1(I,J)
 449       CONTINUE
 448   CONTINUE
C
C
C
       RETURN
       END
C
C
C-----------------------------------------------------------------------
C
C-----------------------------------------------------------------------
       SUBROUTINE INVERSE(A,N)
C-----------------------------------------------------------------------
C
C  This subroutine calculates the inverse of given NxN matrix [A].
C  Taken from "Numerical Recipes for FORTRAN77"
C
C-----------------------------------------------------------------------
C
C      [ Variables ]
C
       IMPLICIT DOUBLE PRECISION (A-H, O-Z)
C
```

```
      PARAMETER ( N1=10, N2=N1*7, N5=N2*2 )
C
      DIMENSION A(N5,N5),Y(N5,N5),INDX(N5),B1(N5)
C
C
      DO 340 I = 1, N
         DO 341 J = 1, N
            Y(I,J) = 0.
 341     CONTINUE
         Y(I,I) = 1.
 340  CONTINUE
C
C
      CALL LUDCMP(A,N,INDX)
C
C
      DO 342 J = 1, N
         DO 345 I = 1, N
            B1(I) = Y(I,J)
 345     CONTINUE
C
C
         CALL LUBKSB(A,N,INDX,B1)
C
         DO 346 I = 1, N
            Y(I,J) = B1(I)
 346     CONTINUE
C
 342  CONTINUE
C
C
      DO 343 I = 1, N
         DO 344 J = 1, N
            A(I,J) = Y(I,J)
 344     CONTINUE
 343  CONTINUE
C
C
      RETURN
      END
C
C
C-----------------------------------------------------------------------
C
C-----------------------------------------------------------------------
      SUBROUTINE LUDCMP(A,N,INDX)
C-----------------------------------------------------------------------
C
C  This subroutine performs LU decomposition.
C  Taken from "Numerical Recipes for FORTRAN77"
C
C-----------------------------------------------------------------------
C
C     [ Variables ]
C
```

```
      IMPLICIT DOUBLE PRECISION (A-H, O-Z)
C
      PARAMETER ( N1=10, N2=N1*7, N5=N2*2 )
      PARAMETER ( TINY=1.0E-16 )
C
      DIMENSION A(N5,N5),INDX(N5),VV(N5)
C
C
C
      D = 1.
C
C
      DO 350 I = 1, N
         AAMAX = 0.
         DO 351 J = 1, N
            IF(ABS(A(I,J)) .GT. AAMAX) AAMAX=ABS(A(I,J))
 351     CONTINUE
         IF(AAMAX .EQ. 0.) AAMAX=TINY
         VV(I) = 1./AAMAX
 350  CONTINUE
C
C
C
      DO 352 J = 1, N
C
         DO 353 I = 1, J-1
            SUM = A(I,J)
            DO 354 K = 1, I-1
               SUM = SUM - A(I,K)*A(K,J)
 354        CONTINUE
            A(I,J) = SUM
 353     CONTINUE
         AAMAX = 0.
C
         DO 355 I = J, N
            SUM = A(I,J)
            DO 356 K = 1, J-1
               SUM = SUM - A(I,K)*A(K,J)
 356        CONTINUE
            A(I,J) = SUM
            DUM = VV(I)*ABS(SUM)
            IF(DUM .GE. AAMAX) THEN
               IMAX = I
               AAMAX = DUM
            ENDIF
 355     CONTINUE
C
         IF(J .NE. IMAX) THEN
            DO 357 K = 1, N
               DUM = A(IMAX,K)
               A(IMAX,K) = A(J,K)
               A(J,K) = DUM
 357        CONTINUE
            D = -D
            VV(IMAX) = VV(J)
```

```
         ENDIF
C
         INDX(J) = IMAX
C
         IF(A(J,J) .EQ. 0.) A(J,J)=TINY
C
         IF(J .NE. N) THEN
            DUM = 1./A(J,J)
            DO 358 I = J+1, N
               A(I,J) = A(I,J)*DUM
 358        CONTINUE
         ENDIF
C
 352  CONTINUE
C
C
      RETURN
      END
C
C
C-----------------------------------------------------------------------
C
C-----------------------------------------------------------------------
      SUBROUTINE LUBKSB(A,N,INDX,B1)
C-----------------------------------------------------------------------
C
C  This subroutine performs LU back-substitution.
C  Taken from "Numerical Recipes for FORTRAN77"
C
C-----------------------------------------------------------------------
C
C     [ Variables ]
C
      IMPLICIT DOUBLE PRECISION (A-H, O-Z)
C
      PARAMETER ( N1=10, N2=N1*7, N5=N2*2 )
C
      DIMENSION A(N5,N5),INDX(N5),B1(N5)
C
C
C
      II = 0
C
C
      DO 360 I = 1, N
         LL = INDX(I)
         SUM = B1(LL)
         B1(LL) = B1(I)
C
         IF(II .NE. 0) THEN
            DO 361 J = II, I-1
               SUM = SUM - A(I,J)*B1(J)
 361        CONTINUE
         ELSE IF (SUM .NE. 0.) THEN
            II = I
```

```
         ENDIF
C
         B1(I) = SUM
 360  CONTINUE
C
C
      DO 362 I = N, 1, -1
         SUM = B1(I)
         DO 363 J = I+1, N
            SUM = SUM - A(I,J)*B1(J)
 363     CONTINUE
         B1(I) = SUM/A(I,I)
 362  CONTINUE
C
C
      RETURN
      END
C
C
C
C-----------------------------------------------------------------------
C
C-----------------------------------------------------------------------
      SUBROUTINE INTGRL2(Ibx,Iby,beta,NX,NY,AX,AY,THETAX,THETAY,IEO,
     &                   BETAX,BETAY,BX,BY,
     &                   CX,CY,DX,DY,EX,EY,
     &                   A11,A22,A12,A16,A26,A66,
     &                   XL,YL,KIII)
C-----------------------------------------------------------------------
C
C  This subroutine computes the stiffness matrix for the nonlinear
C  cubic term.  Note that this matrix is a non-square matrix.
C
C-----------------------------------------------------------------------
C
C
C     [ Variables ]
C
      IMPLICIT DOUBLE PRECISION (A-H, O-Z)
      DOUBLE PRECISION KIII
      INTEGER NX,NY,NXY,i,j
C
      PARAMETER ( N1=10, N2=N1*7, N4=N2**3 )
C
      DIMENSION BETAX(N1),BETAY(N1),BX(N1),BY(N1)
      DIMENSION CX(N1),CY(N1),DX(N1),DY(N1),EX(N1),EY(N1)
      DIMENSION KIII(N2,N4)
C
C
C
C     ------------------------------------------------------------
C     * Defining Beam Functions & Derivatives of Beam Functions
C     ------------------------------------------------------------
C
C
```

```
      q(i,x)  = (SQRT(2.)*SIN(BETAX(i)*x+THETAX)
     &           +AX*EXP(-BETAX(i)*x)
     &           +BX(i)*EXP(-BETAX(i)*(1.-x)))*CX(i)
     &           +2.*EX(i)*(DX(i)*(-x)+0.5)
C
C
      dq(i,x) =((BETAX(i)*SQRT(2.)*COS(BETAX(i)*x+THETAX)
     &           -BETAX(i)*AX*EXP(-BETAX(i)*x)
     &           +BETAX(i)*BX(i)*EXP(-BETAX(i)*(1.-x)))
     &           *CX(i)+DX(i)*(-2.))/XL
C
C
      r(i,y)  = (SQRT(2.)*SIN(BETAY(i)*y+THETAY)
     &           +AY*EXP(-BETAY(i)*y)
     &           +BY(i)*EXP(-BETAY(i)*(1.-y)))*CY(i)
     &           +2.*EY(i)*(DY(i)*(-y)+0.5)
C
C
      dr(i,y) =((BETAY(i)*SQRT(2.)*COS(BETAY(i)*y+THETAY)
     &           -BETAY(i)*AY*EXP(-BETAY(i)*y)
     &           +BETAY(i)*BY(i)*EXP(-BETAY(i)*(1.-y)))
     &           *CY(i)+DY(i)*(-2.))/YL
C
C
C
C
C     ------------------------------------------------------------
C     * Calculating non-square stiffness matrix components for
C       nonlinear (cubic) term by numerical integration using
C       "Extended Trapezoidal Rule"
C     ------------------------------------------------------------
C
C
      xunit = XL/20.
      yunit = YL/20.
C
C
      IF(Ibx .EQ. 0) THEN
         A11 = 0.
      ENDIF
C
      IF(Iby .EQ. 0) THEN
         A22 = 0.
      ENDIF
C
C
C
      i = 0
      DO 320 ix = 1, NX
         DO 321 iy = 1, NY
            i = i+1
            j = 0
            DO 322 kx = 1, NX
               DO 323 ky = 1, NY
                  DO 324 lx = 1, NX
```

```
                  DO 325 ly = 1, NY
                     DO 326 mx = 1, NX
                        DO 327 my = 1, NY
                           j = j+1
C
                           xKee1 = 0.
                           xKee4 = 0.
C
                           yKee1 = 0.
                           yKee4 = 0.
C
                           x = -0.05
                           y = -0.05
C
                           IF(IEO .EQ. 1) NNN = 11
                           IF(IEO .EQ. 0) NNN = 21
C
                           DO 328 KK = 1, NNN
C
                              x = x+0.05
                              y = y+0.05
C
C
                              rc    = 1.
                              IF((KK .EQ. 1) .OR.
     &                           (KK .EQ. 21)) rc = 2.
                              IF(IEO .EQ. 0) THEN
                                IF((KK .EQ. 1) .OR.
     &                             (KK .EQ. 11)) rc=2.
                              ENDIF
C
C
                              xKee1 = dq(ix,x)*dq(kx,x)
     &                                *dq(lx,x)*dq(mx,x)
     &                                *xunit/rc + xKee1
C
C
                              xKee4 = q(ix,x)*q(kx,x)
     &                                *q(lx,x)*q(mx,x)
     &                                *xunit/rc + xKee4
C
C
C
                              yKee1 = r(iy,y)*r(ky,y)
     &                                *r(ly,y)*r(my,y)
     &                                *yunit/rc + yKee1
C
C
                              yKee4 = dr(iy,y)*dr(ky,y)
     &                                *dr(ly,y)*dr(my,y)
     &                                *yunit/rc + yKee4
C
C
 328                          CONTINUE
C
```

```
                                asm=1.
                                IF(IEO .EQ. 1) asm=4.
C
                                KIII(i,j) = beta*
     &                                      (0.5 * A11 * xKee1
     &                                                 * yKee1
     &                                     +0.5 * A22 * xKee4
     &                                                 * yKee4)* asm
C
C
 327                          CONTINUE
 326                        CONTINUE
 325                      CONTINUE
 324                    CONTINUE
 323                  CONTINUE
 322                CONTINUE
 321              CONTINUE
 320  CONTINUE
C
C
C
      RETURN
      END
C
C
C
C-----------------------------------------------------------------------
C
C-----------------------------------------------------------------------
      SUBROUTINE SOLVE(NX,NY,M3,KI,KIII,Ri,vI,mI,k,n,dt,ts,ITI,
     &                 Ibx,Iby,XL,YL,BETAX,BETAY,THETAX,THETAY,
     &                 AX,AY,BX,BY,CX,CY,DX,DY,EX,EY)
C-----------------------------------------------------------------------
C
C  This subroutine solves the system of second-order differential
C  equations with respect to time by numerical time integration
C  scheme of the fourth-order Runge-Kutta method.
C
C-----------------------------------------------------------------------
C
C     [ Variables ]
C
      IMPLICIT DOUBLE PRECISION (A-H, O-Z)
      DOUBLE PRECISION M3,KI,KIII,mI,k,n
      INTEGER ts
C
      PARAMETER ( N1=10, N2=N1*7, N4=N2**3 )
C
      DIMENSION BETAX(N1),BETAY(N1),BX(N1),BY(N1)
      DIMENSION CX(N1),CY(N1),DX(N1),DY(N1),EX(N1),EY(N1)
      DIMENSION M3(N2),KI(N2,N2),KIII(N2,N4),Ri(N2)
      DIMENSION x(N2+1),z(N2+1),A(N2+1),B(N2+1,N2+1),S(N2+1)
C
C
      q(i,xx) = (SQRT(2.)*SIN(BETAX(i)*x+THETAX)
```

```
     &           +AX*EXP(-BETAX(i)*xx)
     &           +BX(i)*EXP(-BETAX(i)*(1.-xx)))*CX(i)
     &           +2.*EX(i)*(DX(i)*(-xx)+0.5)
C
C
      r(i,yy) = (SQRT(2.)*SIN(BETAY(i)*yy+THETAY)
     &           +AY*EXP(-BETAY(i)*yy)
     &           +BY(i)*EXP(-BETAY(i)*(1.-yy)))*CY(i)
     &           +2.*EY(i)*(DY(i)*(-yy)+0.5)
C
C
C
C
C     ----------------------
C     * Preparation of matix
C     ----------------------
C
C
      NXY = NX*NY
C
      DO 510 i = 1, NXY
         A(i) = 1./M3(i)
 510  CONTINUE
C
      A(NXY+1) = 1./mI
C
C
      DO 511 i = 1, NXY
         DO 512 j = 1, NXY
            B(i,j) = A(i) * KI(i,j)
 512     CONTINUE
 511  CONTINUE
C
C
      DO 513 j = 1, NXY+1
         B(NXY+1,j) = 0.
         B(j,NXY+1) = 0.
 513  CONTINUE
C
C
      DO 514 i = 1, NXY
         DO 515 j = 1, NXY**3
            KIII(i,j) = A(i) * KIII(i,j)
 515     CONTINUE
 514  CONTINUE
C
C
      DO 516 i = 1, NXY
         S(i) = Ri(i)
 516  CONTINUE
C
      S(NXY+1) = 1.
C
C
C
```

```
C     -------------------------
C     * Variable initialization
C     -------------------------
C
C
      DO 500 I = 1, NXY+1
         x(I)  = 0.
         z(I)  = 0.
 500  CONTINUE
C
      z(NXY+1) = vI
C
      time  = 0.
      IT    = 0
C
C
C
C     ------------------------------------------------------
C     * Time integration using 4th-order Runge-Kutta method
C     ------------------------------------------------------
C
C
      DO 501 ITT = 1, ts
C
         IT = IT+1
C
C
         CALL RK4(NX,NY,A,B,KIII,S,x,z,dt,Ibx,Iby,k,n)
C
C
         SUM = 0.
C
         DO 502 i = 1, NXY
            PR = S(i)*x(i)
            SUM = SUM+PR
 502     CONTINUE
C
         w = SUM
C
C
         alpha = w + x(NXY+1)
         IF(alpha .LT. 0.) THEN
            FI = 0.
         ELSE
            FI = k*(alpha**n)
         ENDIF
C
         w0 = -w
         u0 = x(NXY+1)
         time = time+dt
C
C
         IF(IT .EQ. ITI) THEN
            CALL OUTPUT(time,FI,w0,u0)
            IT = 0
```

```
         ENDIF
C
C
 501  CONTINUE
C
C
C
      RETURN
      END
C
C
C
C-----------------------------------------------------------------------
C
C-----------------------------------------------------------------------
      SUBROUTINE RK4(NX,NY,A,B,KIII,S,x,z,dt,Ibx,Iby,k,n)
C-----------------------------------------------------------------------
C
C  This subroutine performs a numerical integration using fourth-
C  order Runge-Kutta method.
C
C-----------------------------------------------------------------------
C
C     [ Variables ]
C
      IMPLICIT DOUBLE PRECISION (A-H, O-Z)
      DOUBLE PRECISION KIII,k,n
C
      PARAMETER ( N1=10, N2=N1*7, N4=N2**3 )
C
      DIMENSION A(N2+1),B(N2+1,N2+1),KIII(N2,N4),S(N2+1)
      DIMENSION x(N2+1),z(N2+1),x1(N2+1),z1(N2+1)
      DIMENSION ak1(N2+1),ak2(N2+1),ak3(N2+1),ak4(N2+1)
      DIMENSION bk1(N2+1),bk2(N2+1),bk3(N2+1),bk4(N2+1)
C
C
C
C     ----------------------------------------
C     * Solving 2nd-order differential equations
C     ----------------------------------------
C
C
      NXY = NX*NY
C
C
      DO 550 i = 1, NXY+1
         x1(i) = x(i)
         z1(i) = z(i)
 550  CONTINUE
C
C
C
      DO 551 i = 1, NXY+1
         ak1(i) = dt*func(NXY,i,x,A,B,KIII,S,Ibx,Iby,k,n)
         bk1(i) = dt*z1(i)
```

```
 551  CONTINUE
C
C
      DO 552 i = 1, NXY+1
         x(i) = x1(i)+0.5*bk1(i)
 552  CONTINUE
C
C
      DO 553 i = 1, NXY+1
         ak2(i) = dt*func(NXY,i,x,A,B,KIII,S,Ibx,Iby,k,n)
         bk2(i) = dt*(z1(i)+0.5*ak1(i))
 553  CONTINUE
C
C
      DO 554 i = 1, NXY+1
         x(i) = x1(i)+0.5*bk2(i)
 554  CONTINUE
C
C
      DO 555 i = 1, NXY+1
         ak3(i) = dt*func(NXY,i,x,A,B,KIII,S,Ibx,Iby,k,n)
         bk3(i) = dt*(z1(i)+0.5*ak2(i))
 555  CONTINUE
C
C
      DO 556 i = 1, NXY+1
         x(i) = x1(i)+bk3(i)
 556  CONTINUE
C
C
      DO 557 i = 1, NXY+1
         ak4(i) = dt*func(NXY,i,x,A,B,KIII,S,Ibx,Iby,k,n)
         bk4(i) = dt*(z1(i)+ak3(i))
 557  CONTINUE
C
C
      DO 558 i = 1, NXY+1
         z(i) = z1(i) + (ak1(i)+2.*ak2(i)+2.*ak3(i)+ak4(i))/6.
         x(i) = x1(i) + (bk1(i)+2.*bk2(i)+2.*bk3(i)+bk4(i))/6.
 558  CONTINUE
C
C
C
      RETURN
      END
C
C
C
C-----------------------------------------------------------------------
C
C-----------------------------------------------------------------------
      FUNCTION func(NXY,i,x,A,B,KIII,S,Ibx,Iby,k,n)
C-----------------------------------------------------------------------
C
C
```

```
C
C     [ Variables ]
C
      IMPLICIT DOUBLE PRECISION (A-H, O-Z)
      DOUBLE PRECISION KIII,k,n
C
      PARAMETER ( N1=10, N2=N1*7, N4=N2**3 )
C
      DIMENSION A(N2+1),B(N2+1,N2+1),KIII(N2,N4),S(N2+1),x(N2+1)
C
C
C
      SUM = 0.
C
      DO 580 J = 1, NXY+1
         PR = B(i,J)*x(J)
         SUM = SUM+PR
 580  CONTINUE
C
      S1 = SUM
C
C
C
      IF((Ibx .EQ. 0) .AND. (Iby .EQ. 0)) THEN
         S2 = 0.
         GOTO 584
      ENDIF
C
      IF(i .EQ. NXY+1) THEN
         S2 = 0.
         GOTO 584
      ENDIF
C
      SUM = 0.
      JJJJ = 0
C
      DO 581 J = 1, NXY
         DO 582 JJ = 1, NXY
            DO 583 JJJ = 1, NXY
               JJJJ = JJJJ+1
               PR = KIII(i,JJJJ)*x(J)*x(JJ)*x(JJJ)
               SUM = SUM+PR
 583        CONTINUE
 582     CONTINUE
 581  CONTINUE
C
      S2 = SUM
C
 584  CONTINUE
C
C
C
      SUM = 0.
C
      DO 585 J = 1, NXY+1
```

```
         PR = S(J)*x(J)
         SUM = SUM+PR
 585  CONTINUE
C
      IF(SUM .LT. 0.) THEN
         SUM = 0.
      ENDIF
C
      F = k*(SUM**n)
C
C
      S3 = F*A(i)*S(i)
C
C
      func = -S1-S2-S3
C
C
      RETURN
      END
C
C
C
C-----------------------------------------------------------------------
C
C-----------------------------------------------------------------------
      SUBROUTINE SOLVE2(NX,NY,M3,KI,KIII,Ri,vI,mI,k,n,dt,ts,ITI,
     &                  Ibx,Iby,XL,YL,BETAX,BETAY,THETAX,THETAY,
     &                  AX,AY,BX,BY,CX,CY,DX,DY,EX,EY,Rii)
C-----------------------------------------------------------------------
C
C  This subroutine solves the system of second-order differential
C  equations
C  with respect to time by numerical time integration scheme of the
C  fourth-order Runge-Kutta method.  Cosine-type distributed patch
C  loading is also considered.
C
C-----------------------------------------------------------------------
C
C     [ Variables ]
C
      IMPLICIT DOUBLE PRECISION (A-H, O-Z)
      DOUBLE PRECISION M3,KI,KIII,mI,k,n
      INTEGER ts
C
      PARAMETER ( N1=10, N2=N1*7, N4=N2**3 )
C
      DIMENSION BETAX(N1),BETAY(N1),BX(N1),BY(N1)
      DIMENSION CX(N1),CY(N1),DX(N1),DY(N1),EX(N1),EY(N1)
      DIMENSION M3(N2),KI(N2,N2),KIII(N2,N4),Ri(N2),Rii(N2)
      DIMENSION x(N2+1),z(N2+1),A(N2+1),B(N2+1,N2+1)
      DIMENSION S(N2+1),S2(N2+1)
C
C
      q(i,xx) = (SQRT(2.)*SIN(BETAX(i)*x+THETAX)
     &          +AX*EXP(-BETAX(i)*xx)
```

```
     &           +BX(i)*EXP(-BETAX(i)*(1.-xx)))*CX(i)
     &           +2.*EX(i)*(DX(i)*(-xx)+0.5)
C
C
      r(i,yy) = (SQRT(2.)*SIN(BETAY(i)*yy+THETAY)
     &           +AY*EXP(-BETAY(i)*yy)
     &           +BY(i)*EXP(-BETAY(i)*(1.-yy)))*CY(i)
     &           +2.*EY(i)*(DY(i)*(-yy)+0.5)
C
C
C
C     ----------------------
C     * Preparation of matix
C     ----------------------
C
C
      NXY = NX*NY
C
      DO 510 i = 1, NXY
         A(i) = 1./M3(i)
 510  CONTINUE
C
      A(NXY+1) = 1./mI
C
C
      DO 511 i = 1, NXY
         DO 512 j = 1, NXY
            B(i,j) = A(i) * KI(i,j)
 512     CONTINUE
 511  CONTINUE
C
C
      DO 513 j = 1, NXY+1
         B(NXY+1,j) = 0.
         B(j,NXY+1) = 0.
 513  CONTINUE
C
C
      DO 514 i = 1, NXY
         DO 515 j = 1, NXY**3
            KIII(i,j) = A(i) * KIII(i,j)
 515     CONTINUE
 514  CONTINUE
C
C
      DO 516 i = 1, NXY
         S(i) = Rii(i)
         S2(i)= Ri(i)
 516  CONTINUE
C
      S(NXY+1) = 1.
      S2(NXY+1)= 1.
C
C
C
```

```
C     -------------------------
C     * Variable initialization
C     -------------------------
C
C
      DO 500 I = 1, NXY+1
         x(I)  = 0.
         z(I)  = 0.
 500  CONTINUE
C
      z(NXY+1) = vI
C
      time  = 0.
      IT    = 0
C
C
C
C     ------------------------------------------------------
C     * Time integration using 4th-order Runge-Kutta method
C     ------------------------------------------------------
C
C
      DO 501 ITT = 1, ts
C
         IT = IT+1
C
C
         CALL RK4p(NX,NY,A,B,KIII,S,S2,x,z,dt,Ibx,Iby,k,n)
C
C
         SUM = 0.
C
         DO 502 i = 1, NXY
            PR = S2(i)*x(i)
            SUM = SUM+PR
 502     CONTINUE
C
         w = SUM
C
C
         alpha = w + x(NXY+1)
         IF(alpha .LT. 0.) THEN
            FI = 0.
         ELSE
            FI = k*(alpha**n)
         ENDIF
C
         w0 = -w
         u0 = x(NXY+1)
         time = time+dt
C
C
         IF(IT .EQ. ITI) THEN
            CALL OUTPUT(time,FI,w0,u0)
            IT = 0
```

```
         ENDIF
C
C
 501  CONTINUE
C
C
C
      RETURN
      END
C
C
C
C-----------------------------------------------------------------------
C


C-----------------------------------------------------------------------
      SUBROUTINE RK4p(NX,NY,A,B,KIII,S,S2,x,z,dt,Ibx,Iby,k,n)
C-----------------------------------------------------------------------
C
C  This subroutine performs a numerical integration using fourth-
C  order Runge-Kutta method. Cosine-type distributed patch loading is
C  also considered.
C
C-----------------------------------------------------------------------
C
C     [ Variables ]
C
      IMPLICIT DOUBLE PRECISION (A-H, O-Z)
      DOUBLE PRECISION KIII,k,n
C
      PARAMETER ( N1=10, N2=N1*7, N4=N2**3 )
C
      DIMENSION A(N2+1),B(N2+1,N2+1),KIII(N2,N4)
      DIMENSION S(N2+1),S2(N2+1)
      DIMENSION x(N2+1),z(N2+1),x1(N2+1),z1(N2+1)
      DIMENSION ak1(N2+1),ak2(N2+1),ak3(N2+1),ak4(N2+1)
      DIMENSION bk1(N2+1),bk2(N2+1),bk3(N2+1),bk4(N2+1)
C
C
C
C     ----------------------------------------
C     * Solving 2nd-order differential equations
C     ----------------------------------------
C
C
      NXY = NX*NY
C
C
      DO 550 i = 1, NXY+1
         x1(i) = x(i)
         z1(i) = z(i)
 550  CONTINUE
C
C
```

```
C
C
      DO 551 i = 1, NXY+1
         ak1(i) = dt*func1(NXY,i,x,A,B,KIII,S,S2,Ibx,Iby,k,n)
         bk1(i) = dt*z1(i)
 551  CONTINUE
C
C
C
      DO 552 i = 1, NXY+1
         x(i) = x1(i)+0.5*bk1(i)
 552  CONTINUE
C
C
C
      DO 553 i = 1, NXY+1
         ak2(i) = dt*func1(NXY,i,x,A,B,KIII,S,S2,Ibx,Iby,k,n)
         bk2(i) = dt*(z1(i)+0.5*ak1(i))
 553  CONTINUE
C
C
C
      DO 554 i = 1, NXY+1
         x(i) = x1(i)+0.5*bk2(i)
 554  CONTINUE
C
C
C
      DO 555 i = 1, NXY+1
         ak3(i) = dt*func1(NXY,i,x,A,B,KIII,S,S2,Ibx,Iby,k,n)
         bk3(i) = dt*(z1(i)+0.5*ak2(i))
 555  CONTINUE
C
C
C
      DO 556 i = 1, NXY+1
         x(i) = x1(i)+bk3(i)
 556  CONTINUE
C
C
C
      DO 557 i = 1, NXY+1
         ak4(i) = dt*func1(NXY,i,x,A,B,KIII,S,S2,Ibx,Iby,k,n)
         bk4(i) = dt*(z1(i)+ak3(i))
 557  CONTINUE
C
C
C
      DO 558 i = 1, NXY+1
         z(i) = z1(i) + (ak1(i)+2.*ak2(i)+2.*ak3(i)+ak4(i))/6.
         x(i) = x1(i) + (bk1(i)+2.*bk2(i)+2.*bk3(i)+bk4(i))/6.
 558  CONTINUE
C
C
C
```

```
      RETURN
      END
C
C
C
C-----------------------------------------------------------------
C
C-----------------------------------------------------------------
      FUNCTION func1(NXY,i,x,A,B,KIII,S,S2,Ibx,Iby,k,n)
C-----------------------------------------------------------------
C
C
C
C     [ Variables ]
C
      IMPLICIT DOUBLE PRECISION (A-H, O-Z)
      DOUBLE PRECISION KIII,k,n
C
      PARAMETER ( N1=10, N2=N1*7, N4=N2**3 )
C
      DIMENSION A(N2+1),B(N2+1,N2+1),KIII(N2,N4)
      DIMENSION S(N2+1),S2(N2+1),x(N2+1)
C
C
C
      SUM = 0.
C
      DO 580 J = 1, NXY+1
         PR = B(i,J)*x(J)
         SUM = SUM+PR
 580  CONTINUE
C
      A1 = SUM
C
C
C
      IF((Ibx .EQ. 0) .AND. (Iby .EQ. 0)) THEN
         A2 = 0.
         GOTO 584
      ENDIF
C
      IF(i .EQ. NXY+1) THEN
         A2 = 0.
         GOTO 584
      ENDIF
C
      SUM = 0.
      JJJJ = 0
C
      DO 581 J = 1, NXY
         DO 582 JJ = 1, NXY
            DO 583 JJJ = 1, NXY
               JJJJ = JJJJ+1
               PR = KIII(i,JJJJ)*x(J)*x(JJ)*x(JJJ)
               SUM = SUM+PR
```

```
 583         CONTINUE
 582      CONTINUE
 581   CONTINUE
C
      A2 = SUM
C
 584   CONTINUE
C
C
C
      SUM = 0.
C
      DO 585 J = 1, NXY+1
         PR = S2(J)*x(J)
         SUM = SUM+PR
 585   CONTINUE
C
      IF(SUM .LT. 0.) THEN
         SUM = 0.
      ENDIF
C
      F = k*(SUM**n)
C
C
      A3 = F*A(i)*S(i)
C
C
      func1 = -A1-A2-A3
C
C
      RETURN
      END
C
C
C
C-----------------------------------------------------------------------
C
C-----------------------------------------------------------------------
      SUBROUTINE OUTPUT(time,F0,w0,u0)
C-----------------------------------------------------------------------
C
C  This subroutine writes desirable information in the output data
C  file "global2.out".
C  Time [sec], force [N], plate midplne displacement [m], impactor
C  displacement [m] are produced.
C
C-----------------------------------------------------------------------
C
C     [ Variables ]
C
      IMPLICIT DOUBLE PRECISION (A-H, O-Z)
C
C
      WRITE(11,*)time,F0,w0,u0
C
```

```
C
      RETURN
      END
C
C
C-----------------------------------------------------------------------
```

Sample Input Data File "global2.dat"

```
IM7G/X8553-50  [+45/-45/+45/-45/0/0]s  252mm x 89mm plate
Nonlinearity in x-direction (beta=0.05)
1.53kg impactor @ 5m/s
9 x 9 modes (only odd modes)    5 microsec time increment
3000 time steps     Recording every 10th time step data
1 0 0.05
3 4 5 5
1
0.252 0.089 0.00174 1540.
143591000. 54249900. 37682300. 0. 0. 42568300.
22.5264 20.1778 15.0949 3.5227 3.5227 16.5905
10266000. 10266000. 0. 0.833
1.53 5.0 0. 5.0E8 1.5
0.000005 3000 10
```

The format of the "global2.dat" is described as follows:

Line 1-5 : comment lines (program does not read)
Line 6 : Ibx Iby beta
Line 7 : IBCX IBCY NX NY
Line 8 : IEO
Line 9 : XL YL THICK ROU
Line 10 : A11 A22 A12 A16 A26 A66
Line 11 : D11 D22 D12 D16 D26 D66
Line 12 : G44 G55 G45 sc
Line 13 : mI vI cf k n
Line 14 : dt ts ITI

where,

Ibx, Iby : nonlinearity index numbers (integer) in the x- and y-direction

	1 => include nonlinear effect 0 => do not include nonlinear effect (linear)
beta :	geometrical nonlinearity factor ranging from 0.0 to 1.0 0.0 => linear case 1.0 => perfectly nonlinear case
IBCX, IBCY :	index numbers for the boundary conditions in x and y directions 1 => simply supported - simply supported 2 => clamped - free 3 => clamped - clamped 4 => free - free 5 => simply supported - clamped 6 => simply supported - free
NX, NY :	number of modes in the x and y directions
IEO :	switch for turning off even modes 0 => both odd and even modes 1 => odd modes only
XL, YL :	dimensions of plate in the x and y directions (m)
THICK, ROU :	thickness of the plate (m), density of the plate (kg/m^3)
A's : D's : G's : sc :	tensor components of A matrix (N/m) tensor components of D matrix (N-m) shear stiffness components (N/m) shear correction factor
mI, vI :	mass of impactor, initial impactor velocity
cf :	dimension of the square shape of the patched loading for point loading, let cf = 0.0 (This program is capable of dealing with double-cosine type distributed patch loading, although there has not been verified, yet.)
k, n :	local contact stiffness (N/m^n), nonlinearity exponent
dt, ts :	time increment (sec), number of time steps
ITI :	number of time steps to be skipped for reducing the output results. (i.e. for ITI=10, every 10th data will be recorded in the output data file.)

Sample Output Data File "global2.out"

First Column	Second Column	Third Column	Fourth Column
Time [sec]	Impact Force [N]	Plate Midplane Displacement [m]	Impactor Displacement [m]

```
5.E-5,  563.9444566804,  1.4143283511979E-4,  2.4978665302005E-4
9.9999999999999E-5,  561.5300020527,  3.9067406494724E-4,  4.9871839325297E-4
1.5E-4,  489.8141990071,  6.4805422765267E-4,  7.4669146746603E-4
1.9999999999999E-4,  197.1448177938,  9.4011445903343E-4,  9.9388489703504E-4
2.4999999999999E-4,  137.7189637977,  1.1983886311825E-3,  1.2407219672911E-3
2.9999999999999E-4,  186.3529445234,  1.4355325612436E-3,  1.4873223536263E-3
3.4999999999999E-4,  84.64649828287,  1.7030468658694E-3,  1.7336495365059E-3
3.9999999999999E-4,  201.8817150805,  1.9251416199655E-3,  1.9797699579251E-3
4.4999999999998E-4,  216.9672580041,  2.168261242569E-3,  2.225578156295E-3
4.9999999999998E-4,  239.2794938581,  2.4097734244457E-3,  2.4709554218636E-3
      :                    :                    :                    :
      :                    :                    :                    :
      :                    :                    :                    :
```